THE JOURNAL OF CHEMICAL PHYSICS

VOLUME 11 NUMBER 6

JUNE, 1943

Published by the
AMERICAN INSTITUTE OF PHYSICS
Lancaster, Pa. and New York, N. Y.

THE JOURNAL OF CHEMICAL PHYSICS

ADVISORY EDITORIAL BOARD

R. T. BIRGE
A. H. COMPTON
JAMES FRANCK
IRVING LANGMUIR
JOHN T. TATE
HAROLD C. UREY

BOARD OF EDITORS

JOSEPH E. MAYER, *Editor*

Associate Editors

Term ending December 31, 1949	*Term ending December 31, 1944*	*Term ending December 31, 1945*
SIMON FREED	CHARLES O. BECKMAN	L. O. BROCKWAY
MAURICE L. HUGGINS	BRYCE L. CRAWFORD, JR.	RONALD W. GURNEY
J. G. KIRKWOOD	P. DEBYE	KENNETH S. PITZER
GEORGE SCATCHARD	DAVID HARKER	ALFRED L. SKLAR
J. H. VAN VLECK	FRANK H. WESTHEIMER	E. W. R. STRACIE
		HUGH S. TAYLOR

THE JOURNAL OF CHEMICAL PHYSICS is published monthly by the American Institute of Physics. Its purpose is to bridge a gap between journals of physics and journals of chemistry. The artificial boundary between physics and chemistry has now been in actual fact completely eliminated, and a large and active group is engaged in research which is as much the one as the other. It is to this group that the Journal is rendering its principal service and makes its greatest appeal, both as a prompt and efficient medium for publication of research and as a convenient and carefully edited assemblage of pertinent information.

Manuscripts for publication should be submitted to Joseph E. Mayer, Havemeyer Hall, Columbia University, New York, New York.

Proof and all correspondence concerning papers in the process of publication should be addressed to the Publications Manager, American Institute of Physics, 175 Fifth Avenue, New York, New York.

Subscriptions and orders for single copies should be addressed to Prince and Lemon Streets, Lancaster, Pennsylvania, or to the American Institute of Physics, 175 Fifth Avenue, New York, New York.

Change of address should be addressed to the Publications Manager.

Subscription Price

The United States and Possessions, Canada and Mexico $10.00
Elsewhere 11.00

Back Numbers

Complete set: Vol 1, 1933—Vol 10, 1942 ..... $100.00
Yearly rate: $11.00.
Single copies: $1.00 each.

The Journal of Chemical Physics is published monthly at Prince and Lemon Streets, Lancaster, Pennsylvania.

Entered as second-class matter December 30, 1932, at the Post Office at Lancaster, Pa., under the Act of August 24, 1912. Acceptance for mailing at special rate of postage provided for in the Act of February 28, 1925, embodied in paragraph 4, Section 538, P. L. & R., authorized [illegible].

THE JOURNAL
OF
CHEMICAL PHYSICS

VOLUME 11, NUMBER 6 JUNE, 1943

The Infra-Red Absorption Spectrum and Configuration of Cyclohexane

ROBERT S. RASMUSSEN
Shell Development Company, Emeryville, California

(Received March 9, 1943)

The infra-red absorption spectrum from 2 to 14.5μ was determined for cyclohexane vapor. The number of bands found in the 700–1350 cm^{-1} region confirms the chair structure (symmetry D_{3d}) as the most stable at room temperature. The band envelopes are discussed and compare well with the theory of Gerhard and Dennison.

I. INTRODUCTION

THE infra-red absorption spectrum of cyclohexane vapor has an important bearing on the question of the configuration of the cyclohexane molecule. The evidence in favor of the "chair" form (symmetry D_{3d}), and hence of the staggered configuration of groups about a C–C single bond, has been summarized by Schomaker and Stevenson[1] and by Kohlrausch and Wittek.[2] Langseth and Bak[3] pointed out that if the opposed configuration of groups about a C–C single bond were the more stable, the cyclohexane molecule would assume the "cradle" form (symmetry C_{2v}) or the planar form (symmetry D_{6h}) or some compromise between the two. The exact form in this case would depend on the relative magnitudes of the potential restricting rotation about the C–C bond and the energy of distortion of the tetrahedral valence angles of the carbon atoms. The latter authors also presented data drawn from the Raman spectrum of liquid cyclohexane to indicate that the structure is the planar one. Kohlrausch and Wittek[2] called attention to an error in the polarization data used by these authors and showed that the correct polarization data lead unambiguously to the chair structure, assuming the usual selection rules to hold in the liquid. As shown below, this is also the conclusion drawn from the infra-red spectrum of the vapor, where the selection rules hold exactly.

The Raman spectrum of liquid cyclohexane is recapitulated in Table I. The values shown are averages of those given by various workers.[2–4] The infra-red absorption spectrum has been given previously by Kettering and Sleator[5] but without any tabulated wave-length data or any discussion.

II. EXPERIMENTAL DETAILS AND RESULTS

The spectrometer employed was an automatic-recording rocksalt prism instrument,[6] capable of

[1] V. Schomaker and D. P. Stevenson, J. Chem. Phys. **8**, 637 (1940).
[2] K. W. F. Kohlrausch and H. Wittek, Zeits. f. physik. Chemie **B48**, 177 (1941).
[3] A. Langseth and B. Bak, J. Chem. Phys. **8**, 403 (1940).
[4] A. Petrikaln and J. Hochberg, Zeits. f. physik. Chemie **B3**, 217 (1929); E. Canals, M. Godchot, and G. Cauquil, Comptes rendus **194**, 1574 (1932); K. W. F. Kohlrausch and W. Stockmair, Zeits. f. physik. Chemie **B31**, 382 (1936); R. Ananthakrishnan, Proc. Ind. Acad. Sci. **3**, 52 (1936); K. Matsuno and K. Han, Bull. Chem. Soc. Japan **11**, 321 (1936); A. I. Sidorova, Acta Phys. (U.S.S.R.) **7**, 193 (1937).
[5] C. F. Kettering and W. W. Sleator, Physics **4**, 39 (1933).
[6] To be described in a forthcoming article in *The Review of Scientific Instruments.*

resolving six reciprocal centimeters at eleven mu. The total absorption path used was 58 cm. The spectrum was obtained at a pressure of 40 mm Hg, and at regions of heavy absorption at 5 mm Hg also.

The cyclohexane used was a pure sample prepared under the direction of Professor C. E. Boord of the Department of Chemistry of the Ohio State University as part of the American Petroleum Institute Hydrocarbon Research Project in the Industrial Research Foundation of the University.

The spectrum obtained (Fig. 1) is in good agreement with that of Kettering and Sleator, but shows a little better resolution. The wavelengths (Table I) are accurate to $\pm.01\mu$ for $\lambda>5\mu$, as indicated by a test run on ethylene vapor and comparison with grating data. At $\lambda<5\mu$, the accuracy is somewhat lower, becoming about $\pm.02\mu$ at 3μ.

The bands with centers at 7.93μ, 9.60μ, and 11.57μ are clearly resolved into P, Q, and R branches. The peak at 9.85μ appears to be the Q branch of a band whose P and R branches are obscured by the P branch of the 9.60μ band. The band at 11μ seems to be different in appearance from the other long wave bands, having two equally intense peaks at 10.97μ and 11.075μ. The absorption near 14.6μ is seen, from reference to the curve of Kettering and Sleator, to be the R branch of a band with Q branch at 14.85μ.

TABLE I. Raman and infra-red spectra of cyclohexane (frequencies in cm^{-1}).

	Raman (liquid)	Infra-red (vapor)
Fundamentals	382 (2) P	673.4 (2)
	426 (3) D	
	802 (10) P	864.3 (6)
	1028 (7) D	902.9 (5)
	1155 (4) $\frac{1}{2}P$	1015 (1)
	1266 (7) D	1042 (3)
		1261 (5)
	1346 (2) (D?; harmonic?)	
	1443 (7) D	1456 (10)
	2853 (11) P	2865 (1)
	2871 (2)	2920 (1)
	2888 (3) D	2960 (9)
	2897 (3) } resonance	
	2909 (1) } splitting	
	2923 (8) D	
	2937 (8) P	
Higher harmonics	762 (0)	1348 (0)
	1424 ($\frac{1}{2}$)	1684? (0)
	1464 (1)	1792 (0)
	2349 (0)	1842? (00)
	2466 (1)	1887 (0)
	2536 (0)	2004 (0)
	2554 (0)	2079 (0)
	2604 (0)	2179? (00)
	2629 (1)	2217 (1)
	2663 (3) P	2294? (0)
	2698 (2)	2427 (1)
		2530 (0)
		2665 (0)
		2705 (5)
		3210 (1)
		3360 (0)
		3495 (0)
		3815 (0)
		4000 (0)
		4150 (0)
		4290, 4330 (2)

Figures in parentheses give relative intensities (based on 40-mm curve for infra-red). P = polarized, D = depolarized. Infra-red frequencies for $\lambda<4\mu$ rounded off to closest 5 cm^{-1}. (?) indicates doubtful bands, possibly due to wiggles in energy curve.

III. DISCUSSION

The forty-eight normal modes of vibration of cyclohexane can be conveniently divided into the following sets: twelve C−H stretching vibrations, six H−C−H bending vibrations, six C−C stretching vibrations, six C−C−C bending vibrations, and eighteen vibrations in which CH_2 groups twist or rock as units. This division, which is of course only a first approximation to the true motions, is sufficiently accurate to enable the frequency range to be stated in which each set of vibrations will be found. For a given symmetry of the whole molecule the symmetry classes to which the vibrations in each set belong are readily found by application of the usual group theory methods to the set of internal coordinates which describe the vibrations of the required type. In Table II are given the frequency ranges for each set of vibrations and the symmetry classes into which these vibrations fall, for the chair, cradle, and planar forms. Infra-red and Raman selection rules are shown for each case. The frequency ranges are known through reasonable extrapolations from corresponding vibrations in the simpler molecules methane, ethane, and ethylene.

The region 1350 to 700 cm^{-1} (7.4 to 14.3μ), which includes the C−C stretching frequencies and CH_2 rocking and twisting frequencies is the most fruitful one to examine, since here the frequencies are by their nature most spread apart, and resolution is highest in the prism-

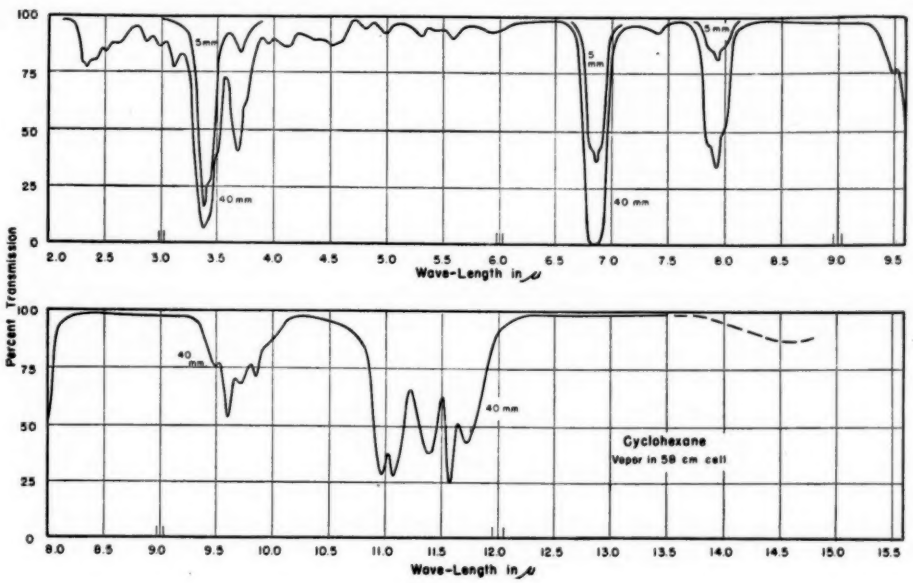

FIG. 1.

dispersed infra-red spectrum. In the observed spectrum there are five bands here, exactly the number to be predicted on the chair structure. The cradle and planar structures would require eighteen and three, respectively. Any structure intermediate between the cradle and planar would require even more, being of lower symmetry than either. Hence, the infra-red spectrum directly confirms the chair form as the stablest at room temperature. Reference to the Raman data and to Table II shows that both in polarization requirements (the polarized frequency shifts 382, 802, 1155 cm^{-1} being totally symmetric) and in distribution of frequencies the chair form is indicated.

Only one of the two expected infra-red bands is found in the 1400 cm^{-1} region. However, this band is so strong and resolution is so relatively poor in this region that this may very well be a case of a strong band completely hiding a weaker one. One of the low frequency infra-red bands is still unobserved, lying at a wave-length greater than 16μ. In the Raman spectrum 1400 cm^{-1} region, only one strong line has been found, the depolarized 1443 cm^{-1} frequency. There should be a polarized shift in this region, but it is apparently rather weak. Possibly the weak 1424 cm^{-1} line (listed as a harmonic) is this fundamental, although its polarization has not been measured because of its low intensity. The usual rule that the totally symmetrical (polarized) Raman shifts are more intense than the non-totally symmetrical seems to be violated here. In the 700–1350 cm^{-1} region, two polarized and two depolarized lines are found; two more depolarized ones should be present but are apparently too weak to be observed. The shift at 1346 cm^{-1} is possibly one of these.

Any more specific assignment of the observed frequencies, other than the symmetry of the

TABLE II. Symmetry classes of vibrations of cyclohexane for chair, cradle, and planar forms.

Type and range	Chair, D_{3d}						Cradle, C_{2v}				Planar, D_{6h}									
	A_{1g}	A_{1u}	A_{2g}	A_{2u}	E_g	E_u	A_1	A_2	B_1	B_2	A_{1g}	A_{1u}	A_{2g}	A_{2u}	B_{1g}	B_{1u}	B_{2g}	B_{2u}	E_{1g}	E_{1u}	E_{2g}	E_{2u}
12 C–H stretching 2850–3000 cm^{-1}	2	0	0	2	2	2	4	2	4	2	1	0	0	1	0	1	1	0	1	1	1	1
6 H–C–H bending 1350–1500 cm^{-1}	1	0	0	1	1	1	2	1	2	1	1	0	0	0	0	1	0	0	0	1	1	0
18 CH_2 rocking and twisting 700–1350 cm^{-1}	1	2	2	1	3	3	4	5	4	5	0	1	1	1	1	0	1	1	2	1	1	2
6 C–C stretching 700–1350 cm^{-1}	1	1	0	0	1	1	2	1	1	2	1	0	0	0	0	0	0	1	0	1	1	0
6 C–C–C bending <700 cm^{-1}	1	0	0	1	1	1	2	2	2	0	0	0	0	0	0	1	1	0	0	0	1	1
Activity: IR = infra-red, R = Raman, I = inactive	R	I	I	IR	R	IR	R, IR	R	R, IR	R, IR	R	I	I	IR	I	I	I	I	R	IR	R	I

Raman frequencies as shown by polarization data, is impossible at this time. The infra-red band envelopes seem to be incapable of yielding knowledge as to the symmetry characters of the infra-red active frequencies, as discussed below. Lack of knowledge of the five inactive frequencies and of one infra-red and several Raman frequencies makes it of little use to attempt to interpret the overtones and combinations. These specific details of the vibrational spectrum must await an adequate force constant treatment for their elucidation.

Using accepted carbon-carbon and carbon-hydrogen bond lengths (1.54 and 1.09A, respectively) and tetrahedral angles, the principal moments of inertia of the chair structure are calculated to be:

$$A = B = 116.8 \text{ at. wt. units} \cdot \text{A}^2,$$
$$C = 201.8 \text{ at. wt. units} \cdot \text{A}^2.$$

The value of the parameter $\beta = (A/C) - 1$, used by Gerhard and Dennison[7] to describe the asymmetry of a symmetrical top molecule, is -0.421; i.e., the cyclohexane molecule approximates somewhat a flat disk ($\beta = -\frac{1}{2}$). Reference to the band envelope curves for perpendicular bands given by Gerhard and Dennison shows that for this value of β, these bands still have a good deal of the character of bands of a spherically symmetrical rotator, the zero branches ($\Delta J = 0$, $\Delta K = \pm 1$) forming a strong central maximum, giving the whole band the appearance of a parallel band. This explains the parallel type envelopes found in four of the five bands in the 700–1350 cm^{-1} region of the infra-red spectrum, where there are to be expected four perpendicular and one parallel band. The apparently anomalous envelope of the 11μ band can be interpreted as being due to a vibration involving a relatively large change in moments of inertia between the ground and first excited vibrational states. The resulting degrading (to the red, in this case) causes the Q branch at 902.9 cm^{-1} (11.075μ) to be considerably broadened; the R branch at 912.4 cm^{-1} (10.97μ) to be shifted to a lower frequency than normal and to pile up until its maximum intensity is comparable to the Q branch; and the P branch to be shifted to lower frequency than normal and decreased in intensity so that it is hidden by the R branch of the 864.3 cm^{-1} (11.57μ) band.

Using the "separation" function of Gerhard and Dennison,[7] the calculated P–R separation of the parallel bands is 23 cm^{-1}. The perpendicular band P–R separation should be slightly less than this. The observed values for the 1042 cm^{-1} and 864.3 cm^{-1} bands (the only two which were free enough from interference and sufficiently resolved to measure accurately) are 25 cm^{-1} for each, in very good agreement considering the limitations of the simple theory applied to actual cases.

Recently data have been published on the heat capacity of cyclohexane vapor over a temperature range from 370° to 410°K.[8] Because of lack of knowledge of the several inactive or unobserved frequencies and of the degeneracies of known frequencies it seems improbable that any significant result would be obtained by a statistical calculation and comparison with experiment.

[7] S. L. Gerhard and D. M. Dennison, Phys. Rev. **43**, 197 (1933).

[8] J. B. Montgomery and T. DeVries, J. Am. Chem. Soc. **64**, 2375 (1942).

THE JOURNAL OF CHEMICAL PHYSICS VOLUME 11, NUMBER 6 JUNE, 1943

Determination of Chlorine Vibrations in Dichlorobenzenes from Intensities and Polarizations of Their Raman Lines

GERTRUD NORDHEIM AND H. SPONER
Department of Physics, Duke University, Durham, North Carolina
(Received January 22, 1943)

Intensities and polarization properties of vibrations in which mainly chlorine atoms are participating, are investigated theoretically for the dichlorobenzenes. It is assumed that the change of polarizability in these vibrations is connected primarily with displacements of the chlorine atoms and that contributions from the individual atoms are additive. The Raman tensors belonging to the chlorine vibrations are then obtained by either adding or subtracting the single C−Cl contributions with reference to a chosen system of axes rigidly connected with the molecule. Intensity ratios were obtained for the symmetrical and unsymmetrical valence vibrations and deformation vibrations, respectively. Very small depolarization factors were found for lines representing symmetrical valence vibrations. For deformation vibrations the simplified theory gives complete depolarization for all allowed Raman lines. The results are discussed in connection with existing experimental data.

INTRODUCTION

RAMAN spectra of substituted benzenes have been investigated by several authors and correlations of the observed lines to particular modes of vibration have been proposed in many cases. In spite of the great number of vibrations it is possible to follow such a correlation through whole series of substitutions for certain vibrations. However, in general, it is extremely difficult or impossible to find an unambiguous assignment for all observed lines. Such difficulties were encountered in the course of an investigation of the Raman spectra of the dichlorobenzenes and their depolarization factors.[1,2]

In this paper, we are interested in vibrations of the dichlorobenzenes in which mainly chlorine atoms are involved and in the correlation of these vibrations to observed Raman lines. To supplement the existing data we have studied from a theoretical point of view the intensity and polarization properties of these vibrations. We have used the following simplified assumptions: a. The change of polarizability in these particular vibrations is connected mainly with the displacements of the chlorine atoms. b. The contributions to the change of polarizability from the individual atoms are treated as additive.

Among the vibrations of the dichlorobenzenes there must occur two valence and two deformation vibrations of the C−Cl bonds in the molecular plane and two deformation vibrations perpendicular to the plane whereas there is only one of each kind in monochlorobenzene. The valence vibrations will have larger frequencies than the deformation vibrations. All of them have frequency values below 1000 cm^{-1}.

GENERAL THEORETICAL OUTLINE

The induced electric moment m is given by

$$m=\alpha E,$$

where E is the vector of the electric field strength of the incident radiation and α is the polarizability tensor. α depends on the coordinates describing the motion of the vibrating or rotating molecules. We are not concerned here with the effect of rotation, but rather with the dependence of the polarizability on molecular vibration. Since the displacements of the atoms during the vibration are small compared to nuclear dimensions, α can be developed in powers of the normal coordinates q_i which themselves are periodical with time ($q_i=a_i\cos 2\pi\nu_i t$, where a_i is the amplitude and ν_i the frequency of the i-th vibration). Including only linear terms, we have for a typical element α_{xy} of the polarizability tensor

$$\alpha_{xy}^{\text{total}}=\overset{T}{\alpha}_{xy}+\sum_i \frac{\partial \overset{T}{\alpha}_{xy}}{\partial q_i} q_i$$

$$=\overset{T}{\alpha}_{xy}+\sum \overset{iR}{\alpha}_{xy}\cos 2\pi\nu_i t \qquad (1)$$

where

$$\frac{\partial \overset{T}{\alpha}_{xy}}{\partial q_i} a_i=\overset{iR}{\alpha}_{xy}.$$

[1] H. Sponer and J. S. Kirby-Smith, J. Chem. Phys. **9**, 667 (1941). See this paper for previous references.
[2] O. Paulsen, Monatsh. d. Chemie **72**, 244 (1939); K. W. F. Kohlrausch and O. Paulsen, ibid. 268 (1939) *p*-dichlorobenzene.

Here the first term $\overset{T}{\alpha}_{xy}$ gives the Tyndall or Rayleigh scattering and in the second term the i-th member of the sum represents the Raman scattering due to the i-th vibration. The contributions from the different vibrations are independent of each other (incoherent) and we will drop the index i when discussing the Raman tensor $\overset{R}{\alpha}_{xy}$ due to one particular vibration.

Such a tensor (assumed to be symmetrical) may be split into two parts, a spherically symmetrical and an anisotropic one (unless specified otherwise, α_{xy} means the Raman tensor $\overset{R}{\alpha}_{xy}$ from here on)

$$\alpha_{xy}=\overset{s}{\alpha}_{xy}+\overset{b}{\alpha}_{xy}=\frac{s}{\sqrt{3}}\delta_{xy}+\left(\alpha_{xy}-\frac{s}{\sqrt{3}}\delta_{xy}\right). \quad (2)$$

Here $s=(1\sqrt{3})(\alpha_{xx}+\alpha_{yy}+\alpha_{zz})$ is the trace of the tensor multiplied by $(1/\sqrt{3})$ and $\delta_{xy}=1$ for $x=y$ and $\delta_{xy}=0$ for $x\neq y$. Since s is an invariant of the tensor, this splitting is valid for any coordinate system, also for the special one of the principal axes in which the tensor α_{xy} is diagonal.

Intensity and polarization of the Raman light can be expressed with the help of these tensors. The intensity of the total Raman scattering in all directions due to one particular vibration is proportional to the square of the corresponding tensor α_{xy}, i.e., to the sum of the squares of all the components (the square is also an invariant of the tensor).

$$I\sim\sum_{xy}\alpha^2_{xy}=\alpha^2_{xx}+\alpha^2_{yy}+\alpha^2_{zz}+\alpha^2_{xy}+\cdots=s^2+b^2,$$

where s^2 and b^2 are the squares of the tensors $\overset{s}{\alpha}_{xy}$ and $\overset{b}{\alpha}_{xy}$. However, the intensity of a Raman line is generally observed at right angles to the incident beam. This intensity is given by the expression

$$I_{\text{obs}}=10s^2+13b^2. \quad (3)$$

The depolarization factor (for natural light) is given by the expression*

$$\rho_n=\frac{6b^2}{10s^2+13b^2}. \quad (4)$$

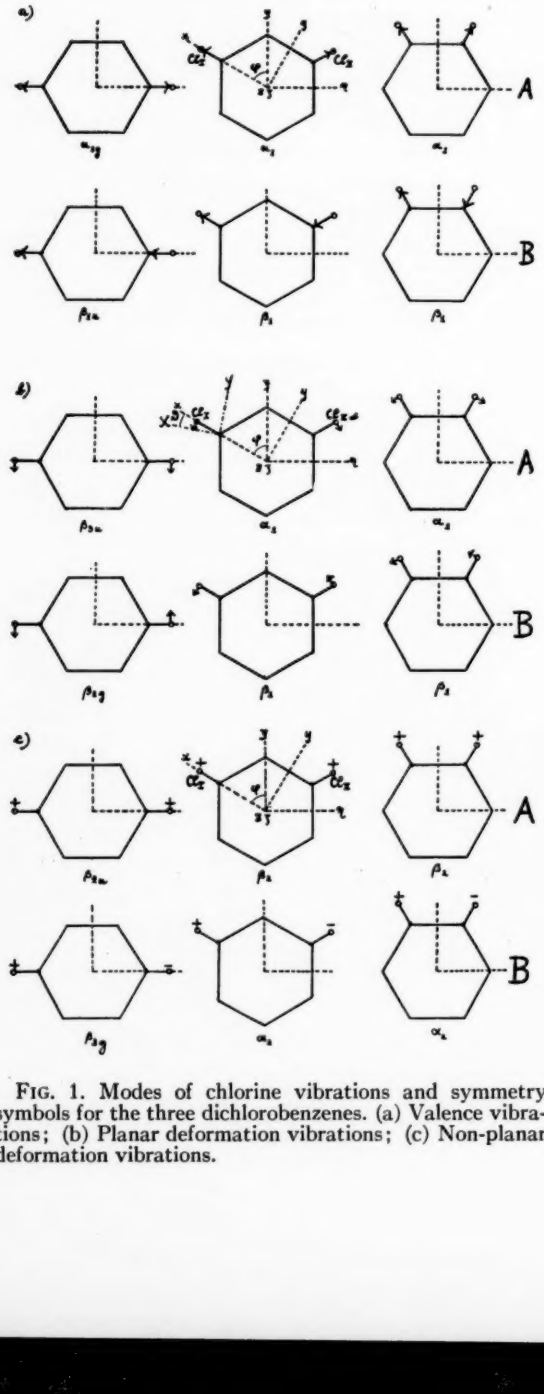

FIG. 1. Modes of chlorine vibrations and symmetry symbols for the three dichlorobenzenes. (a) Valence vibrations; (b) Planar deformation vibrations; (c) Non-planar deformation vibrations.

THEORETICAL TREATMENT OF CHLORINE VIBRATIONS

With this general outline in mind we shall now attack the problem of the chlorine vibrations of the dichlorobenzenes. We shall try to obtain values for the depolarization factors of their Raman lines and also an estimate of the intensity ratios between the lines belonging to the two valence vibrations in the molecular plane, to the

* The formula frequently found in the literature

$$\rho_n=\frac{6b'^2}{45a'^2+7b'^2}$$

follows from the one given in the text by putting $a'^2=s^2/3$ and $b'^2=3b^2/2$. Both the formulae for ρ_n are valid in any coordinate system but for the special one of the principal axes the invariant b'^2 becomes

$$b'^2=\tfrac{1}{2}[(\alpha_{xx}-\alpha_{yy})^2+(\alpha_{yy}-\alpha_{zz})^2+(\alpha_{zz}-\alpha_{xx})^2]. \quad (4a)$$

b' is called the optical anisotropy.

TABLE I. Transformation coefficients for the Raman tensor α_{xy}.

	α_{xx}	α_{yy}	α_{zz}	α_{xy}	α_{yz}	α_{zx}	α_{zz}	α_{yz}	α_{xy}
$\alpha_{\xi\xi}$	$\cos^2\varphi$	$\sin^2\varphi$	0	$\cos\varphi\sin\varphi$	$\sin\varphi\cos\varphi$	0	0	0	0
$\alpha_{\eta\eta}$	$\sin^2\varphi$	$\cos^2\varphi$	0	$-\sin\varphi\cos\varphi$	$-\cos\varphi\sin\varphi$	0	0	0	0
$\alpha_{\zeta\zeta}$	0	0	1	0	0	0	0	0	0
$\alpha_{\xi\eta}$	$-\cos\varphi\sin\varphi$	$\sin\varphi\cos\varphi$	0	$\cos^2\varphi$	$-\sin^2\varphi$	0	0	0	0
$\alpha_{\eta\xi}$	$-\sin\varphi\cos\varphi$	$\cos\varphi\sin\varphi$	0	$-\sin^2\varphi$	$\cos^2\varphi$	0	0	0	0
$\alpha_{\xi\zeta}$	0	0	0	0	0	$\cos\varphi$	0	$\sin\varphi$	0
$\alpha_{\zeta\xi}$	0	0	0	0	0	0	$\cos\varphi$	0	$\sin\varphi$
$\alpha_{\eta\zeta}$	0	0	0	0	0	$-\sin\varphi$	0	$\cos\varphi$	0
$\alpha_{\zeta\eta}$	0	0	0	0	0	0	$-\sin\varphi$	0	$\cos\varphi$

two deformation vibrations in the molecular plane and the two deformation vibrations out of the plane. The results will be compared with experimental data.

The vibrations with which we are concerned here are represented schematically in Fig. 1 together with their symmetry symbols.[3] In each pair of vibrations the two chlorine atoms vibrate in phase for one vibration and out of phase for the other one (called A and B vibrations respectively in Fig. 1). If we assume that in first approximation the Raman tensor for these vibrations is determined by the change of polarizability in the C−Cl bonds alone and moreover that the contributions from the two bonds are additive, then we can construct the Raman tensors by either adding or subtracting the single C−Cl contributions with reference to a chosen system of axes rigidly connected with the molecule. This system with axes ξ, η, ζ is indicated in Fig. 1. ξ and η lie in the molecular plane, ζ is perpendicular to it. If the Raman tensor of a particular C−Cl bond has the six components α_{xy} with the x axis in the C−Cl direction, the y axis perpendicular to it in the plane and the z axis orthogonal to the plane then we may express this tensor in the coordinate system ξ, η, ζ by making the usual tensor transformation

$$\alpha_{\xi\eta}=\sum_{xy}\alpha_{xy}\cos(x\xi)\cos(y\eta). \tag{5}$$

From the special choice of the six axes it follows that all terms in the sum containing factors $\cos(\zeta x)$, $\cos(\zeta y)$, $\cos(\xi z)$, and $\cos(\eta z)$ are zero.

[3] The symmetry symbols used are listed for instance in H. Sponer and E. Teller, Rev. Mod. Phys. **13**, 76 (1941). See also A. Langseth and R. C. Lord, Kgl. Danske Vid. Sels. Math.-fys. Medd. **16**, No. 6 (1938) for the classification of the vibrations of the deuterobenzenes according to symmetry and type, and H. Sponer and J. S. Kirby-Smith, reference 1, for the vibrations of the chlorobenzenes.

If φ is the angle $(x\xi)$ we may express all the coefficients occurring in the transformations (5) as functions of φ as indicated in Table I.

The Raman tensor $\overset{I}{\alpha}_{xy}$ belonging to the displacement of the chlorine atom Cl_I becomes, with the help of the angle of transformation φ, $\overset{I}{\alpha}_{\xi\eta}$ in the reference system ξ, η. Similarly the angle of transformation is $-\varphi$ for the chlorine atom Cl_{II}. To indicate this, the corresponding tensors are called $\overset{I}{\alpha}_{\xi\eta}(\varphi)$ and $\overset{II}{\alpha}_{\xi\eta}(-\varphi)$. Their addition and subtraction gives the resulting Raman tensors for each pair of vibrations A, B.

$$\begin{aligned} A&=\overset{I}{\alpha}_{\xi\eta}(\varphi)\pm\overset{II}{\alpha}_{\xi\eta}(-\varphi),\\ B&=\overset{I}{\alpha}_{\xi\eta}(\varphi)\mp\overset{II}{\alpha}_{\xi\eta}(-\varphi). \end{aligned} \tag{6}$$

The + and − signs in (6) have to be determined for each of the three pairs separately (see below).

The intensity ratio of the two vibrations ν_A and ν_B can be calculated from Eq. (3) and the depolarization factors ρ_A and ρ_B from Eq. (4), after A^2 and B^2 have been determined.

A. The Chlorine Valence Vibrations

We assume, as is customary, that for small amplitudes the change of polarizability varies linearly with nuclear displacements. In our case this change for one C−Cl group may be taken as the one which occurs during the totally symmetrical chlorine vibration in C_6H_5Cl. If we make the simplifying assumption that the Raman tensor α_{xy} corresponding to this vibration has cylindrical symmetry about the C−Cl axis (which we take as x axis), then the tensor has the form

$$\alpha_{xy}=\begin{vmatrix}\alpha_{xx}&0&0\\0&\alpha_{yy}&0\\0&0&\alpha_{zz}\end{vmatrix}=\begin{vmatrix}\alpha_{xx}&0&0\\0&\alpha_{yy}&0\\0&0&\alpha_{yy}\end{vmatrix}. \tag{7}$$

We can determine the ratio α_{xx}/α_{yy} from the experimentally known[4] depolarization factor $\rho_n=0.13$. From (4) and (4a) follows then

$$\frac{s^2}{b^2}=\frac{6-7\rho_n}{10\rho_n}=3.91$$

with

$$s^2=\tfrac{1}{3}(\alpha_{xx}+2\alpha_{yy})^2 \quad \text{and} \quad b^2=\tfrac{2}{3}(\alpha_{xx}-\alpha_{yy})^2.$$

Since we are interested in the ratio s^2/b^2 only, i.e., in relative intensity values, we may arbitrarily fix one constant, for example $s^2=3$. With this value we obtain for the intensity using Eq. (3)

$$I_{\text{mono}}\sim 10s^2+13b^2=30+10=40$$

and, if we take the positive root of s^2/b^2, we have

$$\alpha_{xx}=1.716; \quad \alpha_{yy}=\alpha_{zz}=0.642.$$

This choice does not mean a restriction of generality in the final results given below because the intensity and depolarization factors always depend on s^2/b^2 only, and the negative root leads to the same result. The shape of the polarizability ellipsoid, however, depends on the sign. The positive sign, yielding $\alpha_{xx}>\alpha_{yy}=\alpha_{zz}$ is physically more plausible since it corresponds to an ellipsoid with the major axis in the direction of the C–Cl bond.

In order to find the Raman tensors belonging to the two valence vibrations A and B of the dichlorobenzenes (Fig. 1a), we calculate $\overset{I}{\alpha}_{xy}$ and $\overset{II}{\alpha}_{xy}$ in the coordinate system ξ, η from (7) with the help of Table I. We can see from Fig. 1a that the Raman tensor A belonging to the totally symmetrical valence vibration, in which the chlorine atoms are in phase, will be given by adding $\overset{I}{\alpha}_{\xi\eta}(\varphi)$ and $\overset{II}{\alpha}_{\xi\eta}(-\varphi)$ and the tensor B (chlorine atoms out of phase) by subtracting them. (6) becomes here

$$A=\overset{I}{\alpha}_{\xi\eta}(\varphi)+\overset{II}{\alpha}_{\xi\eta}(-\varphi),$$
$$B=\overset{I}{\alpha}_{\xi\eta}(\varphi)-\overset{II}{\alpha}_{\xi\eta}(-\varphi),$$

with

$$A_{\xi\xi}=2(\alpha_{xx}\cos^2\varphi+\alpha_{yy}\sin^2\varphi),$$
$$A_{\eta\eta}=2(\alpha_{xx}\sin^2\varphi+\alpha_{yy}\cos^2\varphi),$$
$$A_{\zeta\zeta}=2\alpha_{zz},$$
$$A_{\xi\eta}=A_{\eta\xi}=A_{\xi\zeta}=A_{\zeta\xi}=A_{\eta\zeta}=A_{\zeta\eta}=0,$$
$$B_{\xi\xi}=B_{\eta\eta}=B_{\zeta\zeta}=0,$$
$$B_{\xi\eta}=B_{\eta\xi}=-2(\alpha_{xx}-\alpha_{yy})\sin\varphi\cos\varphi,$$
$$B_{\xi\zeta}=B_{\zeta\xi}=B_{\eta\zeta}=B_{\zeta\eta}=0.$$

With the values of α_{xx}, α_{yy}, α_{zz} determined above we find for all three dichlorobenzenes $s_A^2=(2s)^2=12$; $s_B^2=0$.

The squares of the tensors are given by

$$A^2=4[3.36(\cos^4\varphi+\sin^4\varphi)+4.4\sin^2\varphi\cos^2\varphi+0.41], \quad (8)$$
$$B^2=4\times 2.32\sin^2\varphi\cos^2\varphi.$$

Thus

$$b_A^2=A^2-s_A^2=4[3.36(\cos^4\varphi+\sin^4\varphi)+4.4\sin^2\varphi\cos^2\varphi-2.59],$$
$$b_B^2=B^2=4\times 2.32\sin^2\varphi\cos^2\varphi.$$

The intensities I_A and I_B and their ratios can be found with the help of (3) and the depolarization factors ρ_A from (4). Since $s_B^2=0$, it follows $\rho_B=6/7$ which means that the non-totally symmetrical vibrations are completely depolarized as expected.

The intensity ratios and depolarization factors for the vibrations of the three individual dichlorobenzenes can be calculated with the above expressions by putting $\varphi=90°$, 60°, 30° respectively for the para- meta-, and ortho-compound, (comp. Fig. 1(a)). The results are summarized in Table II together with the data on the totally symmetrical valence vibration of monochlorobenzene. The discussion of this table will be given in a later section.

B. The Chlorine Deformation Vibrations

We assume that the main effect of the chlorine deformation vibrations consists in a rotation of the polarizability tensors α connected with the C–Cl bonds. We neglect the distortion of α due to changes in the C–Cl distance. This is analogous to the procedure for the valence vibrations where we considered the change in distance only and neglected the angular changes. However, it might lead to less reliable results because the distortion of the carbon-ring might give a relatively larger contribution to the Raman tensors

[4] L. Simons, Soc. Sci. Fennica, Comm. Phys.-Math. **6**, No. 13 (1932).

TABLE II. Calculated relative intensities and depolarization factors for the chlorine valence vibrations of the dichlorobenzenes.

Chlorobenzene	I_A	I_B	I_A/I_B	ρ_A	ρ_B
$p-di$ $\varphi=90°$	4×40	0	∞	0.13	—
$m-di$ $\varphi=60°$	4×34.4	4×5.56	6.1	0.063	6/7
$o-di$ $\varphi=30°$	4×34.4	4×5.65	6.1	0.063	6/7
mono	40	—	—	0.13*	—

* Taken from experimental data (reference 4) to adjust the constants.

of the deformation vibrations than the angular changes to the valence vibrations.

A deformation vibration consists in a rotation of the C−Cl bond (axes X, Y, Z) against a system of axes x, y, z in which the C−Cl bond is at rest. We have to calculate first the Raman tensor $\overset{R}{\alpha}_{xy}$ (change of polarizability) produced by such a rotation of a single C−Cl group. The effect of the two C−Cl groups in the dichlorobenzenes can then be composed with the help of (6) in the same manner as for the valence vibrations by transformation into a coordinate system ξ, η, ζ fixed in the molecule.

For the deformation vibrations in the plane the rotation of one C−Cl group will take place in the x, y plane (ϑ = angle of rotation), the z and Z axes being coincident. The coordinate systems used for the calculation of the Raman tensors belonging to these vibrations are shown in Fig. 1(b). The calculation for the non-planar deformation vibrations is analogous; there the rotation of one C−Cl group takes place in the x, z plane perpendicular to the plane of the molecule and the y and Y axes coincide. (See Fig. 1(c).)

The polarizability tensor α_{XY} rigidly connected with one oscillating C−Cl bond (diagonal terms only) can be expressed in the system x, y, z (C−Cl bond at rest) by again using Table I. The coefficients will be functions of the angle of rotation ϑ. Since the rotation of the C−Cl axis out of the position of equilibrium will be small, the angle ϑ will be small and may be written as $\vartheta=\epsilon\cos 2\pi\nu_i t$ where ν_i is the frequency of the vibration. We can then develop the tensor α_{xy} in ϵ and only keep linear terms in ϵ ($\sin\vartheta\backsimeq\vartheta$, $\cos\vartheta\backsimeq 1$). Corresponding to the second row in Eq. (1) the terms of zeroth order give the Rayleigh scattering and the terms of first order the components of the Raman tensors.

For a C−Cl bond rotating in the x, y plane we have

$$\alpha_{xx}=\overset{T}{\alpha}_{XX}\cos^2\vartheta+\overset{T}{\alpha}_{YY}\sin^2\vartheta\sim\overset{T}{\alpha}_{XX},$$
$$\alpha_{yy}=\overset{T}{\alpha}_{XX}\sin^2\vartheta+\overset{T}{\alpha}_{YY}\cos^2\vartheta\sim\overset{T}{\alpha}_{YY},$$
$$\alpha_{zz}=\overset{T}{\alpha}_{ZZ};\quad \alpha_{xz}=\alpha_{zx}=\alpha_{yz}=\alpha_{zy}=0,$$
$$\alpha_{xy}=\alpha_{yx}=(-\overset{T}{\alpha}_{XX}+\overset{T}{\alpha}_{YY})\sin\vartheta\cos\vartheta$$
$$=(-\overset{T}{\alpha}_{XX}+\overset{T}{\alpha}_{YY})\epsilon\cos 2\pi\nu_i t.$$

For the angle of rotation $-\vartheta$, $\alpha_{xy}=\alpha_{yx}$ changes its sign; the other components remain the same.

In the system where the molecule is at rest, the Raman tensor belonging to one C−Cl group vibrating in the plane will have the components

$$\overset{R}{\alpha}_{xx}=\overset{R}{\alpha}_{yy}=\overset{R}{\alpha}_{zz}=\overset{R}{\alpha}_{xz}=\overset{R}{\alpha}_{zx}=\overset{R}{\alpha}_{yz}=\overset{R}{\alpha}_{zy}=0,$$
$$\overset{R}{\alpha}_{xy}=\overset{R}{\alpha}_{yx}=(-\overset{T}{\alpha}_{XX}+\overset{T}{\alpha}_{YY})\epsilon=c. \tag{9}$$

A similar calculation for the rotation of a C−Cl bond in the x, z plane leads to the following components of the corresponding Raman tensor

$$\overset{R}{\alpha}_{xx}=\overset{R}{\alpha}_{yy}=\overset{R}{\alpha}_{zz}=\overset{R}{\alpha}_{xy}=\overset{R}{\alpha}_{yx}=\overset{R}{\alpha}_{yz}=\overset{R}{\alpha}_{zy}=0,$$
$$\overset{R}{\alpha}_{xz}=\overset{R}{\alpha}_{zx}=(\overset{T}{\alpha}_{XX}-\overset{T}{\alpha}_{ZZ})\epsilon'=c'. \tag{10}$$

c and c' in (9) and (10) are certain unknown constants in which the intensities of the vibrations can be expressed.

The Raman tensors of the deformation vibrations of the dichlorobenzenes can now be easily obtained. $\overset{I}{\alpha}_{\xi\eta}$ and $\overset{II}{\alpha}_{\xi\eta}$ denote again the Raman tensors belonging to the two C−Cl bonds in the coordinate system ξ, η, ζ. These tensors can be found by transformation with the angle φ of tensors of the form (9) (for the planar deformation vibrations) or (10) (for the non-planar vibrations) using again Table I. The dependence on the angle can be read from Figs. 1(b) and 1(c). We see that Eqs. (6) become for the planar vibrations

$$A=\overset{I}{\alpha}_{\xi\eta}(\vartheta,\varphi)+\overset{II}{\alpha}_{\xi\eta}(-\vartheta,-\varphi)$$
$$=\overset{I}{\alpha}_{\xi\eta}(\vartheta,\varphi)-\overset{II}{\alpha}_{\xi\eta}(\vartheta,-\varphi), \tag{11a}$$
$$B=\overset{I}{\alpha}_{\xi\eta}(\vartheta,\varphi)+\overset{II}{\alpha}_{\xi\eta}(\vartheta,-\varphi),$$

TABLE III. Calculated intensities and depolarization factors for the planar chlorine deformation vibrations of the dichlorobenzenes.

Chloro-benzene	I_A	I_B	I_A/I_B	ρ_A	ρ_B
p−*di* $\varphi=90°$	0	$13\times 8c^2$	0	—	6/7
m−*di* $\varphi=60°$	$13\times 6c^2$	$13\times 2c^2$	3	6/7	6/7
o−*di* $\varphi=30°$	$13\times 6c^2$	$13\times 2c^2$	3	6/7	6/7
mono	—	$13\times 2c^2$	–	—	6/7

and for the non-planar vibrations

$$A=\overset{I}{\alpha}_{\xi\eta}(\vartheta,\varphi)+\overset{II}{\alpha}_{\xi\eta}(\vartheta,-\varphi),$$
$$B=\overset{I}{\alpha}_{\xi\eta}(\vartheta,\varphi)+\overset{II}{\alpha}_{\xi\eta}(-\vartheta,-\varphi) \qquad (11b)$$
$$=\overset{I}{\alpha}_{\xi\eta}(\vartheta,\varphi)-\overset{II}{\alpha}_{\xi\eta}(\vartheta,-\varphi).$$

For the pair of vibrations in the plane the components of the Raman tensors become

$$A_{\xi\xi}=\overset{R}{\alpha}_{xy}[2\cos\varphi\sin\varphi-2\cos(-\varphi)\sin(-\varphi)]$$
$$=c[4\cos\varphi\sin\varphi],$$
$$A_{\eta\eta}=\overset{R}{\alpha}_{xy}[-2\cos\varphi\sin\varphi+2\cos(-\varphi)\sin(-\varphi)]$$
$$=c[-4\cos\varphi\sin\varphi],$$
$$A_{\xi\eta}=A_{\eta\xi}$$
$$=\overset{R}{\alpha}_{xy}[\cos^2\varphi-\sin^2\varphi-\cos^2(-\varphi)+\sin^2(-\varphi)]$$
$$=0,$$
$$A_{\zeta\zeta}=A_{\xi\zeta}=A_{\zeta\xi}=A_{\eta\zeta}=A_{\zeta\eta}=0,$$
$$B_{\xi\xi}=B_{\eta\eta}=B_{\zeta\zeta}=B_{\xi\zeta}=B_{\zeta\xi}=B_{\eta\zeta}=B_{\zeta\eta}=0,$$
$$B_{\xi\eta}=B_{\eta\xi}=\overset{R}{\alpha}_{xy}2[\cos^2\varphi-\sin^2\varphi]$$
$$=c2[\cos^2\varphi-\sin^2\varphi].$$

As before, we obtain a measure for the intensity with the help of (3) after determining the squares of these tensors

$$A^2=c^2\times 32\cos^2\varphi\sin^2\varphi,$$
$$B^2=c^2\times 8(\cos^2\varphi-\sin^2\varphi)^2. \qquad (12)$$

Since $s_A{}^2=s_B{}^2=0$, we have $I_A=13A^2$, $I_B=13B^2$, and $I_A/I_B=A^2/B^2$. From Eq. (4) we have $\rho_A=\rho_B=6/7$ which means that all the deformation vibrations in the plane are completely depolarized.

For the deformation vibrations out of the plane the components of the Raman tensors become with the help of (10), (11b), and Table I

$$A_{\xi\xi}=A_{\eta\eta}=A_{\zeta\zeta}=A_{\xi\eta}=A_{\eta\xi}=0,$$
$$A_{\xi\zeta}=A_{\zeta\xi}=\overset{R}{\alpha}_{xz}[\cos\varphi+\cos(-\varphi)]=c'(2\cos\varphi),$$
$$A_{\eta\zeta}=A_{\zeta\eta}=\overset{R}{\alpha}_{xz}[-\sin\varphi-\sin(-\varphi)]=0,$$
$$B_{\xi\xi}=B_{\eta\eta}=B_{\zeta\zeta}=B_{\xi\eta}=B_{\eta\xi}=B_{\eta\zeta}=B_{\zeta\eta}=0,$$
$$B_{\xi\zeta}=B_{\zeta\xi}=\overset{R}{\alpha}_{xz}[-\sin\varphi+\sin(-\varphi)]=c'(-2\sin\varphi).$$

Since $s_A{}^2=s_B{}^2=0$, the intensities are again directly proportional to the squares

$$I_A=13A^2=13c'^2\times 8\cos^2\varphi,$$
$$I_B=13B^2=13c'^2\times 8\sin^2\varphi. \qquad (13)$$

The intensity ratio is given by $\cos^2\varphi/\sin^2\varphi$ and $\rho_A=\rho_B=6/7$.

The intensity ratios for the pairs of deformation vibrations of the three dichlorobenzenes can be obtained by putting $\varphi=90°$, 60°, 30° respectively. The results are summarized in Tables III and IV. Their discussion and the comparison with the experimental data will be given in the next section.

TABLE IV. Calculated intensities and depolarization factors for the non-planar chlorine deformation vibrations of the dichlorobenzenes.

Chloro-benzene	I_A	I_B	I_A/I_B	ρ_A	ρ_B
p−*di* $\varphi=90°$	0	$13\times 8c'^2$	0	—	6/7
m−*di* $\varphi=60°$	$13\times 2c'^2$	$13\times 6c'^2$	1/3	6/7	6/7
o−*di* $\varphi=30°$	$13\times 6c'^2$	$13\times 2c'^2$	3	6/7	6/7
mono	$13\times 2c'^2$	—	—	6/7	—

DISCUSSION AND COMPARISON WITH EXPERIMENTAL DATA

To facilitate the discussion of the results of the previous section in relation to existing experimental data, all observed low frequency Raman lines (up to the strong 1000 cm^{-1} region which corresponds to the totally symmetrical ring vibrations) of the dichlorobenzenes have been collected in Table V, together with the estimated intensities and observed depolarization factors. All

TABLE V. Raman spectra of dichlorobenzenes.

Substance	Raman lines: Swaine and Murray (Ref. 5)	Raman lines: Paulsen (Ref. 2)	Depolarization factors: Sponer and Kirby-Smith (Ref. 1)	Depolarization factors: Paulsen (Ref. 2)	Calc.	Assignment
		219(00)				
$p-C_6H_4Cl_2$		232(00)				
	302(4)	298(65)	0.8	0.73	0.86	β_{2g} (C−Cl def.)
$\varphi=90°$	333(8)	330(134)	0.5	0.21		α_{1g} (ϵ_g^+)
	355(1)				0.86	β_{3g} (C−Cl def.)
		479(00?)				
		509(00?)				
	627(5)	631(36)	0.8	0.78		β_{2g} (ϵ_g^+)
	710(00)					
	748(10*b*)	748(104)	0.2	0.06	0.13	α_{1g} (C−Cl valence)
		794(00)				
		812(1)				
		Dadieu, Pongratz, and Kohlrausch (Ref. 7)				
	178(3)	176(5)	0.9		0.86	α_2
$m-C_6H_4Cl_2$	202(3)	199(8*b*)	0.9		0.86	β_2 or α_1 (α_1 / β_1 or α_2 / α_2 or β_1)
	216(2)	210(8*b*)			0.86	α_1 or β_2
$\varphi=60°$	366(1)	360(3)				
	399(4*b*)	397(8)	0.10			α_1 (ϵ_g^+)
	428(2)	428(4)	0.6			β_1 (ϵ_g^+)
	530(0)					
	666(4)	662(6)	0.25		0.06	α_1 (C−Cl valence)
	154(10)	152(10*b*)	0.8		0.86	β_2
$o-C_6H_4Cl_2$	203(3)	199(4)	0.8		0.86	α_2 (α_1 / β_1 or β_2 / β_2 or β_1)
	239(1*b*)	240(5*b*)	0.8		0.86	α_1
$\varphi=30°$	330(0*b*)	336(3)				
	430(1)	427(5)	0.8			β_1 (ϵ_g^+)
	469(1)	469(5)				
	483(2)	486(6)	0.45			α_1 (ϵ_g^+)
	658(5)	660(8)	0.35		0.06	α_1 (C−Cl valence)
	756(0*b*)	747(1/2)				
	860(1*b*)					

measurements refer to the liquid. Swaine and Murray's[5] measurements of the lines and Sponer and Kirby-Smith's[1] measurements of the depolarization factors are given for all three substances. For para-dichlorobenzene a careful study with improved technique has been published by Paulsen.[2] We have reproduced here all his lines, also the very weak and doubtful ones, together with his depolarization factors which at present represent the most reliable values. The calculated depolarization factors have been taken from Tables II–IV of the preceding section. The assignments are partly the same as in reference 1 and are partly suggested from our theoretical results.

The discussion will be carried through according to types of vibrations as in the previous section.

[5] J. W. Swaine and J. W. Murray, J. Chem. Phys. **1**, 512 (1933).

A. The Chlorine Valence Vibrations

As mentioned in the Introduction (see also Fig. 1(a)), there are two types of valence vibrations in each dichlorobenzene which are distinguished by motions of the two chlorine atoms in phase and out of phase (generally denoted by *A* and *B* in this paper). As pointed out in reference 1, they originate from a linear combination of benzene hydrogen vibrations in the 3000 cm^{-1} region, when replacing two hydrogen by two chlorine atoms, and they belong to the following symmetry classes: α_{1g} (para) from α_{1g}, ϵ_g^+ in benzene, β_{1u} (para) from β_{1u}, ϵ_u^-; α_1 (meta) from α_{1g}, β_{1u}, ϵ_g^+, ϵ_u^-; β_1 (meta) from ϵ_g^+, ϵ_u^-; and α_1 (ortho) from α_{1g}, ϵ_g^+, ϵ_u^-; β_1 (ortho) from β_{1u}, ϵ_g^+, ϵ_u^-. The totally symmetrical vibration has been observed with certainty in all three cases in the lines 748 cm^{-1} (α_{1g} para), 666 cm^{-1} (α_1 meta), and 658 cm^{-1} (α_1 ortho), as has been noticed by many

authors. The intensity estimates of these lines given in Table V agree with our calculations, as far as the ratios between the lines of the various compounds are concerned. The lines in the meta- and ortho-compounds are of about the same intensity while the corresponding line in para-dichlorobenzene is stronger. All three lines are highly polarized. The depolarization factor of α_{1g} (para) should theoretically coincide with $\rho=0.13$ of α_1 in C_6H_5Cl which we have used as fixed value.* Sponer and Kirby-Smith's value is slightly higher and Paulsen's more accurate figure is lower than the one calculated by our rough method so that the agreement can be called satisfactory. The ρ's for the α_1-line in the meta- and ortho-compound should theoretically have the same value, namely about $\frac{1}{2}$ of that for α_{1g} (para). This result is not confirmed experimentally. Although, according to the experimental method, the measured ρ-values represent upper limits and more accurate values will probably be noticeably lower (analogous to Paulsen's $\rho=0.06$ of α_{1g} (para) instead of 0.2), it is improbable that they will be below the ρ-value for the α_{1g} para-frequency. The assumption of cylindrical symmetry for the change of polarizability tensor for one vibrating C—Cl group is conceivably not a good approximation for this vibration. However, the assumption cannot be very wrong and it seems to us that a slight deviation from it does not alter the results in the desired direction so that other effects like non-additivity might be responsible.

An assignment for the unsymmetrical valence vibration which must have a similar frequency value has never been reported with certainty. For the para-compound the vibration β_{1u} is forbidden in the Raman effect but may occur in the infra-red. Lecomte[6] assigns the symmetry β_{1u} to the weak infra-red line 620 cm^{-1}. This interpretation is somewhat doubtful. The fact that this line changes its frequency value somewhat with the substituents is in favor of his assignment; its low value is against it since the unsymmetrical valence vibration is frequently larger than the symmetrical one. Besides the infra-red band just mentioned, Lecomte observed quite a number of bands in the region in which we are interested, namely a strong band at 820 cm^{-1} and weak ones at 650, 680, 720, 750, and 780 cm^{-1}. He interpreted the bands at 820 and 720 cm^{-1} as coming from the non-planar hydrogen vibrations ϵ_u^+ (about 850 cm^{-1}) and α_{2u} (671 cm^{-1} infra-red) in benzene. Both of them lead to β_{2u} vibrations in the para-compound which are allowed in the infra-red. However, this assignment cannot be correct, as one of these two β_{2u} vibrations becomes a non-planar chlorine deformation vibration which must be considerably lower in frequency. We would prefer to assign the weak 620 cm^{-1} in the infra-red to the same vibration as the medium strong Raman line at 631 cm^{-1}, namely to the β_{2g} (coming from the ϵ_g^+ in benzene), which is forbidden in the infra-red but might appear weakly in the liquid on account of intermolecular forces. The strong infra-red line 820 cm^{-1} could be assigned to the valence vibration β_{1u}; this vibration might be accompanied by a sufficiently strong variation of the electric moment so that the corresponding infra-red band could be fairly intense. Paulsen's very faint line at 812 cm^{-1} might be caused by the same vibration which is forbidden in the Raman effect but might appear weakly because of intermolecular forces. The band 720 cm^{-1} (infra-red) and the extremely faint Raman line at 710 cm^{-1} reported by Swaine and Murray might be due to the other β_{2u} vibration as suggested by Lecomte. For his tentative assignment of the weak bands 680 and 750 cm^{-1} to non-planar β_{3g} vibrations (β_{2g} and ϵ_g^- H-vibrations in benzene), forbidden in the infra-red, the same is true as for the β_{2u} vibrations; one of them should become a Cl-bending vibration with smaller frequency. On the whole, it seems premature to offer definite assignments for all weak lines, particularly because selection rules may break down in the liquid and thus may cause forbidden lines to appear in the Raman effect or infra-red respectively.

In the meta- and ortho-compounds the unsymmetrical C—Cl valence vibration has the symmetry β_1 and it is allowed although the corresponding line is much weaker than the α_1. It is completely depolarized in the Raman effect. It should have a frequency value similar to the line

* The intensity of the Cl-vibration α_1 in C_6H_5Cl of frequency value 702 cm^{-1} is slightly weaker than α_{1g} in p-$C_6H_4Cl_2$, although the intensity ratio should theoretically be about $\frac{1}{4}$. However, a comparison is difficult since the intensity estimates were made by different authors.

[6] J. Lecomte, J. de phys. et rad. **9**, 13 (1938).

of the totally symmetrical valence vibration. We see from Table V that no lines of reasonable intensity are available for this interpretation. We already know from Table II that the intensity ratio between the two valence vibrations should be about 6, i.e., the symmetrical valence vibration should occur about 6 times stronger than the unsymmetrical one. This places the expected Raman lines at once among the very weak observed lines. The only lines which occur in the right region are the weak lines at 756 and 860 cm^{-1} in ortho- and possibly 530 cm^{-1} in meta-dichlorobenzene. However, a number of weak and stronger bands have been reported in the infrared. Lecomte gives tentative explanations for all of them. According to him the lines at 756 and 860 cm^{-1}, both of which appear also in the infrared, result from the H-vibrations ϵ_g^- and ϵ_u^+ in benzene, respectively. The interpretation is possibly correct. Lecomte places the β_1 chlorine valence vibration at about 820 cm^{-1} in both the meta- and ortho-compounds. Since this fits in well with our interpretation of the same line in the para-compound, we consider this as probable. From our computations we can only conclude that the unsymmetrical halogen valence vibrations will not show up at all or as very weak Raman lines although they are allowed by selection rules.

B. The Chlorine Deformation Vibrations

The two groups of deformation vibrations of the three dichlorobenzenes (in the molecular plane and out of it) belong to the following symmetry classes: Planar vibrations have the symmetries β_{3u} and β_{2g} for the para- and α_1 and β_1 for the meta- and ortho-compounds. Non-planar vibrations have the symmetries β_{2u} and β_{3g} (para) and β_2 and α_2 (meta and ortho). The two types are denoted with A and B in this paper and are shown in Fig. 1(b) and 1(c). The monochlorobenzene has only one type of chlorine vibration in each group of symmetry, β_1 (planar) and β_2 (non-planar). It is unessential for our discussion from which benzene vibrations these vibrations originate.

As can be seen from Tables III and IV we expect the following results from our computations regarding the appearance of these vibrations: The vibrations β_{3u} and β_{2u} of *p*-dichlorobenzene are forbidden in the Raman effect. For the planar vibrations, the α_1's in *m*- and *o*-dichlorobenzene should appear with the same intensity and should be three times as strong as the β_1 vibrations. The β_{2g} para-vibration should be four times as strong as these β_1-vibrations. For the non-planar vibrations, we expect the α_2 (meta) to be of the same intensity as the β_2 (ortho) and three times as strong as the β_2 (meta) and α_2 (ortho). The β_{3g} para-vibration is, according to calculations, slightly stronger than α_2 (meta).

In our approximation all the deformation vibrations give completely depolarized Raman lines, including the totally symmetrical ones, so that we cannot distinguish between them in this respect. The reason for this is, of course, our neglecting all deformations of the change of polarizability tensors and considering their rotation only. Such a computation leads to a zero trace of the tensor. A better approximation which takes the deformations into account would lead to a small trace value for the totally symmetrical vibrations so that their depolarization factors would be slightly less than 6/7.

We turn now to a comparison of these theoretical results with the observed low frequency Raman lines of the dichlorobenzenes. Para-dichlorobenzene has a strong and highly polarized line at 330 cm^{-1} which has been interpreted as caused by a symmetrical carbon vibration (resulting from ϵ_g^+ in benzene). A line of medium intensity was found at 298 cm^{-1} by all observers. It occurs also in the ultraviolet spectrum and might well correspond to the β_{2g} vibration. A weaker line has been reported at 355 cm^{-1} by Swaine and Murray but not by Paulsen. It represents perhaps the β_{3g} vibration. The extremely faint lines which Paulsen reports at 219,232,479, and 509 cm^{-1} must correspond to vibrations forbidden in the Raman effect. Besides the two Cl-deformation vibrations of symmetry β_{3u} and β_{2u}, carbon frequencies of symmetry β_{2u} and α_{1u} (ϵ_u^+ in benzene) might appear weakly. Furthermore, besides the already mentioned carbon vibration $\beta_{2g}(\epsilon_g^+)$ of probable frequency 631 cm^{-1}, another allowed carbon vibration of symmetry β_{3g} (β_{2g} in benzene) should occur in this region. The infrared band at 540 cm^{-1} of medium intensity reported by Lecomte might correspond to Paulsen's

509 cm^{-1} and could be any β_u vibration since they are allowed in the infra-red.

The correlation is more difficult for the *m*- and *o*-dichlorobenzene since all vibrations are allowed in the Raman effect. Also, the intensity estimates are less accurate than for the *p*-compound. The essential question is, which type of bending vibration belongs to the lowest frequency value. The values lie close enough to make either choice possible. We have pointed out before that the calculated intensity ratios are the only indication which the theory gives us: $\alpha_1 : \beta_1 = 3 : 1$ (*m* and *o*) and $\alpha_2(m) : \beta_2(m) = \alpha_2(m) : \alpha_2(o) = 3 : 1$, where $\alpha_2(m)$ has the same intensity as $\beta_2(o)$. Consulting Table V we may first rule out the frequencies 399 cm^{-1} in $m-C_6H_4Cl_2$ and 483 cm^{-1} in $o-C_6H_4Cl_2$ which belong to the symmetrical carbon vibration α_1 resulting from the 606 ϵ_g^+ vibration in benzene. The non-symmetrical component lies in the same frequency region and is probably the 428 in meta and the 469 or 430 cm^{-1} in ortho. This leaves us with the lines 178(3), 202(3), 216(2), 366(1), 530(0) for $m-C_6H_4Cl_2$ and 154(10), 203(3), 239(1*b*), 330(0*b*), and 430(1) or 469(1) in $o-C_6H_4Cl_2$, from which we have to select the lines belonging to the deformation vibrations. We see immediately that it is impossible to fulfill the theoretical intensity relations. Several different sets give more or less equally good fits depending on whether one uses the intensity estimates by Swaine and Murray[5] or by Dadieu, Pongratz, and Kohlrausch[7] throughout for consistent comparisons. Each set has its own advantages and disadvantages. As long as we do not have more precise intensity measurements, it seems useless to prefer one of these correlation sets. We must try to take recourse to other sources. The ultraviolet absorption spectra of all three dichlorobenzenes[8] have been studied. From the occurrence of the low frequencies in these spectra one can draw certain conclusions about the symmetries of the vibrations concerned. Combining all the information available we would believe that the sets, in which we identify the line 154 cm^{-1} (*o*) with β_2 and 178 (*m*) with α_2 are more probable than sets with 154 (*o*) and 178 (*m*) as α_1. Probable assignments, giving more weight to the more recent measurements, are indicated in the last column of Table V. We refrain from more definite assignments until accurate intensity measurements are available. We hope that then such simple theoretical calculations as presented here may be of help for the interpretation of Raman spectra of these and similar molecules.

After conclusion of our calculations, a paper by Wolkenstein[9] came to our attention which has some general bearing on the question discussed here. Wolkenstein uses the same principle, but in a more elaborate way, of calculating Raman intensity and depolarization factors for simple molecules. He also assumes additivity of the Raman tensors of individual bonds, but he uses a complete system of force constants to determine the actual deformations and displacements in the various normal vibrations. This is, of course, a more correct method, if it can be carried through. It seems, however, that the results obtained are not superior to those of our simplified procedure. Wolkenstein treats the chlorine and bromine vibrations of CH_3Cl, CH_3Br, CH_2Cl_2, and CH_2Br_2. As an illustration for the applicability of our method, we calculated the depolarization factors and relative intensities of the two C—Cl valence vibrations of CH_2Cl_2 using the depolarization factor of the C—Cl valence vibrations of CH_3Cl, and obtained results which are in as good agreement with observations as Wolkenstein's.

In conclusion we should like to express our thanks to Dr. E. Teller who stimulated the theoretical treatment of the problem presented here and to Dr. L. W. Nordheim for helpful discussions. We also wish to acknowledge a grant-in-aid from the Duke University Research Fund for carrying out this research.

[7] A. Dadieu, A. Pongratz, and K. W. F. Kohlrausch, Monatsh. f. Chemie **61**, 426 (1932).
[8] H. Sponer, Rev. Mod. Phys. **14**, 224 (1942).
[9] M. W. Wolkenstein, J. Phys. Acad. Sci. U.S.S.R. **5**, 185 (1941).

Optical Sensitizing of Silver Halides by Dyes

IV. The Optical Sensitizing Properties of Fluorescein Dyes in Relation to Their Spectral Absorption and Constitution*

S. E. SHEPPARD, R. H. LAMBERT, AND R. D. WALKER
Kodak Research Laboratories, Eastman Kodak Company, Rochester, New York

(Received March 6, 1943)

A comparison of increasingly halogenated fluoresceins shows that, with increasing weight of halogen introduced, the principal visible absorption moves steadily to longer waves, as also the first ultraviolet band. At the same time the acid dissociation constants of the phenolic and carboxylic groups tend to become indistinguishable, while the solubilities of the silver compounds decline. The various structures involved in the resonance of the alkaline, hydrogen, and silver compounds are discussed. Measurements of the solubility of silver erythrosinate show this to vary with "aging" and particle size. The solubility of silver erythrosinate on adsorption to silver bromide is apparently lower than that of the pure compound. The adsorption is oriented, an edge-on or end-on monolayer being formed. Although not irreversible, there is a peculiar deviation from the Langmuir isotherm. The optical sensitizing appears to occur by a mechanism similar to that with basic dyes. Initially, transfer of an exciton to the silver halide seems indicated, rather than of an electron.

1. THE ABSORPTION SPECTRA OF FLUORESCEIN DYES IN RELATION TO CONSTITUTION AND SOLUTION

CERTAIN fluorescein dyes, *viz.*, eosin and erythrosin, are the oldest of the practical color sensitizers for silver halide emulsions.[1] Although they have been displaced almost entirely by cyanine (polymethine) dyes, even in their own region of green-yellow (orthochromatic) sensitizing, they exhibit certain characteristics of definite importance for the basic theory of optical sensitizing. Some essentials of the molecular constitution of dyes of this category have been excellently described by G. Schwarz.[2]

The archetype of the substances is *xanthene*

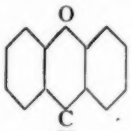

(acid form)

in which, however, the O-atom can be replaced by such bivalents as S, Se, $CH_2 \cdots$. Of more immediate importance is the genotype fluorescein which is (water) soluble by ionization with alkali of the $-OH$ group in the xanthene skeleton, and of the $-COOH$ group in the pendent phenyl nucleus. Also the xanthene skeleton has become an extended resonance system because of the $=O : -O^-$ groups. For all

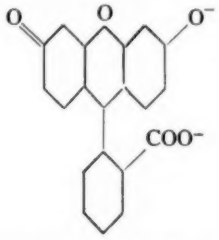

of this, fluorescein is quite incompetent as an optical sensitizer for the silver halides. This property appears, with strengthening of the resonance system, by the introduction of halogen atoms in the xanthene skeleton. Specifically,

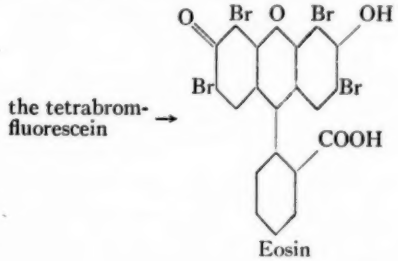

Eosin

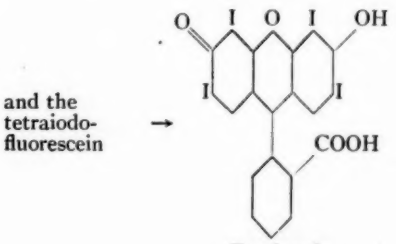

Erythrosin

* Communication No. 914 from the Kodak Research Laboratories.

[1] Cf. S. E. Sheppard, Atti. X. Congr. Internaz. Chim. Rome **1**, 234 (1938).

[2] G. Schwarz, Sci. Ind. Phot. **8**, (2) 97 (1937).

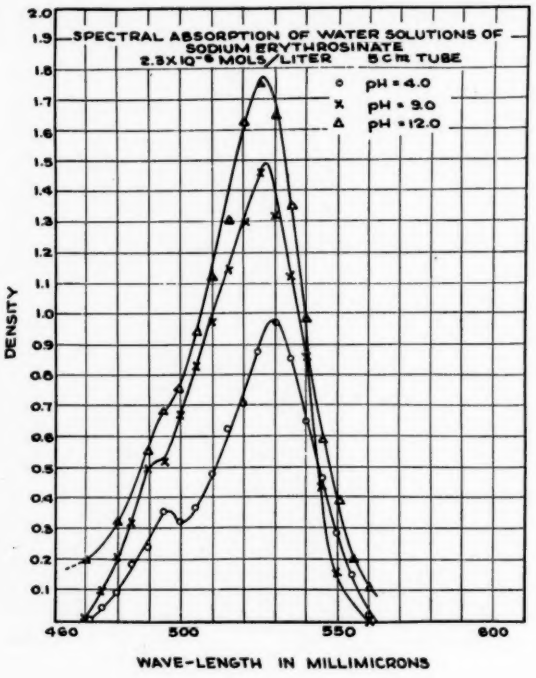

FIG. 1.

are two important sensitizers of this group. It is interesting to observe what occurs by introduction of such electronegative atoms in the xanthene frame. Table I shows that the spectral absorption is only slightly shifted toward the longer waves, and it is evident that the fundamental resonance system is little affected, because the ratio of the wave-lengths (or frequencies) of the visible to the first ultraviolet band is substantially unchanged. This first ultraviolet band probably represents the second excitation level.

Acid Strength

The fluoresceins are acid dyes, and have two potentially acidic groups, *viz.*, the phenolic $-OH$ of the xanthene frame, and the $-COOH$ group in the dependent phenyl nucleus. Attempts were made to determine the corresponding dissociation constants (see Table II) by electrometric titration of the alkaline solutions with acid. Only in the case of fluorescein itself were definite values obtained for the two groups.* In the other cases values were obtained of *one* pK value; this would indicate that in these the pK values were too close to be separated. In fact, the solubilities of the later acids in water are so low that the pK values given may be dictated by the solubilities, and not express the actual dissociation values. The acidification is accompanied by a change in the spectrum, which, in water, is chiefly that occasioned by withdrawal of the fluoresceinate ion from solution. While, for example, the erythrosin acid has (in alcohol) an absorption differing considerably from that of the ion, it can contribute little to the spectrum in water because of its low solubility. Figure 1 shows the nature of the change as the pH is lowered. If the pH is maintained sufficiently high (cf. Fig. 2), erythrosin in alkaline solution —as sodium erythrosinate—follows Beer's law up to fairly high concentrations, when secondary "salt" effects show themselves. These have been studied in the case of eosin (tetrabromfluorescein) by G. Kortum[3] who attributed deviations from Beer's law to the formation of ion aggregates. However, eosin and erythrosin show no such change in spectral distribution (intensification of β-band relative to α-band) with increased concentration as is found with thiazine and cyanine dyes, and which is attributed to dimerization.[4] One of us has indicated elsewhere[4] that it is difficult for the pendant phenyl nucleus to be coplanar with the xanthene frame, and that this would keep the erythrosinate ions from parallel apposition at less than 4–5A interval between them. This distance would probably preclude the spectral anomalies shown in dimerization. The "fluoresceinate" ion can have the two structures shown below:

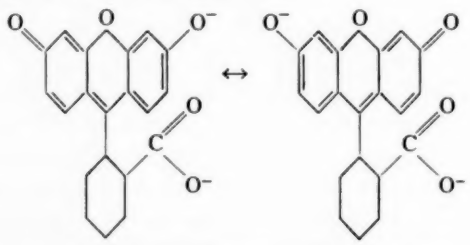

These would have nearly equal energies, and constitute a resonance system accounting for the absorption band in the visible region. The

* Measurements by R. E. Stauffer of these Laboratories.

[3] G. Kortum, Zeits. f. physik. Chemie **34**, 255 (1936).
[4] Cf. S. E. Sheppard, Rev. Mod. Phys. **14**, 305 (1942).

introduction of electronegative groups in the xanthene nucleus would produce secondary electromeric effects[5] somewhat strengthening the resonance but not essentially changing the system. With the addition of protons to form the (undissociated) acids certain complications occur. In the first place, two *tautomeric* forms of the molecule are possible by the addition of a proton to the xanthene nucleus, *viz.*:

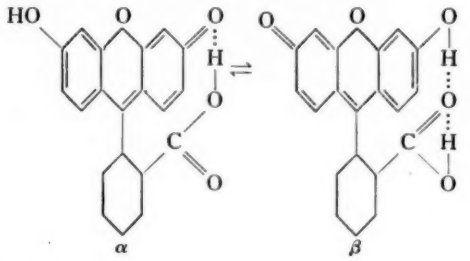

For each of these there can be written a corresponding structure, of higher energy:

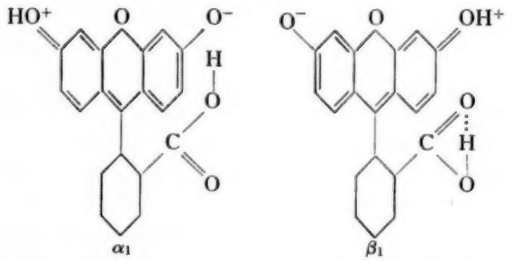

The energy levels of the lower structures α and β will not differ considerably. This will be true also with respect to the higher (dipole) structure α_1 and β_1, so that we should expect an absorption band from the transitions $\alpha \rightarrow \alpha_1$ and $\beta \rightarrow \beta_1$ fairly sharply defined, at least of the same order as that of the erythrosinate ion. However, in respect of the *position* of the band, i.e., the magnitude of $h\nu$ for $\alpha \rightarrow \alpha_1$, $\beta \rightarrow \beta_1$, the energy levels of the $\alpha_1\beta_1$ configurations would appear at first sight to underwrite a band at higher frequency or shorter wave-length than that for the erythrosinate ion, where the two structures are of nearly equal energy. Somewhat surprisingly, the position of the band for the erythrosin acid (prepared by precipitation from aqueous sodium erythrosinate) appears to be in the same spectral region as that of the erythrosinate ion, at least in alcoholic solution, and indeed (in ethanol) at a longer wave-length, 545 mμ, than the ion (sodium erythrosinate) in water at 527 mμ.

TABLE I. Absorption bands of fluoresceins.

Dye	λ_m in mμ	λ_1 (u.v.) in mμ	$R=\lambda_m/\lambda_1$
Fluorescein	491	318	1.55
Dichlorfluorescein	502	334	1.51
Dibromfluorescein	504	328	1.54
Diiodofluorescein	507	335	1.51
Tetrabromfluorescein	518		
Tetraiodofluorescein	526	356	1.48

TABLE II. Dissociation constants.

Compound	pK value
Fluorescein	$pK_1=3-4.0$ $pK_2=5.9$
Dichlorfluorescein	(pK = 4.1)
Tetrachlortetraiodofluorescein	(pK = 4.3)
Tetraiodofluorescein	(pK = 4.55)

[5] A. Sklar, Rev. Mod. Phys. **14**, 232 (1942).

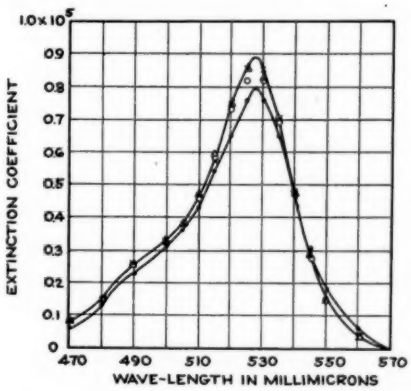

FIG. 2. Spectral absorption of sodium erythrosinate. $\cdot = 10^{-3}$ mole/l; 0.1 mm cell: $\times = 10^{-4}$ mole/l; 1.05 mm cell. $\odot = 10^{-5}$ mole/l; 10 mm cell. $\triangle = 10^{-6}$ mole/l; 100 mm cell. Only limiting curves showing dilution effect from hydrolysis.

A somewhat remarkable result was obtained on comparing the absorption of sodium erythrosinate in ethanol (nearly anhydrous) with erythrosin acid in ethanol saturated with NaOH. It was expected that the absorption curves would be identical, but as may be seen (Fig. 3) the sodium erythrosinate in ethanol gives a maximum at longer wave-length than the erythrosin acid in ethanol saturated with NaOH, and practically identical with that of erythrosin acid in pure ethanol:

Sodium erythrosinate in ethanol	λ_m 544,
Erythrosin acid in ethanol	λ_m 545,
Erythrosin acid in ethanol saturated with NaOH	λ_m 533.

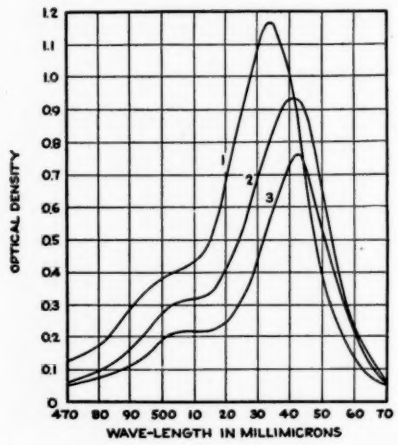

FIG. 3. Spectral absorption of erythrosin. 1 = Erythrosin acid in ethanol saturated with sodium hydroxide, 2 = Sodium erythrosinate in ethanol, 3 = Erythrosin acid in ethanol.

The behavior suggests that sodium erythrosinate in ethanol is converted almost entirely to erythrosin *acid*

$$Na_2^+ E^{=} + 2\ EtOH \rightarrow EH_2 + 2\ EtONa.$$

With increasing addition of water the absorption reverts to that given by the erythrosinate ion in water (see Table III).

The longer wave-length of the erythrosin *acid* in ethanol (also in butanol) than of the erythrosinate *ion* in water is further understandable by the following considerations. A greater influence of polarity of the solvent on the absorption would be expected for the erythrosin *acid* than for the erythrosinate *ion*—on the basis of the structures suggested—because a neutral structure is supposed to be in resonance (to some extent) with a bipolar structure $\alpha \leftrightarrow \alpha_1$, and the latter should be favored by more polar solvents.* On the other hand, the structures of lower energy (α and β) might tend to lose their hydrogen-bonding stability in associating polar solvents, such as alcohols, thereby decreasing the energy difference between α and α_1, β and β_1. The peculiar oscillation of the erythrosin acid absorption with solvent and *p*H may be caused by these factors, affecting both the tautomerism and the mesomerism.

The low solubility of erythrosin acid in water is consistent with a high degree of intermolecular hydrogen-bridging, and the extended absorption spectrum of the solid erythrosin acid (as sublimed film) seems in agreement with this (Cf. Fig. 4). At the same time, in the solid the maximum absorption appears to have shifted to the auxiliary β-band, a "dimerization" effect, which does not appear to occur to any great extent in the *aqueous* solutions of sodium erythrosinate.[4] Perhaps a closer packing side by side of erythrosin structures is allowed in the solid (acid) than is possible in the solution.

According to the structures $\alpha \leftrightarrow \alpha_1$, $\beta \leftrightarrow \beta_1$ suggested for the erythrosin acid, this could take on a third proton, giving the resonating structures

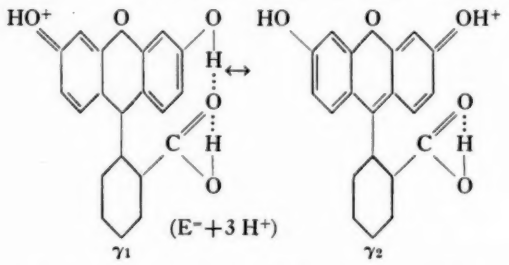

γ_1 and γ_2 shown above. Of these, γ_1 would tend to be somewhat more stable because of the possibility of double hydrogen-bonding as indicated. Thus, there would be *de jure* a crossing over of hydrogen-bonding stabilization from the β to the α side, but not actually, because γ_1 and γ_2 are mesomers, not tautomers. The spectrum of erythrosin acid dissolved in sulfuric acid and alcohol, which is shown in Fig. 5, seems to agree with this. There is apparently a residue of the two-proton addition structure, indicated by the band at 540 mμ, but in addition there appears a diffuse band having its principal maximum at 487 mμ; the addition of a third proton has been markedly hypsochromic.

There are two other points concerning the relations of the erythrosinate *ion* and erythrosin acid. The first is that the alkaline erythrosinates,

TABLE III. Wave-length of maximum absorption of sodium erythrosinate in water-ethanol mixtures.

Percent water	λ_{max} in mμ
0	540–544
10	538
50	533
99	528
100	527

* The alcohols act with merocyanines as super-polar solvents. See reference 4.

e.g., the sodium salt, are somewhat hydrolyzed in water. This results in some deviation from Beer's law on dilution, if not kept sufficiently alkaline, but it is not serious, and can be corrected. The other point is that in the exposition of structures for the acid form we have not taken account of deviations from coplanarity of the $-COOH$ group with the xanthene residue. This is discussed fully in dealing with silver erythrosinate, when it assumes a greater importance.

2. THE ADSORPTION OF FLUORESCEIN DYES TO THE SILVER HALIDES

Very extensive and solid foundations for our understanding of this field were laid by K. Fajans and his collaborators, in work extending over a period of years and from which they developed the important analytical technic of the "adsorption indicators." In general, we shall not need to cite specific publications, since we can refer to two summary articles covering the field, by K. Fajans and T. Erdey-Grúz up to 1931[6] and by K. Fajans up to 1937.[7]

The Initial Mechanism of Adsorption

Various "adsorption rules" are discussed by Fajans: There has been considerable disagreement as to the relative preponderance in the initial adsorption act (a) of simple electrostatic attraction (of negative fluoresceinate ions to positive silver ions); (b) of exchange adsorption or displacement, e.g., of Br^- ions by fluoresceinate; (c) of syncrystallization with the adsorbent; (d) of the "solubility" of the adsorbate. As regards the adsorption of erythrosin to the silver halides, we may say that it is undoubtedly initiated by the electrostatic attraction of (positive) Ag^+ ions for the negative $E^=$ ions of (sodium) erythrosinate. However, the degree of adsorption (e.g., as measured for a specific surface by x/m—moles dye adsorbed per gram adsorbent) is not exclusively and definitively determined by the pAg (or pX) of the solution in the sense that the half-degree of adsorption coincides with the isoelectric point of the silver halide—as indicated in the theoretical curves of Fig. 6. These curves are constructed (a) for silver bromide, for which the equivalence point and the isoelectric points nearly coincide—as they do for silver chloride. The deviations of silver iodide will not be considered at present in this connection. (b) For silver erythrosinate, isoelectric point at pAg 5.12; (c) experimental results.

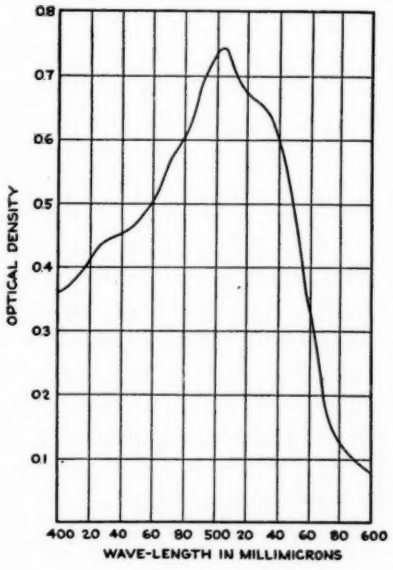

FIG. 4. Spectral absorption of sublimed erythrosin acid.

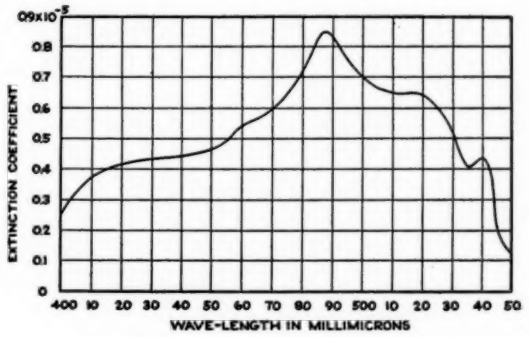

FIG. 5. Spectral absorption of erythrosin acid in ethanol acidified with 1 cc sulfuric acid per 100 cc ethanol.

Qualitatively, Fajans and his collaborators[7] and Sheppard, Lambert, and Keenan[8] have shown that the pAg determines the adsorption in the sense of the electrostatic theory. But it is believed that quantitatively there are deviations from the expected adsorption densities because of (α) the bulk factor of the dye ion. For example,

[6] K. Fajans and T. Erdey-Grúz, Zeits. f. physik. Chemie A158, 97 (1931).

[7] K. Fajans, Die chemische Analyse **33**, 161–222 (1935).

[8] S. E. Sheppard, R. H. Lambert, and R. L. Keenan, J. Phys. Chem. **36**, 174 (1932).

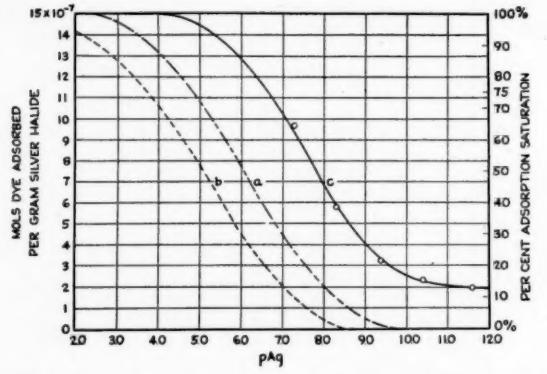

FIG. 6. Effect of pAg on adsorption of erythrosin. (a) Theoretical curve through I_p AgBr, (b) Theoretical curve through I_p Ag_2E, (c) Observed values for erythrosin adsorbed to AgBr.

as discussed later, according to their orientation, a dye ion may be equivalent spatially to from three to ten or more of surface silver or halide ions. (β) Reversibility and solubility. Thus, the electrostatic hypothesis actually assumes a reversible equilibrium in which the equilibrium constant depends upon the solubilities (or solubility products) of the adsorbent and adsorbate—and that these are independent of the fact of adsorption itself. Now the adsorption may not be reversible, because of orientation of the dye ion to present a non-lyophile aspect.[4] Again, the solubility of the adsorbed layer may be less than that of the substance in the mass, also probably the consequence of orientation. It is suspected that this is the case with silver erythrosinate.

The existence of "exchange" adsorption (β) is really tantamount to deviation from equilibrium determined by simple electrostatic attractions and the solubility product. From experiments on the adsorption of radioactive bromide ions, Fajans[7] concluded that bromide ions are replaced by erythrosin, and are found in the solution, indicating that the solubility of "adsorbed" silver erythrosinate became equal or less than that of silver bromide.

Something of the sort seems indicated by our experimental results in certain optical sensitizing experiments. Thus, a silver bromide emulsion at a pAg of 8.3 was found to show quite strong adsorption and optical sensitizing. The aforementioned equilibrium pAg measurements show that bromide ions must have been displaced. It is true that the solubility product of silver erythrosinate seems to vary with the particle size (see later), but the lowest value, i.e., 1×10^{-6} mole/liter, is still much higher than that of silver bromide. At pAg$\sim$8, from the solubility products, silver erythrosinate should not be able to form on silver bromide. The explanation of these anomalies may lie in the structure of solid silver erythrosinate, and in particular, of an adsorbed layer of this.

Syncrystallization, in the sense of full isomorphism, is excluded with dye ions like erythrosin; from their magnitude and structure these ions are incapable of building in to the silver halide lattice.

The solubility factor has required a rather full study of the formation and properties of silver erythrosinate. According to a reversible electrostatic adsorption, at sufficiently low pAg values, the maximum adsorption densities of the fluoresceinates would be in the inverse order to the solubilities of their silver salts. Qualitatively, the data are in agreement with this. Thus, fluorescein and dichlorfluorescein do not show appreciable adsorption or sensitizing. However, in accordance with a reversible adsorption to a monomolecular layer, the magnitude of the adsorption approaches a limit with increasing concentration of erythrosin.

The mathematical expression for this would be Langmuir's equation for reversible formation of a monolayer, e.g., in simplified form:

$$x/m = a = \alpha\beta c_r/(1+\beta c_r),$$

where $x/m=a$ is the adsorption density, c_r is the residual (equilibrium) concentration of the solution, and α and β are constants. Fajans[7] states that the equation holds for erythrosin and eosin on silver iodide over the whole concentration range. Our results with erythrosin on silver bromide are not representable by this simple form of the Langmuir equation, but show approach to accord as high concentrations and adsorption densities are reached.

The degree of fulfillment of the simple Langmuir equation is most readily exhibited by a plot of a against a/c_r, which should be linear. In Fig. 7 may be seen the deviation of our results, and their approach to agreement at high adsorption densities.

An explanation for this may be found on consideration of the physical meaning of Langmuir's equation, as he originally developed it. Writing the equation in the form

$$\eta = \tau\mu/(1+\mu\alpha/V_1),$$

where η = number of molecules (ions) adsorbed per unit area, τ = average life of adsorbed ion (time of relaxation), μ = g moles impinging per cm² per sec., α = fraction adhering per cm², V_1 = rate of evaporation or solution. It will be seen on comparison with the preceding empirical form that a is proportional to η, that c_r is proportional to μ, and that simple relations obtain between the constants. It is now suggested that the discrepancy may be explained by supposing that τ, the average life of an adsorbed ion, is not constant and independent of the degree of adsorption in the case of erythrosin. We may suppose that τ is affected by an "accommodation coefficient," such that as the adsorption density increases, τ decreases, approaching a small constant value. This would be caused by the increasing difficulty of later adsorbed erythrosinate ions to accommodate themselves to the sparser sites, i.e., in attaching silver ions of the silver halide lattice to themselves, and building in to the already formed monolayer of silver erythrosinate. This would give a curve deviating from the simple Langmuir function in the manner shown in Fig. 7.

The determination of the limiting adsorption density (saturation) brings us to the effective area occupied by the dye ion and therewith to consideration of its orientation on adsorption. Because the solubility of silver erythrosinate is lowest for the dyes considered—and indeed (see later) appears to be effectively still lower for the adsorbed state—only this case need be considered. The theoretical limit values for monolayers, first calculated by M. L. Huggins[9] gave the following:

Dye	Vertical End-on	Vertical Edge-on	Flat	Experimental
Erythrosin	6	6	10	5.25 to 6

The area covered by $E^{=}_{vert}$ in projection is about 76A² and, as shown in Fig. 8, for $E^{=}_{flat}$ about 144A². It is evident from these that $E^{=}_{flat}$ must cover >9 Ag^+ ions, while $E^{=}_{vert} \leqq 6$ Ag^+ ions.

The data of O. J. Walker[10] gave $E^{=} \leqq 3$ Ag^+ ions, which is definitely too high for any monolayer. There seems to be no evidence for bimolecular layers with erythrosin; it is probable that his determination of specific surface was considerably in error, since no size-frequency determinations were made of the microcrystals, but only random counts of linear measurements. Our own data for "saturation"—which was not actually reached, because of independent formation of silver erythrosinate—indicate a value of *ca.* 1 $E^{=}$ to 5~6 Ag^+, using an area of 75A² for that occupied by erythrosin adsorbed edge-on or end-on.

To secure more definitive ideas as to the nature of the orientation, it is necessary to consider the constitution of solid silver erythrosinate, because the spectroscopic and sensitizing data show this to be fundamentally identical with erythrosin adsorbed to silver halide.

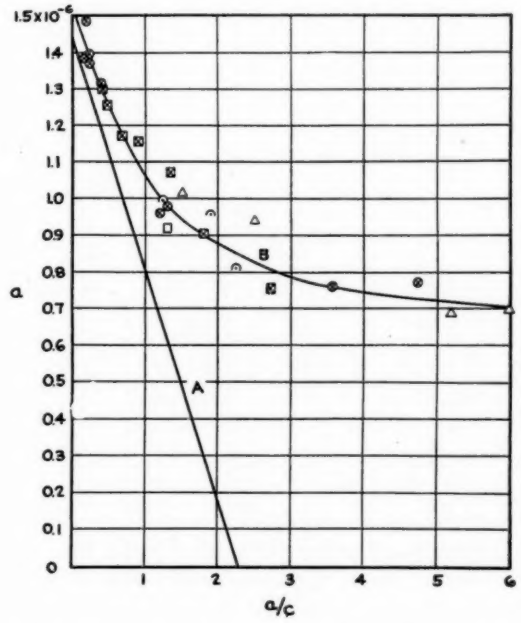

FIG. 7. Adsorption of erythrosin to silver bromide. Curve A = Langmuir equation in linear form, Curve B = Composite curve of experimental data.

[9] Cf. S. E. Sheppard, R. H. Lambert, and R. D. Walker, J. Chem. Phys. **7**, 265 (1939).

[10] O. J. Walker, Diss. München, 1926–27.

3. CONSTITUTION OF ADSORBED LAYER AND OF SILVER ERYTHROSINATE

Upon adsorption of the fluorescein dyes to silver halides, there is a notable deepening of the color, compared with that of the ion in water. This deepening of the color is the basis of Fajan's "adsorption indicator" method and results from a displacement of the absorption band to longer wave-lengths. The displacement from that of the (hydrated) erythrosinate ion is quite considerable, amounting to some 430A, or, as $h\nu_1 - h\nu_2$, about $=0.17$ ev. Not only is that absorption band $h\nu_2$ responsible for the "adsorption indicator" function of eosin and erythrosin, but it is also that effective in optical sensitizing.[11] As we have shown previously, it also corresponds to the absorption spectrum of silver erythrosinate. It has appeared desirable, therefore, to investigate more fully the formation, properties, and structure of silver erythrosinate. This can be formed as a finely divided (microcrystalline) precipitate of quite low solubility by mixing aqueous solutions of silver nitrate and sodium erythrosinate, followed by thorough washing and drying. O. J. Walker[10] found that the wet precipitate tended to disperse colloidally, and only became microcrystalline after evaporating to dryness. He measured the solubility in water (probably near 20°C) by shaking for about 24 hours with water, average value 1.10×10^{-6} mole/liter. Kieser[12] had previously obtained a value of 0.5×10^{-6} and Pohl* 5.8×10^{-6} mole/liter.

The formation and solubility product were investigated by electrometric titration of sodium erythrosinate with silver nitrate, accompanied by spectrophotometric measurements of the solutions and hydrosols. At the outset no special precautions were taken to exclude either light or carbon dioxide. Later, such precautions were observed, although any photolysis appears to be extremely slight or negligible. Since silver carbonate has a solubility of about 3.7×10^{-4} mole/liter (25°C), it was possible that it might affect the titration, but later this appeared improbable.

[11] S. E. Sheppard, R. H. Lambert, and R. D. Walker, J. Chem. Phys. **9**, 96 (1941).
[12] K. Kieser (O. J. Walker, Diss. München, 1926–27).
* Cited by O. J. Walker.

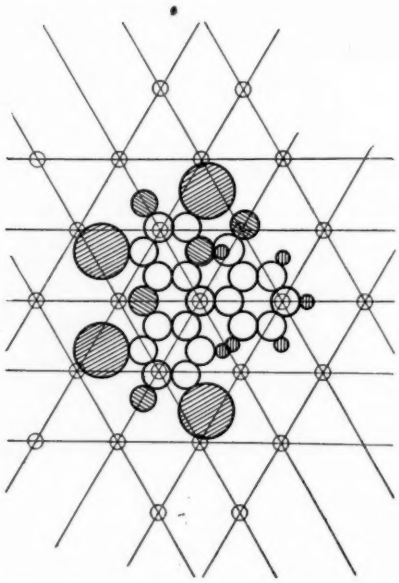

FIG. 8. Erythrosinate ion superimposed flat on a 111 plane of a silver lattice.

Forward and reverse titrations were made of one millimole of one component against number of milliliters of 0.02 N solution of the other. The neutrality point appeared for both curves at two atoms of silver per molecule of sodium erythrosinate, the two curves being nearly symmetrically distributed about this point. This corresponds to the composition Ag_2E; it would follow that the dissociation constants of the two Ag^+ ions must be very nearly equal in magnitude, as was found for the pK values. This neutrality point may be regarded as indicating the silver ion concentration in equilibrium with solid silver erythrosinate, Ag_2E. Assuming *two* silver ions (in solution), i.e.,

$$[Ag_2E]_{(\text{solid})} \rightleftharpoons 2\,Ag^+ + E^=$$

the value $p\text{Ag}=4.30$ should give twice the solubility, or $S=2.5\times10^{-5}$. However, the inflection point was obtained from the differential curves at $p\text{Ag}=5.04$, which, on the above assumptions, gives $S=4.55\times10^{-6}$ mole/liter at 25°C.

Measurement of Solubility of Silver Erythrosinate by Dilution of Suspensions

Suspensions of silver erythrosinate were made, which differed in respect of excess silver or

erythrosinate ion, and the *p*Ag was measured. These suspensions were then successively diluted with water, and *p*Ag was measured at each stage. Curves were plotted for log (Ag_2E) against *p*Ag observed.

Solutions of *p*Ag>5.15 decreased in *p*Ag through a minimum then increased with further dilution. Those of *p*Ag<5.12 increased with similar dilutions to pass through an inflection point at *p*Ag 5.12. This value would imply a solubility of 3.8×10^{-6} mole/liter. Ideally, the point at which all curves intersect should give a value on the dilution axis corresponding, as log *S*, to the solubility. This value appears to be at 4.6–4.8, but is not sufficiently well defined to be considered with confidence.

Spectrophotometry of Suspensions and Solutions

Successive dilutions were made of a suspension 3.24×10^{-4} molar silver erythrosinate (Ag_2E). Absorption curves were measured, and also *p*Ag and *p*H measurements. The data are shown graphically in Fig. 9. During the time of examination, the "solutions" all appeared clear, so that fairly accurate absorption coefficients could be measured. However, on standing 5 to 6 days, all specimens, up to and including that of 4×10^{-6} mole/liter of silver erythrosinate, had precipitated, so that evidently they had not reached equilibrium at the time of measurement.

They show, however, the band at *ca.* 568 mμ of a hydrosol of silver erythrosinate giving place on dilution to the band at 528 mμ of sodium erythrosinate in solution. The data are also given in Table IV to bring out the behavior in respect of *p*Ag. Other similar sets show that the *p*H values are fairly constant.

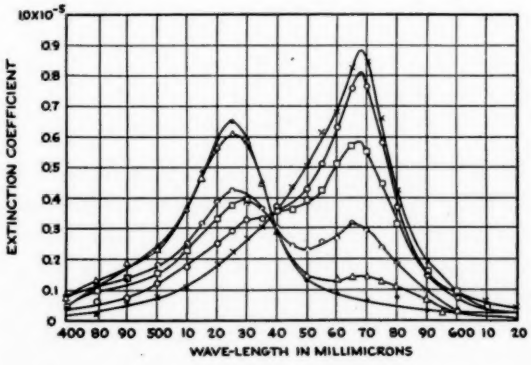

FIG. 9. Effect of *p*Ag on spectral absorption of erythrosin $\times = 3.24\times10^{-4}$ *N* $AgNO_3$, $\odot = 3.24\times10^{-5}$, $\boxdot = 1.62\times10^{-5}$, $\odot = 8.1\times10^{-6}$, $\triangle = 3.24\times10^{-6}$, $\cdot = 1.62\times10^{-7}$, $\sim = 6.5\times10^{-7}$.

Another similar experiment was made with a suspension or hydrosol initially 1.6×10^{-5} mole/liter of silver erythrosinate; the band at 568 mμ became indiscernible between *p*Ag 5.3_3 and *p*Ag 5.5_5. It is evident that silver erythrosinate has a strong tendency to occur and persist in colloidal solution. It is probable that this affects the solubility, making it greater for small particles. This was corroborated by observations on sols freshly prepared, with varying ratio of silver ion and erythrosin, compared with identical systems kept agitated for two weeks by bubbling nitrogen through them, when spectrophotometric measurements were made on the filtrates (Table V). Values obtained directly from the inflection point on titration, *viz.*, $4.5_5\times10^{-6}$ mole/liter, and by dilution of less "aged" sols or precipitates (e.g., $4.5_0\times10^{-6}$, $3.8_0\times10^{-6}$) fall intermediately between these extremes. It appears definite that on "aging" a precipitate with agitation in water, the solubility falls, and may well approach that obtained by O. J. Walker for a well-washed precipitate evaporated to dryness, *viz.*, 1.0×10^{-6} mole/liter. It is possible that the solubility of the adsorbed layer is even lower, at any rate the behavior of erythrosin adsorbed to silver bromide indicates this. Taking the solubility of silver bromide as 0.85×10^{-6} mole/liter, this would not differ greatly from that of O. J. Walker's value for silver erythrosinate. Fajans[7] observed that radioactive bromide ions of— or on —silver bromide could be displaced by erythrosin into the solution, which would point to the solubility of adsorbed silver erythrosinate being $\leqq S_{AgBr}$; and as noted we have observed strong adsorption of erythrosin at *p*Ag 8.3. It is possible that we encounter here an effect of *orientation* of the adsorbed erythrosin. As noted in Section 2, the orientation appears to be either edge-on or end-on, and some consequences of this will be discussed now in connection with the constitution of solid and of adsorbed silver erythrosinate.

We have seen that no separable and soluble ion of the composition AgE^- exists. The band at 567–570 mμ is only produced by [Ag_2E] adsorbed or solid and is an example of what have been termed "cooperative" spectra. The

large displacement from that of sodium erythrosinate was attributed by Fajans to "deformation" of the erythrosinate anion by the large silver cation. If the normal structure of the erythrosin anion is considered (cf. Section 1), it is reasonable to suppose that cations such as Na^+ would tend to place themselves symmetrically with respect to the resonating oxygen atoms:

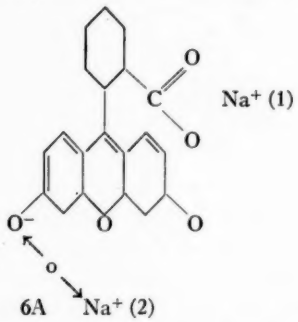

There does not appear to be any reason why substitution of an Ag^+ ion for Na^+ (2) [still less for Na^+ (1)] should change the resonance system so as to displace the absorption by *ca.* 0.2 ev. The Ag^+ (2) ion will be at too considerable distance—of the order of 5 to 6A—to have any considerable polarizing effects on either O-atom. And, otherwise, it appears that the resonance system of the molecule-ion is shielded from any influence of a (coplanar) Ag^+ ion.

Such an arrangement would presume an edge-on orientation of the erythrosin ion relative to an octahedral plane of the silver halide. We must examine the possibilities of an end-on orientation, since the adsorption-density data do not allow any preference. Another "coplanar" arrangement for a silver erythrosinate molecule now suggests itself based on a possible assimilation to erythrosin acid (cf. Section 1). Consider the following graphic formula:

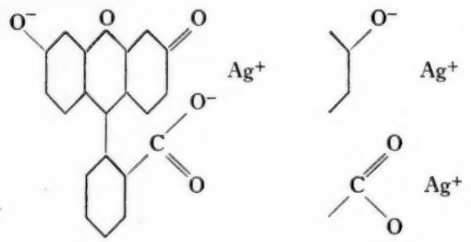

If we conceive that the "phenolic" Ag^+ ion might—as with the H-band of erythrosin acid—extend the resonance system through the "carboxyl" Ag^+ ion—both silver ions being now "chelated" between oxygen atoms in resonance circuits—we have a feasible explanation of the displacement to longer waves of the absorption—by extension of the resonance system as in the case of erythrosin acid. Such a constitution agrees also with the factual equality of the two Ag^+ ions in respect of dissociation, as shown by the titration curves. It must be admitted, however, that the completely coplanar configuration as shown above is very unlikely, if not impossible. The carbon atom of the carboxyl group could hardly come as near to the 4 $-CH$, while with normal 125-degree bond angles the upper O-atom of the carboxyl could not be in the position assigned, but must, through rotation of the dependent phenyl, be in a plane considerably above or below that of the xanthene residue. This would be enforced the more because of the bulk of the iodine atom ($-C-I=2.1A$) attached to the $-C$ atom adjacent to the "phenolic" group. These conditions obtain, however, in much the same degree for erythrosin acid. Rotation of the secondary or accessory resonance system—involving the carboxyl group and the two Ag^+ ions—to a plane making an angle of *ca.* 50 degrees with the xanthene residue might allow the distance between the two Ag^+ ions to be increased to a reasonable extent. In a coplanar configuration they would be separated

TABLE IV. Displacement of absorption.

Concentration moles/liter of Ag^+	Log concentration calculated	pAg	ϵ_{527}	ϵ_{547}
1.59×10^{-5}	−4.80	4.80	0.264×10^5	0.563×10^5
1.18×10^{-5}	−4.927	5.04	0.268	0.543
8.0×10^{-6}	−5.10	5.09	0.323	0.438
6.3×10^{-6}	−5.20	5.16	0.337	0.337
3.16×10^{-6}	−5.50	5.33	0.463	0.115
1.59×10^{-6}	−5.80	5.55	0.474	0.060
8.0×10^{-7}	−6.10	5.78	0.485	0.050

TABLE V. Solubility.

Age	Solubility product	Solubility
Immediate	7.6×10^{-16}	5.74×10^{-6} mole/liter
Two weeks with agitation	0.7×10^{-16}	2.5×10^{-6} mole/liter

only—between centers—by some 2.2A, which is too close. And this also disagrees with their probable interval as dictated by the silver halide lattice for adsorbed erythrosin.

Admitting this non-coplanarity of the auxiliary resonance system (involving the two Ag^+ ions) there still remains another difficulty. With this end-on orientation of the silver erythrosin molecule, the principal transition moment must still be in the xanthene residue—as between the two quasi-phenolate oxygen atoms. But this means—for erythrosin adsorbed to silver halide crystals—that the vibrations absorbed must be polarized in directions more or less perpendicular to the plane of the crystal, that is, parallel to the axis of propagation of the light. This would imply *longitudinal* vibrations in the light ray, which are not admitted as possible.

Whether the part of the suggested resonance system which would be in the plane of the crystal —and, therefore, transverse to the Poynting vector of the incident light ray—could be regarded as taking care of this we cannot say. The configuration offers one possibility, we will consider another. It has been noted that the absorption band of silver erythrosinate is that of the solid phase. This suggests the possibility that in the solid, where a new order of aggregation occurs, the absorption involves this order, and, therefore, more than one molecule. A possible structure of aggregation is shown in Fig. 10. In this arrangement, two erythrosinate ions are supposed in parallel, and separated some 5–6A, both because of the non-coplanarity of the dependent phenyl with its carboxylate group, and also because of the diameters of the $-CI$ groups. The new unit, composed then of two erythrosinate and two silver ions* is capable of resonance between two configurations of identical energy, in which the interstitial silver ions act as alternate acceptors and donors of electrons. The absorption act would involve no permanent reduction of silver ion to metallic silver, which corresponds with observations on the optical stability of silver erythrosinate and with the observations on the photolysis of silver bromide sensitized with erythrosin. In the presence of halogen acceptor, the dye is not destroyed by the absorption of light which produces metallic silver from the silver halide.[11]

As a linear mesophase, this structure could be continued indefinitely,[4] and such a structure may occur in the monolayers of adsorbed erythrosin. But it could hardly be present in solid crystals of silver erythrosinate, because it involves a ratio of "phenolic" silver ions to erythrosinate ions varying continuously with the length of the chain, and this is not compatible with the stoichiometric composition of the crystal. However, this does not affect the identity of the absorptions of the adsorbed layer and of the solid crystal, because the new absorption band is attributed solely, as regards wave-length, to the structure of the optical doublet or dimer. It is evident that this conception of the structure of the absorber for the new band of silver erythrosinate, and of erythrosin adsorbed to silver halides, must remain in the realm of hypothesis until accurate x-ray diffraction data for the crystal, and electron diffraction data for the adsorbed layer, become available.

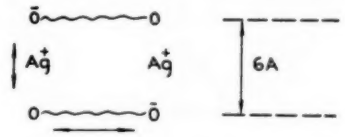

FIG. 10. Suggested structure of adsorbed silver erythrosinate.

Another possibility for a participation of silver atom ions in a new resonance system was suggested by M. L. Huggins, in view of the arrangement shown in Fig. 11. This also involves charge transfer through silver atom ions located, however, between O^--atoms of two successively aligned erythrosinate ions. A possible objection to this is that it might involve dependence of the absorption maximum upon the number of molecules aligned, i.e., on the length of the chain, and there is no evidence of this.

The arrangement previously discussed has evident affinities with one suggested for the mesophase of cyanine dyes[4] and would refer light absorption and optical sensitizing by eosin and erythrosin and the like to similar polymolecular structures. It is possible that the photochemical (quantum) yields in the photolysis of sensitized silver halides may give another datum deciding

* Neglecting the silver ions attached to carboxyls.

this point. Should similarity of sensitizing by the fluorescein type of dye with that by the mesophases of cyanine dyes be established, we could discriminate three main classes of optical sensitizing by dyes:

(1) By neutral (non-ionized) dye molecules: e.g., by merocyanines, by 1,4-diaminoanthraquinone (and other anthraquinone derivatives) by porphyrins, as chlorophyll, phthalocyanine, haemin.
(2) By (basic) cyanine dye molecules, and by thiazines.
(3) By the mesophases of cyanine dyes, and by the fluorescein dyes.

Such a reduction to specific types of absorbing units could give a greater precision to our notions of the mechanism of optical sensitizing of the silver halides.

4. OPTICAL STABILITY AND SENSITIZING

Previous experiments were made with dry silver erythrosinate powder, and with silver erythrosinate suspended in gelatin (de-ashed and thoroughly freed from halide ions), washed with distilled water, and dried. Only with very intense illumination (restricted as well as possible with filters to its own absorption band) could any reduction to silver be observed, and this was attributed to the heating effect. Normal up to large exposures, with the gelatin-emulsified silver erythrosinate, failed to give any latent image developable with regular chemical developers, although prefixation physical development was possible.

In connection with the experiments on the constitution of silver erythrosinate (Section 3), some decomposition of silver erythrosinate suspension was observed on long exposure to daylight, darkening and separation of silver occurring. These were only over periods of time—days—entirely incommensurate with normal photochemical sensitivities, and occurred only with excess of silver ion. It would be attributed to optical sensitizing of adsorbed silver salts.

Silver erythrosinate must be regarded as properly an optically stable absorber in the sense that it is *per se* able to dissipate the energy taken up by absorption of light as heat or fluorescence. This is in good accord with its behavior as an optical sensitizer for the silver halides. It was with erythrosin-sensitized gelatino-silver bromide emulsion that Lescynski[13] first made the basically important observation that one sensitizing dye molecule could produce in photolysis a large number of silver atoms.[14]

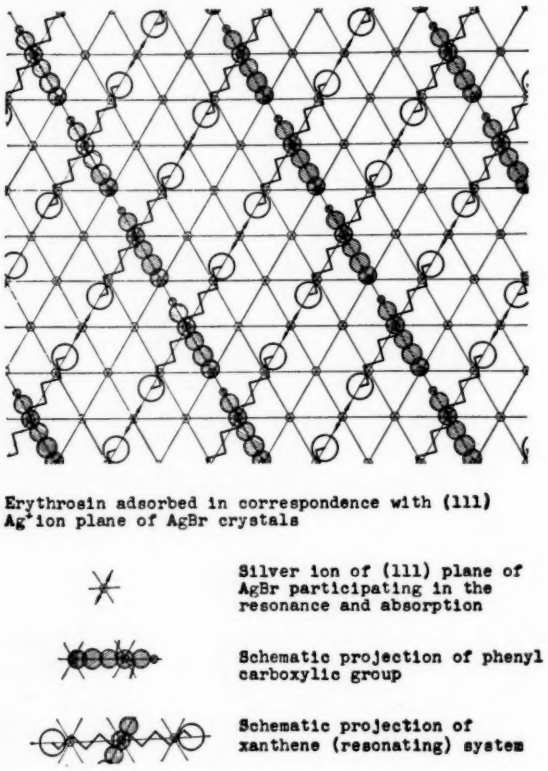
Erythrosin adsorbed in correspondence with (111) Ag⁺ ion plane of AgBr crystals
Silver ion of (111) plane of AgBr participating in the resonance and absorption
Schematic projection of phenyl carboxylic group
Schematic projection of xanthene (resonating) system

FIG. 11.

The persistence of the sensitizing molecule (for silver halide sensitized with silver erythrosinate) only occurs in the presence of a halogen acceptor. For these reasons we consider that the mechanism of optical sensitizing and regeneration of (silver) erythrosinate proposed by S. J. and G. L. Natanson[15] is inacceptable. They suggest the obviously tempting view that a negative charge (electron) is irreversibly transferred from the erythrosin part of the complex to the silver ion part. The chemically changed erythrosin* is supposed to recover an electron,

[13] W. Lescynski, Zeits. f. wiss. Phot. **24**, 275 (1926).
[14] Cf. S. E. Sheppard, R. H. Lambert, and R. D. Walker, J. Chem. Phys. **7**, 426 (1939).
[15] S. J. and G. L. Natanson, J. Phys. Chem. U.S.S.R. **14**, 278, No. 2 (1940).
* The primary products of such electron loss would be free radicals.

either from bromide ion, or from "reducers" such as sodium nitrite—or from gelatin, which is hardly a reducer (of silver ions)—but is a bromine acceptor.

Bromine, as gas, is rather slowly taken up by erythrosin, with some change of color. There appears to be a twofold reaction, in that an irreversible attack on the erythrosin occurs, but also some substitution of bromine for iodine in the molecule.

In the presence of water, bromine forms hypobromous acid, according to the reaction $Br_2+H_2O \rightleftharpoons HOBr+HBr$ (which is shifted to the right by hydroxyl ions, the reaction analyzing to $Br_2+2\ OH^- \rightleftharpoons OBr^-+Br^-+H_2O$). A protective acceptor, in optical sensitizing, should, therefore, not only be a halogen acceptor, but a reducer reacting with the hypobromite, which can destroy the dye. There is evidence[16] that gelatin, in the ordinary photolysis (not optically sensitized) of gelatino-silver bromide, reacts effectively with hypobromite to protect the latent image silver.

It is probable that the erythrosin molecule can act as a temporary or intermediary bromine acceptor by bromine adsorption to the iodine atoms of the molecule. Given sufficient time, and nothing to react with the bromine, there is displacement of iodine by bromine—the cuckoo in the sparrow's nest!—but this probably plays no part in optical sensitizing of silver halides. In this case the bromine may be temporarily held, only to react later with water and with halogen acceptors proper.

The balance of the evidence is that, in optical sensitizing, the silver erythrosin complex on silver halide is not chemically affected by the light it absorbs, but transfers energy as an exciton to the silver halide, with which it is combined by "adsorption." In this primary phase of sensitizing, the mechanism does not differ from that with basic cyanine dyes. These are positive ions, and the emission of an electron, as suggested by various authors[17] is much more difficult to conceive.

[16] Cf. S. E. Sheppard and C. L. Graham, J. Frank. Inst. **230**, 619 (1940).

[17] Cf. G. Kornfeld, J. Phys. Chem. **42**, 795 (1938); also S. E. Sheppard, Atti. X. Congr. Internaz. Chim. Rome **1**, 234 (1938).

Discussion of Energetics

The adsorption of erythrosin may be conceived as implying the participation of silver ions of the silver halide lattice in the resonance system of the erythrosinate. In this sense we may regard the resonance of the new system as equivalent to $AgE \leftrightarrow Ag^+ E^-$ (disregarding for the moment the second electrovalence). We do not know the energies of the two states—of the homopolar and dipolar configurations, respectively, but it is legitimate to suppose that of the dipolar form is higher. Absorption of a quantum of light results in an excited state of $Ag^+ E^-$. In the solid unadsorbed silver erythrosinate, the exciton is dissipated[18] by degeneration to thermoelastic vibrations with relapse of the system into the AgE condition. When adsorbed to a silver halide, the exciton—polarized in the plane of the excited absorber—is transferred to the silver halide lattice and results in the neutralization of a particular pair of $Ag^+ X^-$ ions—probably in an "altered" region of the lattice. It is reasonable to assume that there is such a region immediately contiguous to the adsorbed dye. The dye has been stabilized by adsorption (as shown by its lower solubility than that of the "pure" precipitated material, *vide infra*) at the expense of the stability of the silver halide lattice. The synpolarization of an affected $Ag^+ Br^-$ pair has been considered previously.[11] Where a "sensitizing nucleus" exists, the exciton, handed on by the resonance $Ag^+ X^- \leftrightarrow AgX$, finally provokes an irreversible separation to $Br+(Ag^+ +\theta)$—giving a quasi-free, or photoelectron. There appears nothing in this inconsistent with photoconductance, nor with the Gurney-Mott theory of photolysis. Such a scheme might assume equivalent migrations of electrons *and* positrons (negative potential holes), but effectively it is convenient to assume that positive charges remain attached and move with silver atoms as silver ions—while the electrons move relatively freely.

The question as to whether adsorbed dye and silver halide lattice have preponderantly electrons in common—as part of a new complex—or, have excitons in common, will be discussed later.

[18] J. Franck and E. Teller, J. Chem. Phys. **6**, 861 (1938).

The Transmission Coefficient in the Theory of Absolute Reaction Rates†

HUGH M. HULBURT* AND J. O. HIRSCHFELDER**
Department of Chemistry, University of Wisconsin, Madison, Wisconsin

(Received October 23, 1943)

The activated complex theory of reaction rates is discussed critically. The transmission coefficients for a number of idealized energy surfaces have been computed quantum mechanically. It appears that curvature of the reaction path may introduce activation energy in addition to that caused by constriction and elevation of the energy valley. Except at low temperatures, this additional activation energy is almost negligible. However, it may contribute to the separation of isotopes, where small differences in activation energy are important. For systems in thermal equilibrium at room temperatures and above, the average quantum mechanical transmission coefficient is found to differ insignificantly from that calculated by classical mechanics.

IN the theory of rate processes proposed by Eyring,[1] the process is represented in configuration space by the classical motion of a particle on a surface, the height of which is proportional at each point of the surface to the potential energy of the reacting system whose configuration is represented by that point. Such surfaces have the general shape of long, narrow valleys joined by "passes" through the regions of high energy. The strip of configuration space lying across the deepest of such saddles connecting two regions which correspond to the initial and final states of the system is called the activated state. Whenever the motion of the representative particle on this surface can be treated classically, the rate at which systems move from initial to final configurations is given by

$$k=\frac{P_t\,\bar{v}}{P_i\,\delta}\kappa \qquad (1)$$

and is a direct consequence of statistical mechanics. In this equation, P_i and P_t are the probabilities of the initial and of the activated states, respectively; δ is the width of the transition state; $\bar{v}$, the average velocity of the particles moving across δ; and κ is the transmission coefficient, the fraction of particles successful in completing the journey across the activated state.

Two basic assumptions are involved in this theory:

1. Equilibrium is maintained between the initial and activated states throughout the course of the reaction.

2. Classical mechanics is adequate to describe the motion of the reacting systems over the entire course of the reaction. Both of these assumptions have been the subject of much discussion.[2] The first assumption is justified *a posteriori* by the success of the theory, but it has been difficult to see in advance the conditions under which it holds. As to the second assumption, it is evident that classical mechanics is not applicable to all the motions of the system as it passes through the activated state. A strictly rigorous treatment involves replacing the classical particle by a quantum mechanical wave-packet subject to the potential field represented by the energy surface. It seems probable at first that there should be significant deviations from the behavior predicted classically because of reflection, diffraction, and tunnelling of the quantum mechanical wave packet. Such effects might be expected at barriers, constrictions, and bends in the valley in the energy surface in which the reaction path runs. However, it has previously been shown[2] that for most chemical reactions, the reflection at barriers and constrictions in a straight path is not great enough to modify the classical predictions significantly, except possibly for reactions at very low temperatures, or for reactions involving iso-

† Taken in part from a thesis submitted by H. M. Hulburt to the Graduate School of the University of Wisconsin in partial fulfillment of the requirements for the degree of Doctor of Philosophy.

* Present address: Frick Chemical Laboratory, Princeton University, Princeton, New Jersey.

** Present address: Geophysical Laboratory, Washington, D. C.

[1] H. Eyring, J. Chem. Phys. **3**, 107 (1935).

[2] (a) Summarized in Fowler and Guggenheim, *Statistical Thermodynamics* (Cambridge, 1939) p. 517; (b) J. O. Hirschfelder and E. Wigner, J. Chem. Phys. **7**, 616 (1939).

tope separations. The effect of curvature in the reaction path has not been considered previously and will be discussed here.

QUANTUM EFFECTS

The magnitude of the quantum effects in the motion of the system in curved reaction paths can be estimated by calculating the transmission coefficient for a wave packet traveling in the given potential field. The mathematical difficulty of treating the problem restricts our attention to a few highly idealized potential surfaces, from which, however, we can discern the general features of the more complicated cases. So as to present the results as vividly as possible, most of the detailed mathematical development will be given in the appendix, to which reference may be had for the justification of the qualitative arguments presented here.

It is important to distinguish between two types of reaction at a barrier or bend in the energy surface. If the electronic quantum numbers of the reacting complex do not change throughout the course of the reaction, the reaction is called quasi-static. The activated state method is restricted to such reactions. There are then two possible types of reaction:

1. that in which the vibrational quantum numbers of the reacting complex remain unchanged during the course of the reaction;
2. that in which vibrational transitions take place.

The conditions for good transmission are very different in the two cases.

A. No Vibrational Transitions

We shall consider first the case in which vibrational quantum numbers are unchanged by reflection or transmission at an irregularity in the energy surface. When this is the case, the Eyring formulation of the theory of absolute reaction rates is easily justified for incident systems with sufficiently great translational energy. Mathematically, the condition for no change in quantum number is realized when the potential energy is such that the Schrödinger equation is separable in coordinates parallel and perpendicular to the reaction path. The wave functions for vibrational and translational motions are then completely independent. Such separability is never complete in any actual case, but it will be approximately attainable if the vibrations perpendicular to the reaction path are rapid compared with the motion parallel to the reaction path. The system then executes many vibrations before moving into a region where the vibration frequencies are much different. Hirschfelder and Wigner[2] have shown that, for a straight reaction path, if the change of vibration frequency, ν, along the reaction path, s, satisfies the condition

$$v\frac{d\nu}{ds}\ll\nu^2$$

where v is the translational velocity of the system, there will be no change in the vibrational quantum number.

The transmission coefficient for the case of no change in vibrational quantum number where the reaction path is curved may be studied by considering the potential energy surface to be the channel between two confocal hyperbolae. Such a channel becomes narrower as the system approaches the greatest curvature and then widens out. The potential energy is zero inside the channel and infinite outside. For this case the Schrödinger equation is separable and can be solved explicitly for the whole region. Hence, there is no possibility for a change in vibrational quantum number in rounding the bend. By introducing the elliptic coordinates, μ and ϕ such that

$$\begin{aligned} x&=R\cosh\mu\sin\phi,\\ y&=R\sinh\mu\cos\phi \end{aligned}\qquad(2)$$

we can transform the Schrödinger equation without potential energy into the form:

$$\frac{\partial^2\psi}{\partial\mu^2}+\frac{\partial^2\psi}{\partial\phi^2}-\frac{8\pi^2m}{h^2}\frac{R^2E}{2}(\cosh 2\mu+\cos 2\phi)\psi=0. \qquad (3)$$

The lines $\phi=\phi_0$ are the hyperbolae $(x^2/\sin^2\phi_0)-(y^2/\cos^2\phi_0)=R^2$ whose asymptotes have the slope $dy/dx=\cot\phi_0$. Hence, ϕ_0 is the angle between the asymptote and the y axis. Let the angle between the asymptotes of the two boundary hyperbolae be Δ. Then the boundary condition is that $\psi=0$ on the two hyperbolae whose asymptotes are defined by $\phi=\phi_0+\Delta/2$ and $\phi=\phi_0-\Delta/2$. Equation (3) is separable into the

two one-dimensional equations,

$$\frac{d^2U}{d\mu^2}+\frac{8\pi^2m}{h^2}R^2\left(\frac{E}{2}\cosh 2\mu-\lambda\right)U=0, \quad (4)$$

$$\frac{d^2\Phi}{d\phi^2}+\frac{8\pi^2m}{h^2}R^2\left(\frac{E}{2}\cos 2\phi+\lambda\right)\Phi=0, \quad (5)$$

where $\psi(\mu,\phi)=U(\mu)\cdot\Phi(\phi)$. Here λ is the separation constant whose value is to be determined by the boundary conditions.

Since the lines $\mu=\mu_0$ are ellipses, $(x^2/\cosh^2\mu_0)+(y^2/\sinh^2\mu_0)=R^2$ orthogonal and confocal to the hyperbolae, $\phi=\phi_0$, the factor Φ gives the variation of the wave function ψ as the system moves along any ellipse, i.e., across the channel, while the factor U gives the variation as the system move along the channel, parallel to ϕ_0. It is evident that for a given value of μ and ϕ there are two values of x and y, *viz.*, $(x, +y)$ and $(x, -y)$. Hence, the wave function is symmetrical about the x axis. Its derivatives, however, are different for y positive and for y negative. In order to make them equal at $y=0$, it is necessary to add a component representing a reflected wave to that for the incident wave in the region $y>0$. Thus it is necessary to introduce a reflected wave to satisfy the continuity condition on the wave-function. Physically, however, this reflection is most easily interpreted in terms of a virtual barrier, which can be demonstrated without actually solving the equations (4) and (5) completely.

We solve Eq. (5) for Φ, determining the allowed values of λ. When these values of λ are substituted into Eq. (4) it becomes a one-dimensional equation for the translational motion of the system through the channel. For the lower energies and for values of Δ less than 30°, the equation (5) may be solved using an asymptotic expansion for Φ and the allowed values of λ can be developed in a power series in Δ. (See Appendix). We then find for λ, up to terms in Δ^2,

$$\lambda=\frac{h^2n^2}{8mR^2\Delta^2}-\frac{E}{2}\cos 2\phi_0-\Delta^2b(E) \quad (6)$$

where $b(E)$ is a function of the energy given in the Appendix.

Putting Eq. (6) into Eq. (4) gives a one-dimensional equation for the motion of the particle parallel to any hyperbola. This equation is not in the usual Schrödinger form, however. It can be put into the usual form by the substitutions,

$$s=R\int_0^{\mu}(\sinh^2\mu+\cos^2\phi_0)^{\frac{1}{2}}d\mu, \quad (7)$$

$$\chi=U(\sinh^2\mu+\cos^2\phi_0)^{\frac{1}{4}}. \quad (8)$$

Equation (4) then becomes

$$\frac{d^2\chi}{ds^2}+\frac{8\pi^2m}{h^2}(E-V_\phi-V_\lambda)\chi=0 \quad (9)$$

where

$$V_\phi=\frac{h^2}{8\pi^2mR^2}\times\left[\frac{\frac{3}{2}-\frac{1}{2}\cosh^2 2\mu+2\cosh 2\mu\cos 2\phi_0}{(\cosh 2\mu+\cos 2\phi_0)^3}\right] \quad (10)$$

and

$$V_\lambda=\left[\frac{h^2n^2}{8mR^2\Delta^2}-\Delta^2b(E)\right]\Big/\tfrac{1}{2}(\cosh 2\mu+\cos 2\phi_0). \quad (11)$$

The coordinate s, defined by Eq. (7), is the distance from the narrowest point of the channel measured along the hyperbola asymptotic to $x=y\tan\phi_0$. Thus, s is the coordinate of the reaction path lying midway between the walls of the channel. The substitution of Eq. (8) is made so as to bring the equation into the form (9), where χ now describes the translational motion of a particle in one dimension, moving in a virtual potential field which is the sum of V_λ and V_ϕ.

The separation of the virtual potential into two terms is justified by comparing V_λ with the energy, E_{vib}, of the nth vibrational state for a particle confined to a box of width d given by

$$d^2=4R^2(\sinh^2\mu+\cos^2\phi_0)\sin^2\frac{\Delta}{2}. \quad (12)$$

We see then that V_λ is just equal to E_{vib} for values of Δ small enough that terms in Δ^2 and higher powers can be neglected. Thus we find that though the height of the energy surface is perfectly constant, a system moving in a curved path encounters an effective potential energy barrier, which is partially due to the change in

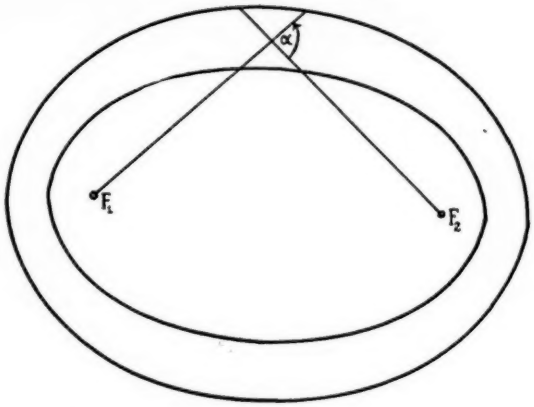

FIG. 1. Elliptic channel. Classically, all particles whose trajectories lie in the angle α are transmitted.

zero-point energy of vibration as the channel narrows (V_λ) and partially due to the curvature of the path (V_ϕ).

If the channel is elliptic rather than hyperbolic, the zero-point energy due to the constriction in the channel has a close connection with the classical conditions for transmission. In the classical case, the particle is reflected in straight lines from the walls of the channel. At any point, its trajectory is specified by the ratio of vibrational to translational energy, for we have $(E_{\text{vib}}/E_{\text{trans}})^{\frac{1}{2}} = v_\perp/v_{||} = \tan\theta$ where $v_\perp$ is the component of velocity perpendicular to the reaction path and $v_{||}$ is the component parallel to the reaction path. Inspection of Fig. 1 shows that all those particles whose trajectories are such that $\theta < \alpha$ are transmitted, whereas those whose trajectories have $\theta > \alpha$ are reflected. Here there is, even in the classical case, a minimum translational energy for each vibrational level which must be exceeded before transmission occurs. An exact calculation shows that precisely the same critical value of $(E_{\text{vib}}/E_{\text{trans}})^{\frac{1}{2}}$ is predicted in the quantum mechanical case. Thus, for an elliptic path, there is a classical analogy for the virtual zero-point energy due to a constriction in the channel.

The term V_ϕ merits closer consideration. It is to be noticed that at large distances, V_ϕ corresponds to an attractive potential, but nearer the narrow part it becomes a repulsion. This peculiar behavior may be interpreted with the help of three analogies from other branches of physics. The presence of V_ϕ arises mathematically from the "straightening out" of the hyperbolic reaction path when the transformations (7) and (8) were made. This result is analogous to the relativistic description of gravitational forces in terms of geodesics in curved space. Thus a particle experiencing gravitational force when its motion is described in euclidean space appears to move on a geodesic in no field in the curved relativistic space.

A second analogy can be made with the classical motion of a particle constrained to move in a prescribed region. Such a particle experiences an apparent "force" due to its constrained motion. For example, the motion of a particle moving in an elliptical orbit may be described by supposing an effective central force, directed toward one focus of the ellipse. Similarly, here, the walls of the channel restrict the particle to move in a definite region of space. This gives rise to a virtual field of force acting on the particle.

A third analogy makes use of the wave properties of matter. A parallel beam of light is made to converge to a point by reflecting it in a parabolic mirror. Similarly, any curved mirror tends to focus waves, concentrating intensity at some point, and diminishing it at others. This focusing effect bears a strong resemblance to the quantum effect observed here, for in regions of low virtual potential energy, one should expect to encounter a concentration of systems, due to the Maxwell-Boltzmann distribution. The presence of curved reflecting walls appears to focus the systems to some extent, concentrating them in the regions where V_ϕ is low and diminishing their numbers where V_ϕ is high.

The magnitude of V_ϕ is indicated by the size of the factor $h^2/8\pi^2 mR^2$, where R is the focal length of the hyperbola $\phi = \phi_0$. For the reaction $H+H_2$, $R \sim 1$A and $M = \frac{2}{3}$ in atomic weight units. For $D+D_2$, R is unchanged, but $M = \frac{4}{3}$. Hence V_ϕ will be only one-half as great. The maximum value of V_ϕ is 0.288 kcal./mole for the $H+H_2$ reaction where $\phi_0 = 60°$. This difference is of the right order of magnitude to account for the discrepancy between the observed and calculated rates.[3]

We may conclude that when there is no change in vibrational quantum number, we should expect fast particles to be transmitted more rapidly

[3] L. Farkas and E. Wigner, Trans. Faraday Soc. **32**, 1 (1936).

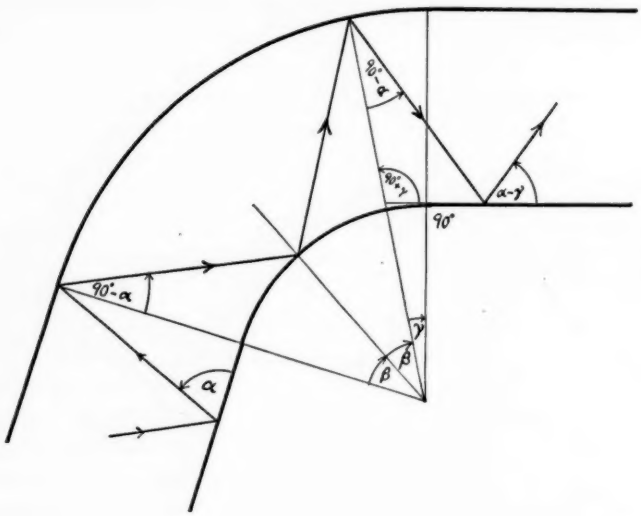

FIG. 2. Classical transmission in a circular channel. The vibrational component of momentum is changed on passing around the bend.

than slow ones. This would appear experimentally as an additional activation energy beyond that necessary to surmount the energy barrier were the reaction path straight.

B. Reflection with Change in Vibrational Quantum Number

Thus far we have investigated only cases where the system is transmitted or reflected without change in vibrational quantum number. For a general potential surface this will be the case, as we saw, if the zero-point energy is a sufficiently slowly varying function of the reaction coordinate. This means that the actual slope of the reaction path must not be too great at any point, and that its curvature must be small. Even then, the curvature of the path will introduce an additional activation energy for the reaction. In general, when these conditions are not satisfied, there will be reflection of the incident system and simultaneous change of its vibrational quantum number. Exceptional conditions prevail when the potential energy surface is such as to render the Schrödinger equation separable everywhere. Then there can be no change in quantum number, but reflection will still occur, due to the increase of zero-point energy as the channel is constricted and to the curvature of the reaction path. These conditions are very special, however. They serve to illustrate the constriction effect and the focusing effect free from the complications of a change in quantum number. In any actual surface, we should not expect to find the Schrödinger equation separable in this fashion, and, even for very smooth reaction paths, the probability of a change in vibrational quantum number is quite high. This is demonstrated by the consideration of an energy surface consisting of three sections. A straight channel is joined to one of circular reaction path, which in turn is joined to a straight section. Consider a particle rebounding elastically from the walls of the channel. Let the last collision in the straight section be just where the channel begins to bend. (See Fig. 2.) The total bend of the channel is $2\beta+\gamma$ and the last collision within the bend is γ before the end of the bend. The path makes an angle $\alpha-\gamma$ with the exit channel, whereas it made an angle γ with the

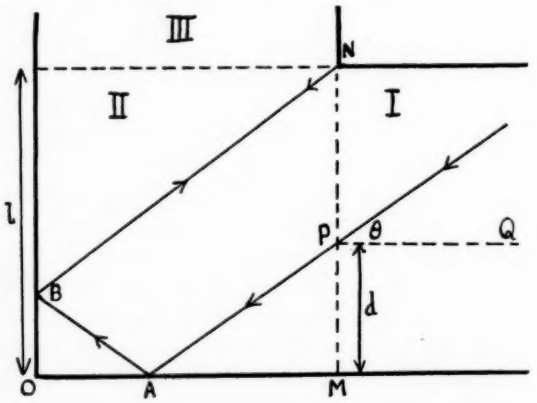

FIG. 3. Rectangular corner. Classically, all particles whose trajectories lie below and parallel to PA are transmitted.

channel before the bend. This shows that the vibrational energy has changed in rounding the bend.

Thus, in any actual case, there will be reflection and transmission of the incident systems into states having a different vibrational quantum number from the initial one. The exact treatment of this problem is more difficult than when no shift in vibrational state is possible, because the ease with which the shift occurs depends quite markedly on the peculiarities of the particular energy surface in question. Often the possibility of shifting into a new vibrational state makes the net reflection much lower than if this possibility were absent. In other cases, there is in reality very little reflection, but that which does occur is almost completely reflection into a different vibrational state.

Some of the main features of these phenomena are illustrated by the behavior of systems traveling down a straight channel having a sharp right angled turn. The potential energy is zero within the channel and infinite outside it. (Fig. 3). Classically, the reaction is represented by a stream of particles rebounding from the walls of the channel. The component of momentum perpendicular to the reaction path is proportional to the square root of the vibrational energy of the system. The component parallel to the reaction path is the translational momentum of the system. Hence, the trajectories of all systems having the same vibrational energy make the same angle with the reaction path. Let

$$\tan\theta = p_y/p_x = [E_{\text{vib}}/(E-E_{\text{vib}})]^{\frac{1}{2}} \qquad (13)$$

where $E=(p_x^2/2m)+(p_y^2/2m)$ is the total energy of the system. Then, referring to Fig. 3, consider a beam of particles crossing MN, each of which has the same total energy and the same distribution of energy between vibration and translation, analogous to a single pure quantum vibrational state. The value of θ is then fixed by Eq. (13), but the position of the point P may be chosen at random so long as it lies on MN. However, inspection of the geometry of the figure shows that all those particles whose trajectories are parallel to PA but lie above it will be reflected, while those whose trajectories are parallel to PA and lying below it will be transmitted. Calling the critical distance MP, d, and the width of the channel l, we have, from the figure,

$$\frac{l-d}{2\sin\theta}=\frac{l}{\cos\theta}-\frac{d}{\sin\theta},$$
$$\tan\theta=\tfrac{1}{2}+d/2l, \qquad (14)$$
$$d_{\text{crit}}=l(2\tan\theta-1).$$

The fraction of particles incident on MN whose trajectories are parallel to PA and which are

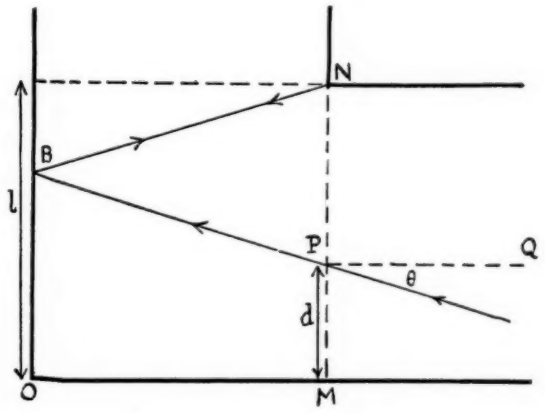

FIG. 4. Rectangular corner. Classically, all particles whose trajectories are parallel to and above PB are transmitted.

transmitted is:

$$T_1=2\tan\theta-1. \qquad (15)$$

From Eq. (14) it is apparent that when $\theta=\tan^{-1}\frac{1}{2}$, no particles are transmitted. For smaller values of θ, inspection of the figure shows that there is also no transmission. When $\theta=\tan^{-1}1$, all the particles are transmitted and for larger values of θ, this is still the case. However, though the total energy and its distribution in vibrational and translational parts determines the value of $\tan\theta$, it does not determine its sign. We must now consider the transmission of particles whose trajectories are perpendicular to the line PA in Fig. 3. Figure 4 demonstrates the critical conditions for this case. All those particles whose trajectories are parallel to PB and lie above it are transmitted; those lying below are reflected. The fraction transmitted is given by

$$T_2=\frac{l-d_{\text{crit}}}{l}=1-\frac{d}{l}=2\tan\theta. \qquad (16)$$

Again, for $\tan\theta=\frac{1}{2}$, $T_2=1$. The over-all fraction transmitted will be the average of T_1 and T_2 since

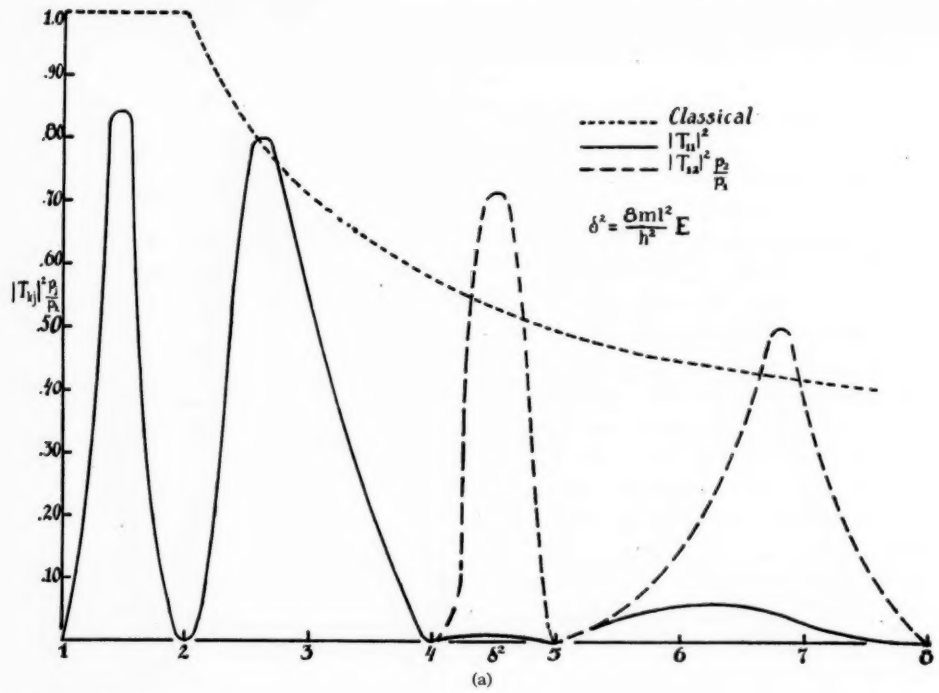

(a)

the probability that θ is positive is equal to that that it is negative. For the various ranges of θ we have the following results:

$$T=\tfrac{1}{2}(T_1+T_2)=\tan\theta \quad 0<\tan\theta<1$$
$$T=1 \qquad\qquad\qquad\qquad \tan\theta>1. \tag{17}$$

If all vibrational energies are equally probable, the *average classical* transmission coefficient is obtained by integrating Eq. (17) with respect to E_{vib}/E, using Eq. (13). The result of this graphical integration is $T=0.785$. For comparison with the quantum mechanical treatment, the classical transmission coefficient was calculated by Eq. (17) for the case where E is restricted to integral multiples of E_{vib}. The total transmission coefficient for an incident particle with one quantum of vibrational energy is shown in Fig. 5. The partial transmission coefficients for transmission into states having one and two quanta of vibrational energy were computed from Eq. (17) and added to give the plotted curve. As in the quantum case to be discussed, the slower moving incident particles have a greater chance of transmission than those having a greater proportion of translational energy, but there are no periodic critical values for which transmission is zero.

The quantum mechanical picture replaces the

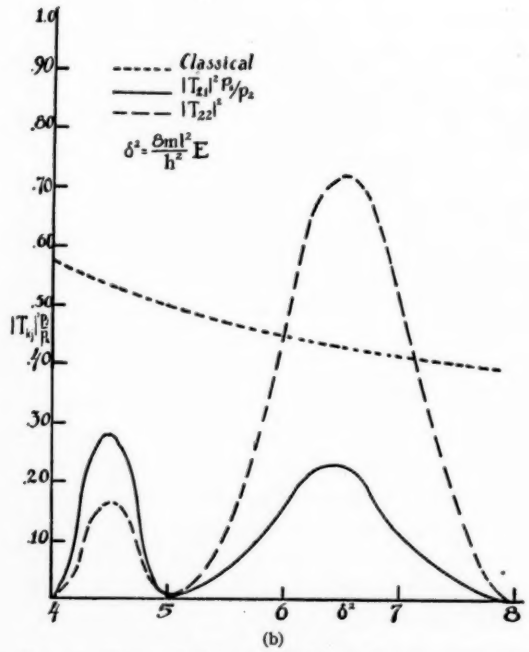

(b)

FIG. 5. Transmission coefficients for a rectangular corner, as a function of the total energy of the system. (a) Particles incident in the lowest vibrational state. (b) Particles incident in the first excited vibrational state.

particles by a train of plane waves whose intensity at any point is proportional to the density of matter there. The boundary conditions of Fig.

3 cannot be satisfied by any single solution to the Schrödinger equation. However, in each of regions marked *I*, *II*, and *III* such solutions can be found. The actual state of the assembly* will be represented in each region by a superposition of the possible stationary states, each with the appropriate amplitude. In region *I*, it is represented by a term corresponding to an incoming plane wave in a particular quantum state, to which must be added an infinite train of waves traveling in the opposite direction in every possible quantum state, including those for which the momentum is imaginary. Such a function is

$$\Psi_k^{\mathrm{I}} = \sin\frac{\pi k}{l}y \exp\left[-\frac{ip_k}{\hbar}x\right] + \sum_{j=1}^{\infty} R_{kj} \sin\frac{\pi j}{l}y \exp\left[\frac{ip_j}{\hbar}x\right] \quad (18)$$

where l is the width of the channel; p_k, the translational momentum of a system in the kth vibrational state; and R_{kj} is the arbitrary amplitude. Those terms in Eq. (18) for which p_j is imaginary correspond, not to traveling waves, but to waves with exponential damping, such as are usually found in diffraction effects. The R_{kj} are determined by the condition that the wave functions and their first derivatives must be equal at each boundary of every two regions. Thus, we have found it necessary to introduce reflection into vibrational states differing from the initial one in order to satisfy the boundary conditions.

The mathematical details are carried through in the Appendix. Here we shall point out some general results of this type of calculation. The most striking result is the oscillation of the transmission coefficient as the energy of the particle increases. Whenever the translational energy of the incident system becomes equal to the vibrational energy of some permissible quantum state for the transmitted particle, we find a zero in the transmission coefficient. Thus, when the system is incident in the first quantum state, its vibrational energy is one unit. If the exit channel is the same width as the incident channel, the vibrational states possible in it have energies of 1, 4, 9, $\cdots n^2$ units. Hence a system incident in the first vibrational state will be totally reflected when its total energy is 1, 2, 4, 5, 8 $\cdots$ (i.e., for any energy $E=j^2+n^2$, where n and j are integers). Figure 5 shows the transmission coefficients for a particle having one quantum of vibrational energy initially. The classical transmission calculated in the manner previously described is also shown.

Reference to Fig. 5 shows that slowly moving particles are most easily transmitted, i.e., those whose total energy is only slightly greater than one unit. However, whenever there is a possibility that the transmitted system has translational energy, the transmission coefficient is markedly increased. Thus, at total energy equal to 4.5 units, the coefficient for transmission into the lowest quantum state (no change in vibrational energy) is very small, in agreement with our previous observations for this case. However, the chance that the transmitted system be in the second quantum state is very much greater, so that the total transmission coefficient is greater than for systems of slightly less energy, e.g., 3.5 units. We conclude that the presence of the corner tends to enhance the probability for a change in vibrational quantum number.

The case may be considered as analogous to the transmission of electromagnetic waves. Waves of very short wave-length (or fast particles) travel in straight lines with negligible diffraction effects at irregularities in the reflecting surface. They are highly reflected at a sharp bend. Waves of longer wave-lengths (slow particles), such as radio waves, are easily diffracted and can be transmitted around sharp corners with much less difficulty. Wave motion of all kinds, electromagnetic, elastic, acoustic, exhibits these same general transmission properties.

It would be of interest to know to what degree the rapidity of oscillation of the transmission coefficient is affected by the asymmetry of the potential surface, the removal of the discontinuous edges, and the averaging due to thermal equilibrium. For the case of a right-angled channel, calculations in the appendix show that narrowing the incident channel increases the rapidity of oscillation, whereas narrowing the exit channel has relatively little effect. This is evident from the fact that total reflection with no change in quan-

* The term "assembly" here denotes the collection of representative points which correspond to the equilibrium distribution of the reacting atoms in all their possible configurations.

tum number occurs whenever the total energy of the system is given by

$$\epsilon^2=\frac{j^2}{l^2}+\frac{n^2}{w^2} \tag{19}$$

where l is the width of the incident channel, w is the width of the exit channel, and j is the vibrational quantum number of the incident system. The number n takes all integral values. For fixed j, diminishing l gives more closely spaced values of ϵ than does diminishing w.

It is also possible to calculate the transmission coefficient for an energy surface like the preceding, but in which the channels meet at an angle θ given by $l=w \sin \theta$ where l and w are the widths of the entrance and exit channels, respectively. In this case, the transmission coefficient shows a fluctuation with θ similar to that calculated for changes in energy. Thus, we should expect optimum angles, differing for different energies, for which the transmission would be greater than at other angles.

Some physical processes may be described as taking place on a potential energy surface on which there is total reflection due to the absence of a pass through the high energy region. When sound is absorbed in gases, the net result is the transfer of the translational energy of the sound wave to the internal vibrations of the colliding molecules. Such a process may be pictured on an energy surface having a blind alley. (Fig 6.) The reflection coefficient then becomes a measure of the ease with which the interconversion of energy takes place. By considering a straight channel of the type described above, one end of which is closed, we find that there can be no interconversion of energy if the channel is perfectly symmetrical. However, if it is L-shaped, or T-shaped with side arms of unequal length, there will be an interchange. Again we find resonant energies for which there is no interchange just as in the cases of total reflection from an open-end channel.

It is evident that the quantitative details of the behavior of the transmission coefficient are very sensitive to minor variations in the potential energy surface. Until these surfaces are known in detail and with greater accuracy than that now available we can hope to calculate no exact values

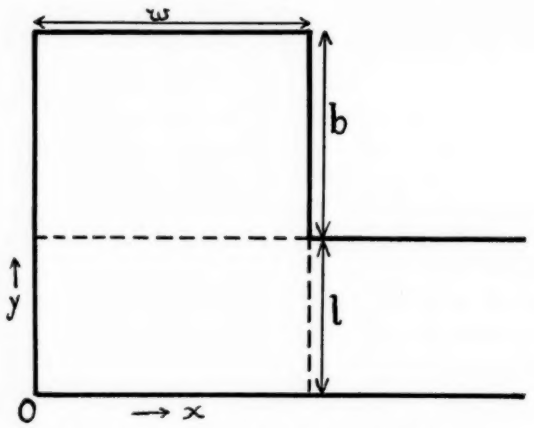

FIG. 6. Closed channel giving total reflection.

for the actual transmission coefficients. However, the results obtained in the simple examples discussed above indicate the general nature of the problem. Reflection on the potential energy surface can arise from three sources: energy humps, constrictions, and bends in the reaction path. If the hump or constriction is sufficiently gradual and the reaction path is straight, we have seen that there will be little tendency for the system to change its vibrational state in traversing the activated state. However, if the reaction path is curved, there is a strong probability that the system will undergo a change in vibrational state, whether it be transmitted or reflected. The magnitude of this probability is an oscillating function of the total energy of the system and of the angle through which the reaction path turns. It is more probable that the reflected or transmitted system be moving slowly than that it be moving rapidly, since the curvature induces transitions to the highest available vibrational state. The actual chance of reflection likewise oscillates with the energy of the system and the angle through which the reaction path turns. Slow systems are more easily transmitted than fast systems, in contrast to the case in which there is no change in quantum number, where the opposite is true. However, the more highly energetic systems are less easily transmitted than those whose total energy is low. The analogy with the optical properties of radiation is very marked and carries over even into the classical treatment, which is analogous to geometrical, or ray, optics.

Any observable experimental result due to

these effects can be expected only if it appears that the peaks in the transmission coefficient are not obscured by the statistical averaging due to the fact that in practice we do not deal with systems all having exactly the same energy and exactly the same vibrational energy, but with an equilibrium mixture. Since in any actual chemical reaction, the initial systems are distributed statistically with respect to their total energies, the experimental transmission coefficient will be an average of those calculated here. Since the energy fluctuates in a range kT about the mean, we can estimate the average transmission coefficient by taking it to be

$$\bar{\kappa} = \int_{E_0-kT}^{E_0+kT} \kappa(E) e^{-E/RT} dE \Big/ \int_{E_0-kT}^{E_0+kT} e^{-E/RT} dE \quad (20)$$

where E_0 is the mean energy, κ, the exact transmission coefficient and $\bar{\kappa}$ the experimentally observable coefficient. If $\kappa(E)$ oscillates rapidly as E is increased by kT, the average value $\bar{\kappa}$ will be a smooth function of E and the maxima and minima would not be observed. In Fig. 5, the energy unit is $h^2/8ml^2$. For ortho-para hydrogen conversion, $l = 0.2 \times 10^{-8}$ cm. Taking m to be the mass of the hydrogen atom, the energy unit is 11.5 kcal./mole, or at 300°K, 19.2 kT. For heavier systems and for wider channels, the energy unit is smaller. The peaks appear to be from $\frac{1}{2}$ to 1 energy unit in width, so that averaging over a width $2kT$ would not smooth them out in this case. Removing the discontinuity and introducing asymmetries into the energy surface will narrow the peaks, so that it would be unsafe to predict any noticeable experimental deviations from a transmission coefficient of unity except in the case of very light atoms, or of isotope separations. For these latter reactions, the relative masses of the isotopes fix the separation of the two systems on the energy scale of Fig. 5, so that whereas when one has an energy such that there is little transmission, its isotopic counterpart with the same energy may automatically fall on a region of Fig. 5 where there is good transmission. Moreover, the angle of the bend is a function of the masses of the atoms in the system, and will be different for different isotopes. Since the transmission coefficient is also a function of the angle, there is a second possibility that different isotopes have different transmission coefficients. These effects will be larger for light atoms, and indeed, for these the observed separation factors are much larger than for heavier isotopes. However, any quantitative prediction of these effects must await more exact knowledge of the energy surfaces involved.

These results have several experimental implications. In the first place, they indicate the impossibility of measuring exactly the height of the energy surface by an experimental determination of the activation energy of a reaction. The virtual barriers due to curvature and constriction of the reaction path amount to at least 0.5 kcal. and prevent any closer estimate being made from experimental data. Since all calculated energy surfaces depend so far upon knowing the height at some point from experimental data, it is evident that they will not be useful in general for predicting the second-order effects dealt with here. Although energy surfaces sufficiently accurate to enable the prediction of relative rates of reaction of isotopes are not known, enough factors have been shown to enter so that one might expect unusual separations in some cases. A third point of interest for experiment is that it seems likely that most newly-formed molecules exist in excited vibrational states. This ought to be observable if a spectroscope were placed in the direction of flow of a streaming system of the reacting molecules. This would amount to observation of infra-red chemi-luminescence, and should give information on many hitherto unobserved higher vibrational levels.

SUMMARY

The quantum effects have been investigated for a number of idealized energy surfaces and have been found to be small except possibly for reactions involving isotope separation and for reactions at low temperatures. It is shown to be highly improbable that no vibrational transitions occur during the course of a reaction, but that they must take place after the system has passed through the activated state. Consequently, the Eyring formulation of the activated state method is justified in its essential features.

The authors take pleasure in acknowledging with gratitude the assistance of Professor Eugene Wigner in several parts of this work. They also

wish to thank Professor C. B. Tompkins for a helpful discussion and the Wisconsin Alumni Research Foundation for financial support while this work was in progress.

APPENDIX

Hyperbolic Channel

Here we shall write down explicit expressions for the wave functions and the separation constant used in calculating the virtual potential barrier to which reflection may be ascribed.

For our purposes it will be sufficiently accurate to take for the solution of the Φ equation:[4]

$$\Phi=(1-k^2\sin^2\phi)^{-\frac{1}{4}} \times\sin\left[A\frac{2\pi R}{k\Lambda}\int_0^{\phi}(1-k^2\sin^2\phi)^{\frac{1}{2}}d\phi+B\right] \quad (21)$$

where

$$A=\left\{1+\frac{\Lambda^2k^2}{4\pi^2R^2}\left[\frac{k\cos 2\phi}{2(1-k^2\sin^2\phi_0)^2}+\frac{5k^2\sin^2 2\phi_0}{16(1-k^2\sin^2\phi_0)^3}\right]\right\}^{\frac{1}{2}}, \quad (22)$$

$$k=(E/[\lambda+E/2])^{\frac{1}{2}}; \quad \Lambda=h/(2mE)^{\frac{1}{2}}. \quad (23)$$

Here Λ is the de Broglie wave-length of the incident waves. This form for the solution of the Mathieu equation is similar to the asymptotic solutions of Langer and Jeffrey. It differs from their solutions in having the constant A different from unity. By using the value of A given above, it may be easily verified by direct substitution in the differential equation that Φ satisfies equation

$$\frac{d^2\Phi}{d\phi^2}+\frac{8\pi^2mR^2}{h^2}\left(\frac{E}{2}\cos 2\phi+\lambda\right)\Phi=0 \quad (24)$$

exactly at the point $\phi=\phi_0$. The error in the solution may be estimated by the difference between the value of A calculated for the two extreme values of ϕ and that for the midpoint between the two hyperbolae. As the energy of the system becomes progressively larger, Eq. (21) becomes a better solution. For small values of the energy, we must confine our discussion to the small values of Δ.

[4] (a) R. E. Langer, Trans. Am. Math. Soc. **36**, 637 (1934); (b) Harold Jeffreys, Proc. London Math. Soc. **23**, 437 (1923); (c) M. J. O. Strutt, Ergeb. d. Math. u. Grenzgebiete **1**, No. 3 (Berlin, 1932); (d) Whittaker and Watson, *Modern Analysis* (Cambridge Press, 1927), fourth edition, Chapter XIX.

The boundary conditions that $\Phi=0$ when $\phi=\phi-(\frac{1}{2})\Delta$ and when $\phi=\phi+(\frac{1}{2})\Delta$ are satisfied if:

$$n_1\pi=A\frac{2\pi R}{k\Lambda}\int_0^{\phi_0+\Delta/2}(1-k^2\sin^2\phi)^{\frac{1}{2}}d\phi+B,$$

$$n_2\pi=A\frac{2\pi R}{k\Lambda}\int_0^{\phi_0-\Delta/2}(1-k^2\sin^2\phi)^{\frac{1}{2}}d\phi+B, \quad (25)$$

$$n\pi=n_1\pi-n_2\pi=A\frac{2\pi R}{k\Lambda}\int_{\phi_0-\Delta/2}^{\phi_0+\Delta/2}\times(1-k^2\sin^2\phi)^{\frac{1}{2}}d\phi.$$

For a given value of the energy, this equation determines the allowed values of k (and hence the separation constant, λ). The integrals occurring in Eq. (25) are the incomplete elliptic integrals of the second kind and they have been tabulated many places in the literature.[5] It is therefore a relatively simple matter to compute the right-hand side of this equation as a function of k and to find those values for which the equation is true.

If the angle between the asymptotes of the limiting hyperbolae is small, i.e., of the order of 30° when the energy is not too large, it is possible to expand the integrals in powers of Δ:

$$\int_{\phi_0-\Delta/2}^{\phi_0+\Delta/2}(1-k^2\sin^2\phi)^{\frac{1}{2}}d\phi=\Delta(1-k^2\sin^2\phi)^{\frac{1}{2}} \times\left\{1-\frac{\Delta^2}{24}\left(\frac{k^2\cos 2\phi_0}{1-k^2\sin^2\phi_0}+\frac{k^4\sin^2 2\phi_0}{4(1-k^2\sin^2\phi_0)^2}\right)\right\}. \quad (26)$$

Then it is easy to obtain the first two terms in the expansion of λ in powers of Δ:

$$\lambda=\frac{h^2n^2}{8mR^2\Delta^2}-\frac{E}{2}\cos 2\phi_0-\Delta^2b(E) \quad (27)$$

where

$$b(E)=\frac{n^2h^2}{8mR^2\Delta^2}\left[\frac{1}{12}-\frac{E\cos 2\phi_0}{12n^2E_0}-\frac{E^2\sin^2 2\phi_0}{48n^4E_0^2}+\frac{\cos^2\phi_0}{2n^2\pi^2}\left\{\cos 2\phi_0\left(\frac{E}{n^2E_0}\right)^{\frac{1}{2}}\times\left(1+\frac{E}{n^2E_0}\sin^2\phi_0\right)^{\frac{1}{2}}+\frac{5}{8}\left(\frac{E}{n^2E_0}\right)\times\sin^2 2\phi_0\left(1+\frac{E}{n^2E_0}\sin^2\phi_0\right)\right\}\right], \quad (28)$$

$$E_0=h^2/8mR^2\Delta^2\cos^2\phi_0. \quad (29)$$

[5] For example, see Jahnke und Emde, *Funktionentafeln* (Teubner, Leipzig, 1933), second edition, p. 124.

Rectangular Corner

Consider next a potential energy surface which consists of a rectangular trough of width l, within which the potential is zero, and outside of which it is infinite. We shall study the effect of a sharp right-angled corner in the trough. This potential surface may be divided into three regions, as shown in Fig. 3, region I being the incident channel, region II, the square corner region, and region III, the exit channel.

The Schrödinger equation is easily solved in regions I and II (Fig. 3). If we consider an incident plane wave which represents the reacting system in its initial state in region I, superposing the reflected waves gives us the wave function:

$$\Psi_k^{\mathrm{I}}=\sum_j (R_{kj}\exp[ip_jx/\hbar] +\exp[-ip_jx/\hbar]\delta_{kj})\sin\frac{\pi j}{l}y. \quad (30)$$

In region III, there are only outgoing waves of the form

$$\Psi_k^{\mathrm{III}}=\sum_j T_{kj}\exp[ip_jy/\hbar]\sin\frac{\pi j}{l}x. \quad (31)$$

In region II there will be standing waves of the form

$$\Psi_k^{\mathrm{II}}=\sum_j A_{kj}\sin\frac{p_j}{\hbar}x\sin\frac{\pi j}{l}y +B_{kj}\sin\frac{\pi j}{l}x\sin\frac{p_j}{\hbar}y. \quad (32)$$

The total energy of the incident wave is $E=(p_j^2/2m)+(j^2h^2/8ml^2)$. The first term is the translational energy, and the second is the vibrational energy for the jth vibrational state. At each junction of two regions, the corresponding wave functions and their derivatives must be equal. After making the expansions

$$\sin\frac{p_j}{\hbar}x=\sum_n C_{jn}\sin\frac{\pi n}{l}x$$

and

$$\sin\frac{p_j}{\hbar}y=\sum_n C_{jn}\sin\frac{\pi n}{l}y$$

application of these boundary conditions gives us the following expressions:

$$R_{kj}=\left(A_{kj}\sin\frac{p_j}{\hbar}l-\exp[-ip_jl/\hbar]\delta_{kj}\right) \times\exp[-ip_jl/\hbar], \quad (33)$$

$$\frac{ip_j}{\hbar}(R_{kj}\exp[ip_jl/\hbar]-\exp[-ip_jl/\hbar]\delta_{kj}) =A_{kj}\frac{p_j}{\hbar}\cos\frac{p_j}{\hbar}l+\sum_n(-1)^n\frac{\pi n}{l}B_{kn}C_{nj}, \quad (34)$$

$$T_{kj}=B_{kj}\sin\frac{p_j}{\hbar}l\exp[-ip_jl/\hbar], \quad (35)$$

$$\frac{ip_j}{\hbar}T_{kj}\exp[ip_jl/\hbar] =B_{kj}\frac{p_j}{\hbar}\cos\frac{p_j}{\hbar}l+\sum_n(-1)^n\frac{\pi n}{l}A_{kn}C_{nj}. \quad (36)$$

These are to be solved simultaneously for R_{kj}, T_{kj}, A_{kj}, and B_{kj}. The C_{nj} are known functions. Putting Eq. (33) into Eq. (34), and Eq. (35) into Eq. (36), and rearranging we get:

$$-\frac{p_j}{\hbar}\exp[-ip_jl/\hbar](A_{kj}+2i\delta_{kj}) =\sum_n(-1)^n\frac{\pi n}{l}B_{kn}C_{nj}, \quad (37)$$

$$-\frac{p_j}{\hbar}\exp[-ip_jl/\hbar]B_{kj} =\sum_n(-1)^n\frac{\pi n}{l}A_{kn}C_{nj}. \quad (38)$$

These equations must be solved for A_{kj} and B_{kj}. This is most easily done in matrix form. Writing the following matrices:

$$P_{kj}=\frac{p_j}{\hbar}\exp[-ip_jl/\hbar]\delta_{kj}, \quad N_{kj}=(-1)^j\frac{\pi j}{l}\delta_{kj}$$

Eqs. (37) and (38) become

$$-(A+2i)P=BNC, \qquad -BP=ANC \quad (39)$$

whence

$$A=-2i(1-G^2)^{-1}, \quad (40)$$

$$B=-2i(1-G^2)^{-1}G \quad (41)$$

where

$$G=NCP^{-1}. \quad (42)$$

Equations (40) and (41) in conjunction with Eqs. (33) and (35) complete the formal solution of the problem.

The matrix elements G_{kj} are given by:

$$G_{kj}=(-1)^{k+j}2\pi^2kj\sin q_k \times\exp[-iq_k]/q_j(q_k^2-\pi^2j^2) \quad (43)$$

where

$$q_j=p_jl/\hbar=\pi(8ml^2E/h^2-j^2)^{\frac{1}{2}}. \quad (44)$$

The necessary matrix elements of $(1-G^2)^{-1}$ had to be calculated numerically. Although this is an infinite matrix, the finite square 6×6 matrix was found to yield sufficiently accurate numerical values.

Effect of Asymmetry

To determine the effect of asymmetry of the potential energy surface on the transmission coefficient, the previous calculation was repeated for the case where the width of one branch of the potential energy surface is a fraction, $1/a$, times the width of the other. The wave function in region II, Fig. 3, is then

$$\Psi_k^{\mathrm{II}}=\sum_j A_{kj}\sin\frac{p_j}{\hbar}x\sin\frac{\pi j}{l}y + B_{kj}\sin\frac{\pi j}{w}x\sin\frac{p_j'}{\hbar}y \quad (45)$$

where p_j' is now the momentum of a particle in the jth vibrational state in the exit branch of the channel.

The analysis proceeds as before, and results in these expressions for R_{kj} and T_{kj}:

$$R_{kj}=(A_{kj}\sin aq_j-\exp[-iaq_j]\delta_{kj})\times\exp[-iaq_j], \quad (46)$$

$$T_{kj}=B_{kj}\sin(q_j'/a)\exp[-i(q_j'/a)], \quad (47)$$

where A_{kj} and B_{kj} are the respective elements of the matrices:

$$A=-2i(1-G''G')^{-1}, \quad (48)$$

$$B=-2i(1-G''G')^{-1}G'', \quad (49)$$

$$G_{kj}''=\frac{2(-1)^{k+i}kj\sin a\pi(\delta^2-k^2)^{\frac{1}{2}}\times\exp[i\pi(a^2\delta^2-j^2)^{\frac{1}{2}}/a]}{(\pi/a)(a^2\delta^2-j^2)^{\frac{1}{2}}(a^2\delta^2-a^2k^2-j^2)}, \quad (50)$$

$$G_{kj}'=\frac{2(-1)^{k+i}kja^2\sin[(\pi/a)(a^2\delta^2-k^2)^{\frac{1}{2}}]\times\exp[i\pi a(\delta^2-j^2)^{\frac{1}{2}}]}{\pi(a^2\delta^2-a^2j^2)^{\frac{1}{2}}(a^2\delta^2-k^2-a^2j^2)}, \quad (51)$$

where $\delta^2=8ml^2E/h^2$ and $a=w/l$.

The general form of the transmission coefficient curve is much the same as for the symmetrical case, but the zeros in T_{kj} are differently spaced.

For $a=2$, i.e., if the exit branch is twice the width of the entrance branch, the zeros are twice as dense as for the case $a=1$. Higher values for a lead to still denser zeros in the transmission coefficient. This means that as the total energy of the system increases the quantum mechanical transmission coefficient will oscillate the more rapidly the wider the exit channel is compared to the entrance channel. Since no actual system is composed of particles all having exactly the same energy, the average transmission coefficient will not display the maxima obtained for a single particle, unless the peaks are considerably broader than the energy range of the particles. This is the case for $a=2$, but for higher values the peaks become much sharper.

Taking $a\leqq1$ corresponds to passage from the wide channel into the narrow one. The general formulae remain the same, but the zeros are now spaced much as before. For $a=\frac{1}{2}$ they come at $E=4, 5, 8, 9, 13$. Since a vibrational quantum in the narrow channel is four times the size of that in the wide one, there can be no transmission below $E=4$ when passing from wide to narrow channel. The subsequent zeros are the same as for the case $a=1$.

Total Reflection

The simplest energy surface for total reflection is a closed straight channel. In this case, however, no exchange of vibrational and translational energy can occur. This is immediately evident when the wave functions for incident and reflected waves are equated at the closed end, $x=0$:

$$\sum_j R_{kj}\sin\frac{\pi j}{l}y=\sin\frac{\pi k}{l}y. \quad (52)$$

Hence, $R_{kj}=\delta_{kj}$. This is apparently the case whenever the energy surface is symmetrical about the reaction path. For an unsymmetrical surface, there will be interchange of energy.

Such a potential surface may be idealized by considering a rectangular channel with a right angle bend in it, but closed at one end (Fig. 6). The general procedure is as before. In each of the three regions indicated in Fig. 6, solutions are found to the Schrödinger equation. In regions I and II, these are given by Eq. (30) and (45), re-

spectively. In region III we can have only standing waves, represented by

$$\Psi_k^{\mathrm{III}}=\sum_j D_{kj}\sin\frac{q_j'}{w}(y-l-b)\sin\frac{\pi j}{w}x \quad (53)$$

where $q_j'=p_j'w/\hbar$ and p_j' is the momentum in region III. Again, the solutions and their first derivatives must be equal at the boundaries of regions I and II and regions II and III. Application of these conditions gives the following results for the reflected amplitudes:

$$R_{kj}=\left(A_{kj}\sin\frac{q_jw}{l}-\exp\left[-iq_jw/l\right]\delta_{kj}\right)\times\exp\left[-iq_jw/l\right], \quad (54)$$

$$A_{kj}=\{-2i(1-G'G)^{-1}\}_{kj}, \quad (55)$$

$$G_{kj}=(-1)^{k+j}\frac{2kj\sin(q_kw/l)\sin(q_j'l/w)}{(q_jw/l)\left[\delta^2l^2-(l^2k^2/w^2)-j^2\right]}, \quad (56)$$

$$G_{kj}'=(-1)^{k+j}\frac{2kj\sin(q_kw/l)\left[\cos(q_j'w/l)+i\sin(q_jw/l)\right]}{l\left[\delta^2w^2-(k^2w^2/l^2)-j^2\right]}, \quad (57)$$

$$\delta^2=8mE/h^2;\quad q_k=\pi(\delta^2l^2-k^2)^{\frac{1}{2}};\quad q_k'=\pi(\delta^2w^2-k^2)^{\frac{1}{2}}. \quad (58)$$

When $b=l$, Eq. (57) becomes indeterminate. The analysis is then simpler, however, and we find that for $b=l$,

$$R_{kj}=-\delta_{kj}\exp\left[-i2q_jw/l\right]. \quad (59)$$

Hence there is no interchange of translational and vibrational energies if $b=l$. Inspection of Eq. (54) shows that, as before, the reflection coefficient is an oscillating function of the total energy, having zeros at the same points as for transmission. The form of the matrix coefficient A_{kj} is different from that of the preceding cases, in that G and G' are no longer symmetrical in a and $1/a$ as before. This however, cannot affect the general shape of the curve for R, but only the magnitudes of its maxima, which appear much as in Fig. 5.

Obtuse Angle

The effect of varying the angle of the bend in the potential energy surface can be calculated for obtuse angles using the wave functions:

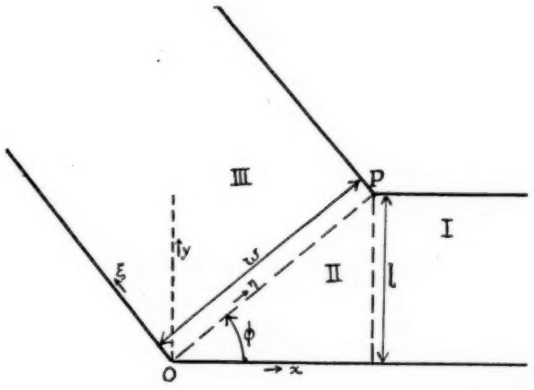

FIG. 7. Obtuse-angled bend. The corner region has the shape of a right triangle.

$$\Psi_k^{\mathrm{I}}=\sum_j(R_{kj}\exp\left[iq_jx/l\right]+\exp\left[-iq_jx/l\right]\delta_{kj})\times\sin\frac{\pi j}{l}y, \quad (60)$$

$$\Psi_k^{\mathrm{II}}=\sum_j\left(\alpha_{kj}\sin\frac{q_jx}{l}+A_{kj}\cos\frac{q_jx}{l}\right)\sin\frac{\pi j}{l}y+B_{kj}\sin\frac{q_j'y}{w\cos\phi}\sin\frac{\pi jx}{w\cos\phi}, \quad (61)$$

$$\Psi_k^{\mathrm{III}}=\sum_j T_{kj}\exp\left[iq_j''\xi/w\right]\sin\frac{\pi j}{w}\eta \quad (62)$$

where $q_j=p_jl/\hbar$, $q_j'=p_j'w\cos\phi/\hbar$, $q_j''=p_j''w/\hbar$, p_j is the momentum of a particle in the jth vibrational state in the incident channel, whose width is l; p_j', is the momentum in the exit channel of width $w\cos\phi$; and p_j'', is the momentum associated with a channel of width w. Region II is a right-triangular region. (Fig. 7.) The cartesian coordinates in region I are x and y; in region III they are ξ, η, related to x and y by the formulas:

$$\xi=y\cos\phi-x\sin\phi,\qquad \eta=y\sin\phi+x\cos\phi. \quad (63)$$

The general method of procedure is now the same as in the previous cases, since wave functions and their derivatives must match at the boundary of each two regions. However, we have an additional relation between the coefficients α_{kj} and A_{kj} which arises from the invariance of the

Schrödinger equation to a rotation of axes about the origin. Thus, when Ψ_k^{II} is transformed into ξ, η coordinates, it must satisfy the boundary condition, $\Psi_k^{II}(\xi, 0)=0$. This gives the condition

$$\sum_j \alpha_{kj} \sin(q_j\xi/w) \sin(\pi j\xi/w \tan\phi) = \sum_j A_{kj} \cos(q_j\xi/w) \sin(\pi j\xi/w \tan\phi) - B_{kj} \sin(q_j'\xi/w) \sin(\pi j\xi/w \cot\phi) \quad (64)$$

connecting α_{kj} with A_{kj} and B_{kj}.

The equations to be solved for R_{kj}, T_{kj}, A_{kj}, and B_{kj} are:

$$R_{kj} \exp[iq_j \cot\phi] + \exp[-iq_j \cot\phi]\delta_{kj} = A_{kj} \cos(q_j \cot\phi) + \alpha_{kj} \sin(q_j \cot\phi), \quad (65)$$

$$\frac{iq_j}{l}[R_{kj} \exp[iq_j \cot\phi] - \exp[-iq_j \cot\phi]\delta_{kj}] = \frac{q_i}{l}[\alpha_{kj} \cos(q_j \cot\phi) - A_{kj} \sin(q_j \cot\phi)] \times \sum_n \frac{(-1)^n \pi n}{w \cos\phi} B_{kn} C_{nj}, \quad (66)$$

$$\sum_j [\alpha_{kj} \sin(q_j\eta/w \tan\phi) + A_{kj} \cos(q_j\eta/w \tan\phi)] \sin(\pi j\eta/w) + B_{kj} \sin(q_j'\eta/w \cot\phi) \sin(\pi j\eta/w) = \sum_j T_{kj} \sin(\pi j\eta/w), \quad (67)$$

$$\sum_j \frac{\pi j}{w \tan\phi}[\alpha_{kj} \sin(q_j\eta/w \tan\phi) + A_{kj} \cos(q_j\eta/w \tan\phi)] \cos(\pi j\eta/w) + B_{kj}\frac{q_j'}{w} \cos(q_j'\eta/w \cot\phi) \sin(\pi j\eta/w) - \frac{q_j}{w}[\alpha_{kj} \cos(q_j\eta/w \tan\phi) - A_{kj} \sin(q_j\eta/w \tan\phi)] \sin(\pi j\eta/w) - \frac{\pi j}{w \cot\phi} B_{kj} \sin(q_j'\eta/w \cot\phi) \cos(\pi j\eta/w) = \sum_j T_{kj}\frac{iq_j''}{w} \sin(\pi j\eta/w) \quad (68)$$

in which the expansion

$$\sin(q_j'y/w \cos\phi) = \sum_n C_{jn} \sin(\pi ny/l)$$

has been made. Similar expansions may be made in the last two equations so as to express both sides of each equation as a Fourier series in the same interval. The resulting coefficients may be set equal term by term, yielding matrix equations for the unknowns as in the previous cases. Since the expansions are complicated, though straightforward, no general information can be gleaned from the equations without extensive numerical computation. However, it is apparent that the transmission coefficient will fluctuate much as before with changes in energy and in the angle ϕ.

THE JOURNAL OF CHEMICAL PHYSICS VOLUME 11, NUMBER 6 JUNE, 1943

Theory of Dissolution of Gels

ARTHUR TOBOLSKY
Department of Chemistry, Princeton University, Princeton, New Jersey

(Received March 6, 1943)

A theory of the dissolution of three-dimensional cross linked polymers is presented. The existence of a definite melting temperature is discussed in terms of molecular constants characterizing the gel.

WHEN a certain critical amount of cross linking occurs in a polymer composed of long chain molecules, continuously linked three-dimensional structures known as gels occur.[1] One of the ways of distinguishing these three-dimensional structures from linear chain polymers is that at ordinary temperatures the gels will exhibit a limited swelling in substances that will dissolve linear chains of the same chemical constitution.

[1] P. J. Flory, J. Am. Chem. Soc. **63**, 3083 (1941).

The existence of a definite temperature above which the swollen gel will be completely disrupted by the swelling pressure of the solvent will be discussed here. The case is especially clear cut when the cross linking bonds are weaker than the primary valence bonds along the chain, because in this case the disruption will occur at the cross linking bonds. In general, however, disruption will occur at the weakest recurring set of primary bonds in the gel structure, and the cause of the periodic weakness in the gel structure might be due to absorbed impurities. For simplicity we shall treat the case where the cross linking bonds are the weakest, but the same considerations apply with slight modification to the other cases.

The disruption of gels at a given temperature bears strong similarities to the melting of a solid. The solid-liquid transition occurs when the unfavorable heat of the transition is overcome by the entropy of randomness gained on melting, in other words $\Delta H = T_m \Delta S$. In the case of the swollen gel, below a certain critical temperature, there will exist two phases, a swollen gel phase and a solvent phase. The solvent will swell the gel a definite amount until the osmotic forces driving the solvent into the gel will be balanced by the elastic reaction of the gel. The elastic reaction of the gel is an entropy elasticity, the driving force being the tendency of the long chain molecules to spend more time in the numerous compact configurations than in less numerous extended ones. At a certain temperature, the unfavorable heat for breaking cross bonds will be counterbalanced by the increase in entropy resulting from the fact that the released chains can assume the more coiled configurations.

Most melting processes occur very rapidly, in fact the melting rate is determined by the diffusion of heat. The rate of dissolution of gels at their melting temperatures is quite slow because of the large entropy and energy change involved in the process. The rate of dissolution is given by $(kT/h) \exp(-\Delta F^{\dagger}/RT)$, where $\Delta F^{\dagger}$ is the free energy required to break the bond and, for the case of primary cross links, $\Delta F^{\dagger}$ is high.

Gelatin gels, which exhibit a reversible sol-gel transformation, appear to be a good example of the considerations presented here. They are presumably composed of long chain molecules with a molecular weight of about 30,000. The cross linking bonds are probably hydrogen bonds, and the weakness of these bonds explains the low melting temperature. The gels are highly elastic and when stretched exhibit double refraction, and give x-ray patterns as does stretched rubber. Below their melting temperatures the gels exhibit a limited swelling in water. The melting is reversible, and by carrying out the operations slowly, the melting and the setting temperatures can be made identical. In fact the slowness of the dissolution is the chief reason why the similarity to the solid-liquid transition has been obscured. For this same reason it is hard to evaluate the experimental evidence obtained to date to decide whether the melting occurs continuously or discontinuously as the temperature is raised, but there certainly does exist some evidence which favors the view that an abrupt change is involved.*

The possibility exists that the breakdown may occur over a small temperature interval, and that extraction of soluble materials and absorption of heat occurs before the large scale breaking of all the cross linking bonds has been completed. More experimental evidence is needed on this point, but the author believes that for a fairly homogeneous gel the dissolution is a cooperative phenomenon involving the simultaneous breaking of many cross bonds. The process is cooperative because every cross bond that breaks results in a gel with a looser structure capable of absorbing more solvent, and this more swollen structure will be more readily soluble than the original structure as will be seen in the forthcoming mathematical discussion. Cooperative processes of similar type give rise to sharp Curie points. The sharp melting points in gelatin gels appear to favor this possibility.

The gain in entropy that will ensue when the cross links are destroyed can be calculated on

* For discussion of this and the other experimental findings on gelatin gels outlined here, and also references to the original literature, see Chapter XV of *Colloids* by E. S. Hedges, published by Edward Arnold and Company (1931), and Chapters 19 and 20 of *Colloid Chemistry* by R. J. Hartmann, published by Houghton Mifflin Company (1939).

the basis of the statistics of long chain molecules. It is known that the probability that the distance between the two ends of a long chain hydrocarbon molecule lies between r and $r+dr$ is given by[2-4]

$$P(r)r^2dr=\frac{4}{\pi^{\frac{1}{2}}\lambda^3}\exp(-r^2/\lambda^2)r^2dr, \qquad (1)$$

where λ is the most probable value of r. λ can be shown for a hydrocarbon of n links to be the following:

$$\lambda=(2/\sqrt{3})l_0\sqrt{n} \qquad (2)$$

(the most probable value is equal to $\sqrt{\frac{2}{3}}$ times the root mean square value).

For hydrocarbons $l_0=1.54$A. For rubber (*cis* structure) Wall[5] has recently calculated a value of $2.01\sqrt{n}$A, and for gutta percha (*trans* structure) a value of $2.90\sqrt{n}$ for the r.m.s. value.

We wish to calculate the entropy change in the following process: the swollen gel breaks its cross linking bonds and the long molecules dissolve in solvent that they had imbibed. There is no appreciable change in the entropy of mixing of solvent and long chain molecules, the greatest contribution arises from the fact that the long chain molecules can now coil up. A contribution of R cal./degree per mole of chains (the communal entropy)[6] arises because the centers of gravity of the molecules are now no longer localized in the network structure but can move through the entire phase.

In order to calculate the entropy of dissolution of the gel, it is necessary to make explicit assumptions about the structure of the gel. The most complete treatment of gel structure[1] indicates that the possible structures may be quite complex. For purposes of calculation and comparison we shall consider two cases. In the first case the highly swollen network will be considered to have the aspect of a three-dimensional fish net, and the possible interpenetration of network units will be neglected. It is to be realized that much looser structures are possible and undoubtedly are important when the cross linking is small.

If in the swollen state of the polymer the average distance between network points is r, then using the Boltzmann relation $S=k\ln P$ the change of entropy in going from the swollen state characterized by r, to the dissolved state where the distance between network units is λ, the gain in entropy per chain of the network is

$$\Delta S=k[(r^2/\lambda^2)-\ln(r^2/\lambda^2)-1]. \qquad (3)$$

If communal entropy be added, then the third term vanishes.

Let ν be the number of cross linking bonds effective in the network structure of the swollen gel per gram of polymer. Then, if γ is the number of chains out of each cross bond, the number of chains s per gram of polymer is $\gamma\nu/2$. In many cases $\gamma=4$ so that the number of chains is twice the number of bonds, that is, $s=2\nu$.

If the distance between neighboring bonds in the swollen gel is r, the volume can be seen to be $8\nu r^3/3\sqrt{3}$, inasmuch as the cross linking bonds can for simplicity be arranged on a diamond lattice. Therefore, for the case of $\gamma=4$, $r^3=V/1.54\nu$, where V is the swollen volume per gram of polymer. If M is the molecular weight of a chain, m the molecular weight divided by the number of atoms in a chain, and N is Avogadro's number, then $\lambda^2=(4/3)l_0^2(M/m)$ and $s=N/M$.

The gain in entropy per mole of "chains" is, therefore,

$$\Delta S=R\left(\frac{3m(2V)^{\frac{1}{3}}}{4(1.54Nl_0^3)^{\frac{1}{3}}M^{\frac{1}{3}}}-\ln\frac{3m(2V)^{\frac{1}{3}}}{4(1.54Nl_0^3)^{\frac{1}{3}}M^{\frac{1}{3}}}\right). \qquad (4)$$

In terms of the density ρ of the polymer and the volume fraction of the polymers, and if the swelling is sufficiently large to neglect the logarithmic term

$$\Delta S=R\left[\frac{3m(2/\phi)^{\frac{1}{3}}}{4(1.54Nl_0^3)^{\frac{1}{3}}M^{\frac{1}{3}}\rho^{\frac{1}{3}}}\right]. \qquad (5)$$

The heat of melting for the case of $\gamma=4$ is equal to $E/2$, where E is the energy per mole of cross bonds. Hence the temperature of melting

[2] H. Eyring, Phys. Rev. **39**, 746 (1932).
[3] W. Kuhn, Kolloid Zeits. **68**, 2 (1934); **76**, 258 (1936).
[4] A. Tobolsky, R. E. Powell, and H. Eyring, Chapter on "Elastic viscous properties of matter" in *Frontiers of Chemistry* (Interscience Publishers, in press).
[5] F. T. Wall, J. Chem. Phys. **11**, 67 (1943).
[6] J. Hirschfelder, D. Stevenson, and H. Eyring, J. Chem. Phys. **5**, 896 (1937).

is given by

$$T_m = E \Big/ 2R\left[\frac{3m(2/\phi)^{\frac{1}{3}}}{4(1.54Nl_0^3)^{\frac{1}{3}}M^{\frac{1}{3}}\rho^{\frac{1}{3}}}\right]. \quad (6)$$

Another possible treatment of the entropy of distortion of a network is that which has been recently used by several authors for the development of the kinetic theory of elasticity.[7] In connection with the theory of limited swelling, Flory and Rehner[8] have developed an equation for the change in elastic entropy on going from undistorted polymer to the swollen state. This is based on the assumption that in the swelling process the relative configuration of the network points are not changed, and the swelling merely magnifies the distance between network points. On this basis r/λ appearing in Eq. (3) can be taken to be the cube root of the ratio of the volumes of the swollen and unswollen states (which is $1/\phi$ in our notation). Their expression for elastic entropy per mole of chains using a tetrahedral model for the network is

$$\Delta S_{\text{elastic}} = -\tfrac{3}{2}R[(1/\phi)^{\frac{1}{3}} - 1]. \quad (7)$$

By a slight extension of Wall's[9] analysis for entropy of stretching one can derive the following expression for the elastic entropy per mole of chains:

$$\Delta S_{\text{elastic}} = -\tfrac{3}{2}R[(1/\phi)^{\frac{1}{3}} - \ln (1/\phi)^{\frac{1}{3}} - 1]. \quad (7')$$

The entropy for the dissolved state of the network per mole of chains neglecting entropy of mixing will differ from the undistorted polymer by $R \ln (1/\phi)$ plus the communal entropy R. If ϕ is small, $\ln 1/\phi$ can be neglected in comparison with $1/\phi$. The entropy change on melting (i.e., going from swollen state to dissolved state) is, therefore [from Eq. (7) or (7')]

$$\Delta S = \tfrac{3}{2}R(1/\phi)^{\frac{1}{3}}. \quad (8)$$

For the tetrahedral model $\gamma = 4$ so that $\Delta H = E/2$ and

$$T_m = \frac{E}{3R(1/\phi)^{\frac{1}{3}}}. \quad (9)$$

On the basis of their theory for $\Delta S_{\text{elastic}}$, Flory and Rehner have derived an expression for ϕ in terms of the molecular weight M, the molar volume V_1 of the solvent, and the density of the polymer. When this is substituted in the expression for T_m, one gets

$$T_m = \frac{E}{3R(M/2\rho V_1)^{2/5}}. \quad (10)$$

This method of treating the entropy of dissolution is based on the assumption that the swollen gel structure is essentially the same (except for a homogeneous dilation) as that of the undistorted polymer, and that the tetrahedral cells interpenetrate to the same extent in both cases. It must be remembered, however, that the undistorted volume of the polymer is determined mainly by the van der Waals volume of the atomic groups (i.e., by energy considerations) and not by statistical considerations, as is proved by the fact that the density of polymers of the same chemical constitution is independent of molecular weight. This fact, as well as the possibility that interpenetration of the elements of the network becomes much less pronounced in the swollen state, limits the accuracy of this method of calculating entropy change.

Experimental work on a series of gels with similar values of E, m, and l_0, with Eqs. (6), (9), and (10) used for comparative purposes, should yield useful information on the structure of gels in the swollen and unswollen states.

---

[7] E. Guth and H. James, Ind. Eng. Chem. **33**, 624 (1941).

[8] P. J. Flory and J. Rehner, New York Academy of Sciences, Preprinted manuscripts on conference on High Polymers (Jan. 1943). A more complete paper on this subject by these authors is forthcoming. The author wishes to thank Drs. Flory and Rehner for useful personal discussion.

[9] F. T. Wall, J. Chem. Phys. **10**, 131 (1942).

An Application of Group Theory to Isomerism in General

TERRELL L. HILL
Morley Chemical Laboratory, Western Reserve University, Cleveland, Ohio

(Received January 30, 1943)

By making use of Polya's theorem and the groups of symmetries of the geometrical models representing unsubstituted parent compounds, it is possible to include the various kinds of isomerism in a single discussion. The number of isomers calculated by this procedure is the total number of all types.

USING group theory, Polya[1] solved a general problem in combinatory analysis applied to geometrical symmetry, and his results have been applied[2] to the calculation of the number of structural isomers in various kinds of organic compounds. However, the applicability of Polya's theorem to isomerism is considerably more general than this. It can be used, for example, to demonstrate mathematically the unity between the three types of isomerism (optical, geometrical, and structural[3]) usually distinguished. Thus, employing the proper three-dimensional models, one obtains by this procedure the total number of isomers of *all* kinds.

We may begin by restating Polya's theorem in an immediately applicable form. Let $\mathfrak{C}$ be the group of symmetries (of order h) of the geometrical model representing the unsubstituted parent compound (e.g., methane, ethylene, benzene, etc.), there being p positions in the parent compound at which substitution can occur. Let P be a permutation group isomorphic to $\mathfrak{C}$. Let $H_{j_1 j_2 \cdots j_p}$ be the number of permutations in P which can be written as the product of j_1 cycles of order one, j_2 cycles of order 2, $\cdots$, and j_p cycles of order p. By placing substituents (hydrogen included) $\varphi_1, \varphi_2, \cdots, \varphi_p$ at positions 1, 2, $\cdots$, p, respectively, one obtains a configuration. Two configurations $(\varphi_1, \varphi_2, \cdots, \varphi_p)$ and $(\varphi_1', \varphi_2', \cdots, \varphi_p')$ are said to be equivalent mod $\mathfrak{C}$ if there exists a permutation

$$S_i = \begin{pmatrix} 1 & 2 & \cdots & p \\ i_1 & i_2 & \cdots & i_p \end{pmatrix}$$

in P such that $\varphi_{i_1} = \varphi_1', \cdots, \varphi_{i_p} = \varphi_p'$. Let $A_{k_1 k_2 \cdots}$ be the number of non-equivalent (mod $\mathfrak{C}$) configurations when k_1 substituents of a first kind, k_2 substituents of a second kind, etc., are substituted into the parent compound. Then

$$\sum A_{k_1 k_2 \cdots} x_1^{k_1} x_2^{k_2} \cdots = \frac{1}{h} \sum H_{j_1 j_2 \cdots j_p} f_1^{j_1} f_2^{j_2} \cdots f_p^{j_p}, \quad (1)$$

where

$$f_1 = 1 + x_1 + x_2 + \cdots, \quad f_2 = 1 + x_1^2 + x_2^2 + \cdots,$$
$$\cdots, \quad f_p = 1 + x_1^p + x_2^p + \cdots.$$

The summation on the right is taken over all permutations in P and the expression on the left is the resulting polynomial in $x_1, x_2, \cdots$. That is, the coefficient

$$A_{k_1 k_2 \cdots} \quad \text{of} \quad x_1^{k_1} x_2^{k_2} \cdots$$

gives the number of isomers possible when k_1 substituents of a first kind, k_2 of a second kind, etc., are introduced into the parent compound.

As has been mentioned above, this theorem has been applied to the calculation of the number of structural isomers in certain cases. However, according to the above definition of non-equivalence, it is clear that two isomers of *any* kind—whether they be optical, geometrical, or structural—correspond to two non-equivalent configurations and will, therefore, be counted if the proper model is employed. That is, two isomers (of any kind) cannot be superimposed one on the other by means of rotations or reflections or both. Therefore $A_{k_1 k_2 \cdots}$ is the *total* number of isomers of *all* types. In the examples previously worked out (in structural isomerism) the geometrical models chosen have been two-dimensional and hence optical isomerism has been excluded. If the geometrical model is the correct three-dimensional one, no such restriction is imposed.

[1] G. Polya, Comptes rendus **201**, 1167 (1935).
[2] G. Polya, Helv. Chem. Acta **19**, 22 (1936); Zeits. f. Krist. **93**, 415 (1936). T. L. Hill, J. Phys. Chem. (in press).
[3] We do not include here structural isomerism of the type (CH_3-O-CH_3, C_2H_5OH).

This method may be used to "prove" *algebraically* the existence of two isomers in the case of a single asymmetric unit or a single geometric unit. Rules for calculating the number of stereoisomers in carbon chain compounds by a process of combining the asymmetric and geometric units have already been worked out.[4] However, when the optical isomerism arises in a ring compound and is the property, in a sense, of the entire ring rather than of particular asymmetric carbon atoms, the use of Polya's theorem is sufficient in itself.

OPTICAL ISOMERISM

The Asymmetric Carbon Atom

In defining an asymmetric carbon atom algebraically one might expect that the existence of only one element, the identity element, in its group of symmetries would be an adequate observation. It is, however, only a necessary condition and not a sufficient one, since the group is derived from *axes* of symmetry, whereas *planes* of symmetry must also be considered. Thus, each of the tetrahedral structures represented in two dimensions by

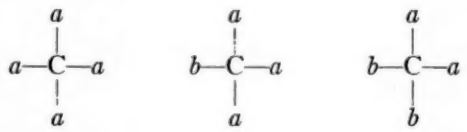

(1) (2) (3)

has more than one element in its group of symmetries (each having at least one axis of symmetry), while neither

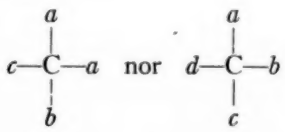

(4) (5)

has an axis of symmetry or more than one element in its group of symmetries, although (4) has a plane of symmetry and (5) has not.

Resorting to Polya's theorem, the geometrical model to be used here is obviously the tetrahedron. As is well known, a permutation group isomorphic to the group of symmetries of the tetrahedron has 12 elements: One permutation can be written as a product of 4 cycles of order one; 8 permutations can be written as a product of one cycle of order 3 and of one cycle of order one; and 3 permutations can be written as a product of 2 cycles of order 2. Therefore, Eq. (1) becomes

$$\sum A_{k_1k_2\cdots}x_1^{k_1}x_2^{k_2}\cdots=\tfrac{1}{12}(f_1^4+8f_3^1f_1^1+3f_2^2). \quad (2)$$

If we choose $f_1=1+x_1+x_2+x_3$, all possibilities are included since this allows the substitution of three different groups in addition to the hydrogen left unsubstituted. That is, the coefficient of $x_1x_2x_3$ in Eq. (2) gives the number of isomers when four different substituents (φ_1, φ_2, φ_3, H) are bonded to the same carbon atom. Similarly, the coefficient of, say, x_1x_2, x_2x_3, $x_1x_2x_3^2$, or $x_1^2x_2x_3$ gives the number of isomers for structures of type (4) above, etc.

Putting $f_1=1+x_1+x_2+x_3$, $f_2=1+x_1^2+x_2^2+x_3^2$, and $f_3=1+x_1^3+x_2^3+x_3^3$ in Eq. (2), one finds

$$\sum A_{k_1k_2k_3}x_1^{k_1}x_2^{k_2}x_3^{k_3}=2x_1x_2x_3+x_1x_2x_3^2+x_1x_3x_2^2+x_2x_3x_1^2+\text{etc.}, \quad (3)$$

all coefficients being unity except the coefficient of $x_1x_2x_3$. This serves, then, as an algebraic confirmation of the possibility of two isomers when four different substituents are attached to the same carbon atom, and of only one isomer in all other cases.

Allene Type Compounds

Optical isomerism of the type found in

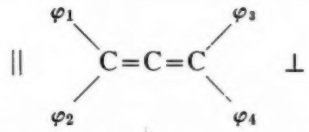

should be mentioned here. The parallel (∥) and perpendicular (⊥) symbols indicate the relative planes in which the two ends of the molecule lie. With this in mind, it is easy to show that the permutation group isomorphic to the group of symmetries of this structure (replacing all φ's by H's) has 4 elements: One permutation can be written as a product of 4 cycles of order one; and 3 permutations can be written as a product of 2 cycles of order 2. Then,

$$\sum A_{k_1k_2\cdots}x_1^{k_1}x_2^{k_2}\cdots=\tfrac{1}{4}(f_1^4+3f_2^2). \quad (4)$$

[4] G. E. K. Branch and T. L. Hill, J. Org. Chem. **5**, 86 (1940); J. K. Senior, Ber. **60B**, 73 (1927).

Choosing again $f_1=1+x_1+x_2+x_3$ and $f_2=1+x_1^2+x_2^2+x_3^2$,

$$\sum A_{k_1k_2k_3}x_1^{k_1}x_2^{k_2}x_3^{k_3}=6x_1x_2x_3+3x_1x_2x_3^2+3x_1x_2^3+x_1^4+\text{etc.} \quad (5)$$

The terms written on the right side of Eq. (5) are representative. The coefficients give the total number of isomers (structural and optical) for the type of substitution indicated. For example, if all substituents are the same (x_1^4), there is one isomer. If all substituents are different ($x_1x_2x_3$), there are six isomers:

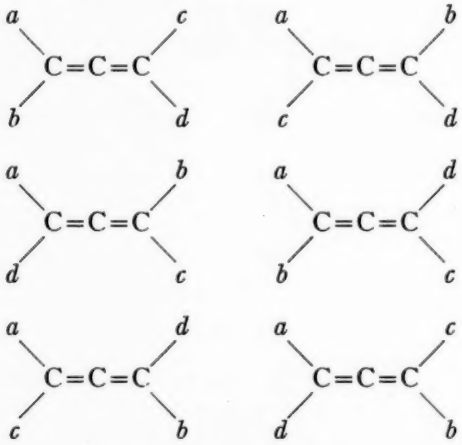

Ring Compounds

Cyclopropane, cyclobutane, and cyclopentane may be considered planar and, therefore, the following may be used as models:

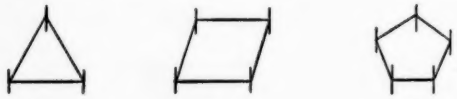

where one set of substituents is undertood to be above the plane of the ring and the other set below this plane. The groups of symmetries of (1), (2), and (3) are easily obtained, and using Eq. (1), one finds, respectively,

$$\text{(a)}\quad \sum A_{k_1k_2\cdots}x_1^{k_1}x_2^{k_2}\cdots=\tfrac{1}{6}(f_1^6+3f_2^3+2f_3^2),$$

$$\text{(b)}\quad \sum A_{k_1k_2\cdots}x_1^{k_1}x_2^{k_2}\cdots=\tfrac{1}{8}(f_1^8+5f_2^4+2f_4^2), \quad (6)$$

$$\text{(c)}\quad \sum A_{k_1k_2\cdots}x_1^{k_1}x_2^{k_2}\cdots=\tfrac{1}{10}(f_1^{10}+5f_2^5+4f_5^2).$$

As an example we may calculate the total number of isomers possible when n OH radicals are substituted into cyclobutane. Since all substituents are to be the same, $f_1=1+x$, $f_2=1+x^2$, and $f_4=1+x^4$. Then, putting these in Eq. (6b), we have

$$\sum A_kx^k=x^8+x^7+6x^6+7x^5+13x^4+7x^3+6x^2+x+1. \quad (7)$$

The coefficient of x^n gives the desired result. Thus, the 13 isomers corresponding to the term $13x^4$ arise as follows:

Structural:

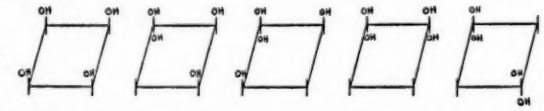

Optical: 4 + 4 + 3 + 1 + 1 = 13

There is some question about the geometrical arrangement in six-membered and higher rings. For any arrangement, of course, one can obtain the group of symmetries of the model and use the above method. For example, if a planar ring for cyclohexane is valid,

$$\sum A_{k_1k_2\cdots}x_1^{k_1}x_2^{k_2}\cdots=\tfrac{1}{12}(f_1^{12}+7f_2^6+2f_3^4+2f_6^2) \quad (8)$$

as may be verified.

Finally, it should be mentioned that applications to rings containing one or more atoms other than carbon and to fused ring systems are also possible. In fact, as is clear from the generality of Polya's theorem, any rigid geometrical model may be subjected to this type of analysis.

GEOMETRICAL ISOMERISM

The group of symmetries of the planar configuration

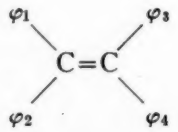

is isomorphic to that of allene type compounds. Therefore Eqs. (4) and (5) are applicable (the total number of isomers being made up here of structural and geometrical contributions). For example, corresponding to the term $3x_1x_2x_3^2$ in

Eq. (5), we have the structures

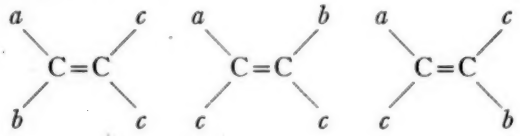

ISOMERISM OF COORDINATION NUMBER *n*

Up to this point we have discussed isomerism in connection with carbon compounds. The treatment need not, however, be confined to carbon, nor, for that matter, to coordination number four.

Structures are known in which coordination numbers from one to eight are exhibited, and Kimball[5] has listed the possible spatial arrangements. Using the group of symmetries of any such arrangement, Polya's theorem leads to the symmetry formula [Eq. (1)]. Thus the total number of isomers may be obtained for any substitution in which the substituents are monovalent coordinating groups.

Marchi, Fernelius, and McReynolds[6] have recently discussed the stereochemistry of coordination number eight, using models and the method of Lunn and Senior.[7]

[5] G. E. Kimball, J. Chem. Phys. **8**, 188 (1940).
[6] L. E. Marchi, W. C. Fernelius, and J. P. McReynolds, J. Am. Chem. Soc. **65**, 329 (1943).
[7] A. C. Lunn and J. K. Senior, J. Phys. Chem. **33**, 1027 (1929).

THE JOURNAL OF CHEMICAL PHYSICS VOLUME 11, NUMBER 6 JUNE, 1943

On the Kinetics of Copolymerization

HERMAN BRANSON AND ROBERT SIMHA
Howard University, Washington, D. C.
(Received March 13, 1943)

TWO general developments of the kinetics of polymerization reactions have been recently given. One[1] involves the assumption of a steady state in regard to the concentration of active nuclei; the other[2] is more general.

Copolymerization reactions have been treated in a few instances[3] by introduction of certain *ad hoc* assumptions. In view of present interests it seems desirable to undertake a more complete analysis of these reactions. Because of the difficulty of a general development, the analysis rests on the steady state method which is valid as long as the rate of initiation is negligibly small in comparison with that of growth and that of termination. Mainly termination involving a radical chain and a stable monomer is considered at present. A few of the results are outlined in the following.

[1] E. F. G. Herrington and Alan Robertson, Trans. Faraday Soc. **38**, 490 (1942).
[2] R. Ginell and R. Simha, J. Am. Chem. Soc. **65**, 706, 715 (1943).
[3] R. G. W. Norrish and E. F. Brookman, Proc. Roy. Soc. **A171**, 147 (1939); F. T. Wall, J. Am. Chem. Soc. **63**, 1846 (1941).

We postulate the mechanism:

$$\text{Initiation:}\quad N_1 \xrightarrow{k_{11}} n_{10};\qquad N_2 \xrightarrow{k_{12}} n_{01},$$

$$\text{Propagation:}\quad n_{rs} \xrightarrow{k_{21}(r,s)} n_{r+1s};\quad n_{rs} \xrightarrow{k_{22}(r,s)} n_{rs+1}, \tag{1}$$

$$\text{Termination:}\quad n_{rs} \xrightarrow{k_{31}(r,s)} N_{r+1s};\quad n_{rs} \xrightarrow{k_{32}(r,s)} N_{rs+1}.$$

N_1 and N_2 are mole fractions of monomer 1 and 2, respectively; n_{rs} are mole fractions of polymer radical of specified composition. N_{rs} are stable polymers. Since

$$dn_{rs}/dt=0,$$

we have from (1)

$$\begin{aligned}&\alpha_{rs}n_{rs}=\beta_{r-1s}n_{r-1s}+\gamma_{rs-1}n_{rs-1} \quad r,s\geqq 1,\\ &\alpha_{10}n_{10}=k_{11}N_1,\\ &\alpha_{01}n_{01}=k_{12}N_2,\end{aligned} \tag{1a}$$

with the definitions

$$\begin{aligned}\alpha_{rs}&=[k_{21}(r,s)+k_{31}(r,s)]N_1\\ &\quad+[k_{22}(r,s)+k_{32}(r,s)]N_2,\\ \beta_{rs}&=k_{21}(r,s)N_1,\\ \gamma_{rs}&=k_{22}(r,s)N_2.\end{aligned}$$

The solution of the difference equations (1a) can be found exactly as a complex function of the

two probabilities for growth of nuclei:

$$\omega_{ik}=\beta_{ik}/\alpha_{ik}, \quad \omega'_{ik}=\gamma_{ik}/\alpha_{ik}.$$

This solution expresses the total number of ways a chain of composition (r, s) can be built. The probabilities may be expected to be functions of the composition of the unstable polymer. In view of the scarcity of experimental data, it seems hardly warranted to carry through an exact treatment. As a first approximation we may, therefore, replace the probabilities by average values obtained on substituting a mean composition for the individual chain composition. The error will be greatest in respect to the pure polymers, n_{r0} and n_{0s}. However, since their number is small, the error will not be large. With these assumptions the solution of (1a) reduces to

$$n_{rs}=\omega^r(\omega')^s\left[\frac{k_{11}}{k_{21}}\binom{r+s-1}{s}+\frac{k_{12}}{k_{22}}\binom{r+s-1}{r}\right], \quad (2)$$

where k_{21} and k_{22} are the average rates of propagation:

$$k_{21}\sum_{i,k} n_{ik}=\sum_{i,k} k_{21}(i,k)n_{ik} \quad (3)$$

with a similar definition for k_{22}. In this equation k_{21} and k_{22} are independent of the composition of monomer in accordance with our assumption. The first term in (2) enumerates all ways of obtaining the polymer n_{rs} from a nucleus n_{10}; the second term, from a nucleus n_{01}.

Going to the kinetics, we have

$$\frac{dN_1}{dt}=-k_{11}N_1-N_1\sum_{i,k}[k_{21}(i,k)+k_{31}(i,k)]n_{ik}$$

and a similar equation for N_2. Introducing average rates of termination k_{31} and k_{32} defined in analogy to (3), we find from (1a):

$$\sum_{i,k} n_{ik}=\frac{k_{11}N_1+k_{12}N_2}{k_{31}N_1+k_{32}N_2}.$$

Substituting into the rate equations for N_1 and N_2 we obtain for the over-all rate

$$dz/dt=(k_{22}-k_{21})z[(k_{11}z+k_{12})/(k_{31}z+k_{32})], \quad (4)$$

where $z=N_1/N_2$ and all rates of propagation are much larger than the rates of termination. This equation or its integral allows a determination of certain combinations of rate constants. It may be noted that the over-all course of the reaction does not follow a simple first-order law as is found in simple polymerization.[1,2] If the second species is used up more rapidly than the first, $z\to\infty$ for $t\to\infty$; otherwise, $z\to 0$. If $z\to\infty$, the limiting rate is

$$\frac{1}{N_1}\frac{dN_1}{dt}=-\frac{k_{11}k_{21}}{k_{31}}; \quad \frac{1}{N_2}\frac{dN_2}{dt}=-\frac{k_{11}k_{22}}{k_{31}},$$

which is a first-order law; similarly a limiting second-order over-all rate results for a second-order initiation. For the final number average molecular weight, we find with the above approximations simply

$$\bar{M}_n=\frac{M_1N_1(0)+M_2N_2(0)}{(k_{31}/k_{21})N_1(0)+(k_{32}/k_{22})N_2(0)}.$$

M_1 and M_2 are the respective molecular weights of monomer; $N_1(0)$ and $N_2(0)$ represent initial mole fractions.

In the case of radical-radical termination with a rate k_3, the over-all rate can be shown to be:

$$\frac{dz}{dt}=z\left[(k_{12}-k_{11})+\frac{(k_{22}-k_{21})}{(k_3)^{\frac{1}{2}}}N_2^{\frac{1}{2}}(k_{11}z+k_{12})^{\frac{1}{2}}\right].$$

For the change of size distribution with composition we find with (1), (2), and (4):

$$\frac{dN_{rs}}{dz}=\frac{N_2(0)}{z_0(k_{22}-k_{21})}\left(\frac{z_0}{z}\right)^{[k_{22}/(k_{22}-k_{21})]+1}\times\frac{k_{31}z+k_{32}}{k_{11}z+k_{12}}f(r,s)\omega^r(\omega')^{s-1},$$

in which

$$f(r,s)=\left[\frac{k_{11}k_{22}k_{31}}{(k_{21})^2}\binom{r+s-2}{s}+\frac{k_{12}k_{32}}{k_{22}}\binom{r+s-2}{s-2}+\left(\frac{k_{12}k_{31}}{k_{21}}+\frac{k_{11}k_{32}}{k_{21}}\right)\binom{r+s-2}{s-1}\right].$$

From the definition of the ω's we see that they can be written as functions of z. The equation may then be integrated to give the final size distribution. Formulae for the weight average molecular weight may also be derived in this manner.

These preliminary results are presented as a contribution to a treatment of copolymerization which will allow a quantitative evaluation of kinetic data and of the structure of copolymers. A detailed paper dealing with this problem and extensions is being prepared.

Interaction of the van der Waals Type Between Three Atoms

B. M. AXILROD AND E. TELLER
George Washington University, Washington, D. C.
(Received May 14, 1943)

IT is recalled that the van der Waals attraction between atoms may be represented in good approximation by a sum of interactions between pairs of atoms.[1] This approximation is obtained by applying perturbation theory to the second order. The resulting interaction potential is of the order of $V\alpha/r^6$ where V is the ionization energy, α is their polarizability, and r is their distance.

If the perturbation calculation is pursued to the third order, interactions between triplets of atoms appear. The order of magnitude of the interaction is

$$\frac{V\alpha^3}{r_{12}^3 r_{23}^3 r_{31}^3},$$

where r_{12}, r_{23}, and r_{31} are the distances between the atoms. The magnitude and even the sign of the interaction potential depend upon the shape of the triangle with the sides r_{12}, r_{23}, and r_{31}. Our purpose is to investigate the character of this dependence.

The term in the third-order interaction energy which depends on triplets of atoms is

$$W_0''' = \sum_{\substack{l \\ l\neq 0}} \sum_{\substack{j\neq 0 \\ j\neq l}} \frac{H_{0j}H_{jl}H_{l0}}{(W_j - W_0)(W_l - W_0)},$$

where W_j, W_l, and W_0 are the unperturbed energies of the intermediate states j and l, and the ground state, respectively. In the numerator H_{0j}, etc., are matrix elements of the perturbation. As the perturbing potential we introduce dipole-dipole interactions between pairs of atoms. We further make the assumption that the lowest states of the interacting atoms are s states. Then in the state designated by subscript j and also in the state designated by subscript l two atoms will be in p levels. One of the three atoms is in the same p level in states j and l. Each of the other atoms is in the lowest s level in one of the states l or j and in a p level in the other of the states l or j.

The dependence of the perturbation potential on the shape of the triangle of the three atoms is due to two reasons. Firstly, the three matrix elements H_{0j}, H_{jl}, and H_{l0} contain the three factors, $1/r_{12}^3$, $1/r_{23}^3$, and $1/r_{31}^3$ (not necessarily in the order given). Secondly, the dipole-dipole interaction depends on the orientation of the interacting dipoles relative to each other and relative to the line connecting them. The orientation of a dipole depends on which particular substate of the degenerate p level was chosen. Subsequently one must carry out the summation over all the substates corresponding to the various p levels that can occur in intermediate states.

The summation can be carried out by a straightforward but lengthy calculation. One obtains

$$W_0''' = C\frac{3\cos\gamma_1\cos\gamma_2\cos\gamma_3 + 1}{r_{12}^3 r_{23}^3 r_{31}^3},$$

where γ_1 is included by the sides r_{12} and r_{31} with similar definitions for γ_2 and γ_3. C is a positive quantity of the order $V\alpha^3$. Its exact magnitude depends on the energies of p levels in the three atoms and on the magnitudes of the dipole matrix elements.

It is of interest to apply the equation to a few special configurations of atoms.

Case 1. *The equilateral triangle.* For $\gamma_1=\gamma_2=\gamma_3$ the interaction energy is

$$W_0''' = C\frac{11/8}{r_{12}^3 r_{23}^3 r_{31}^3}$$

which is positive, and hence the interaction is one of repulsion.

Case 2. *A right triangle.* For $\gamma_1=90°$ the interaction energy is

$$W_0''' = C\frac{1}{r_{12}^3 r_{23}^3 r_{31}^3}$$

and again the interaction is repulsive.

[1] Pauling and Wilson, *Introduction to Quantum Mechanics* (1935), Chap. XIV.

Case 3. *Three atoms in a line.* For $\gamma_1=\gamma_2=0$ and $\gamma_3=180°$ the interaction potential is

$$W_0'''=C\frac{-2}{r_{12}^3r_{23}^3r_{31}^3}$$

which indicates attraction.

Case 4. *One atom far removed from the other two.* For $r_{31}\gg r_{12}r_{31}\backeq r_{23}$ and $\gamma_3\backeq 0$ so that the interaction energy becomes

$$W_0=C\frac{(-3\cos^2\gamma_1+1)}{r_{31}^6r_{12}^3}.$$

THE AMERICAN INSTITUTE OF PHYSICS

INCORPORATED

ADMINISTRATIVE STAFF

HENRY A. BARTON, *Director*

MADELINE M. MITCHELL, *Publications Manager*

JOHN T. TATE, *Adviser on Publications*

Office: 175 Fifth Avenue, New York, New York

JOURNALS

THE PHYSICAL REVIEW

REVIEWS OF MODERN PHYSICS

JOHN T. TATE, *Editor (on leave)*

J. W. BUCHTA, *Acting Editor*

JOURNAL OF THE OPTICAL SOCIETY OF AMERICA

GEORGE R. HARRISON, *Editor*

THE JOURNAL OF THE ACOUSTICAL SOCIETY OF AMERICA

FLOYD A. FIRESTONE, *Editor*

AMERICAN JOURNAL OF PHYSICS

DUANE ROLLER, *Editor*

THE REVIEW OF SCIENTIFIC INSTRUMENTS

GAYLORD P. HARNWELL, *Editor*

THE JOURNAL OF CHEMICAL PHYSICS

JOSEPH E. MAYER, *Editor*

JOURNAL OF APPLIED PHYSICS

ELMER HUTCHISSON, *Editor*

GOVERNING BOARD

PAUL E. KLOPSTEG, *Chairman*
Central Scientific Company

GEORGE B. PEGRAM, *Secretary*
Columbia University

For the American Physical Society:

JOHN T. TATE
University of Minnesota

L. A. DUBRIDGE
University of Rochester

GEORGE B. PEGRAM
Columbia University

For the Optical Society:

A. C. HARDY
Massachusetts Institute of Technology

K. S. GIBSON
National Bureau of Standards

R. C. GIBBS
Cornell University

For the Acoustical Society of America:

HARVEY FLETCHER
Bell Telephone Laboratories

FLOYD A. FIRESTONE
University of Michigan

WALLACE WATERFALL
The Celotex Corporation

For the Society of Rheology:

R. B. DOW
Aberdeen Proving Ground

HERMANN MARK
Brooklyn Polytechnic Institute

N. W. TAYLOR
The Pennsylvania State College

For the American Association of Physics Teachers:

A. G. WORTHING
University of Pittsburgh

PAUL E. KLOPSTEG
Central Scientific Company

T. D. COPE
University of Pennsylvania

The American Institute of Physics is a membership corporation of which five societies are the founding members. These five societies are the principal national societies devoted to pure and applied physics in America. Their names, and those of their representatives who form the Governing Board of the Institute, are given above. The principal work of the Institute is the publication of journals sponsored by the societies or by itself. The names and the editors of the journals are also listed above.

The broad purpose of the Institute is to represent, in all matters of wide or common interest, the five thousand or more members and subscribers associated with the Founder Societies and the journals. It aims to advance the science and profession of physics, and to promote cooperation between pure research, the applied sciences and the industries. To achieve these aims, it is greatly in need of an endowment and is empowered by law to administer grants and funds of any kind.

CONTENTS

The Journal of Chemical Physics Vol. 11, No. 6 June, 1943

The Electronic Spectra and Configurations of Cycloheptatriene . . Robert S. Rasmussen 249

Determination of Chlorine Valences in Trihalomethanes from Intensities and Polarizations of Raman Lines . . . . . Gertrud Nordheim and H. Gilbert 253

Photographic Action of Silver Halides by Dyes. IV. The Optical Sensitizing Properties of Thiacyanine Dyes in Relation to Their Spectral Absorption and Constitution . . . . . S. E. Sheppard, R. H. Lambert, and R. D. Walker 265

Theoretical Investigation of the Efficiency of Alkaline Reaction Rates . . . . . Hugh M. Hulburt and J. O. Hirschfelder 276

Thermal Dissociation of [illegible] . . . . . Arthur Tobolsky 290

Application of Kinetic Theory to Interstellar Material . . . . . Terrell L. [illegible] 294

On the Equation of Clausius-Mosotti . . . . . Herman Branson and Robert [illegible] 297

Dissociation of Bi, Sn, and Weak Type Bonding Three Atoms . . . . . B. M. Axilrod and E. Teller 299

Lancaster Press, Inc. [illegible]